CHARACTERIZATION OF HARMFUL ALGAL BLOOM FREQUENCY, SEVERITY, AND SPATIAL EXTENT IN OKLAHOMA RESERVOIRS UTILIZING THE CYANOBACTERIA ASSESSMENT NETWORK

By

KELLY ROSE HENDRIX

Bachelor of Science in Environment Science

Montana State University

Bozeman, Montana

2021

Submitted to the Faculty of the
Graduate College of the
Oklahoma State University
in partial fulfillment of
the requirements for
the Degree of
MASTER OF SCIENCE
May, 2023

CHARACTERIZATION OF HARMFUL ALGAL BLOOM FREQUENCY, SEVERITY, AND SPATIAL EXTENT IN OKLAHOMA RESERVOIRS UTILIZING THE CYANOBACTERIA ASSESSMENT NETWORK

Thesis Approved:

Dr. Andrew R. Dzialowski

Thesis Advisor

Dr. Scott Stoodley

Dr. Brad Rogers

ACKNOWLEDGEMENTS

I would like to express my sincere gratitude to the people and organizations who have helped me complete my Master's thesis. Firstly, I would like to thank my friends and family for their unwavering support and encouragement throughout my academic journey. Your love and understanding have been invaluable to me, and I could not have made it this far without your support. To my mom, dad, and brother, thank you for always listening intently while I rambled on about my research, even if it often did not always make the most sense at the time. Secondly, I would like to thank my furry companion, Boots, for always being there to cheer me up when I needed it the most. Your unwavering loyalty and unconditional love have been a constant source of joy for me. I would also like to express my gratitude towards the Oklahoma Water Resource Board for their generous funding and guidance. Their financial support has allowed me to pursue my academic goals. Last but not least, I would like to thank my advisors and committee members, Dr. Dzialowksi, Dr. Stoodley, and Dr. Rogers, for their invaluable support and guidance. Their expertise, insights, and constructive feedback have been instrumental in shaping my research, and I could not have completed this thesis without their assistance. Once again, thank you to everyone who has supported me throughout this journey. Your contributions have made a significant impact on my academic and personal growth.

Name: KELLY ROSE HENDRIX

Date of Degree: MAY, 2023

Title of Study: CHARACTERIZATION OF HARMFUL ALGAL BLOOM FREQUENCY, SEVERITY, AND SPATIAL EXTENT IN OKLAHOMA RESERVOIRS UTILIZING THE CYANOBACTERIA ASSESSMENT NETWORK

Major Field: ENVIRONMENTAL SCIENCE

Abstract: Harmful algal blooms (HABs) pose significant threats to human health and the environment. Monitoring them in inland waterbodies is a challenging and costly task. Remote sensing technology is an increasingly useful tool in monitoring and managing HABs, providing timely information on their bloom dynamics. The Cyanobacteria Assessment Network (CyAN) was developed to provide a consistent and uniform program for HAB detection and characterization across the United States. CyAN utilizes the Ocean and Land Colour Imagers (OLCI) aboard Sentinel 3A and 3B to provide near daily imagery of the major waterbodies across the country. The objective of this study is to characterize the frequency, spatial extent, and severity of HABs in Oklahoma Reservoirs utilizing CyAN. Sixty nine waterbodies were selected for analysis. They include the largest lakes and reservoirs in Oklahoma. Frequency, spatial extent, and severity were assessed for trends over the six-year study period (2017-2022). Trend analysis was grouped into four bloom categories: high (>100,000 cells/ml), medium (20,000-100,000 cells/ml), low (<20,000 cells/ml), and total bloom. High, medium, and low-risk bloom thresholds are based off of the World Health Organizations risk of health impact thresholds. Total blooms represent any bloom level above sensor detection. The findings of this research indicate that statewide HABs are increasing in frequency over the study period for all bloom categories. The spatial extent of HABs is increasing statewide for all bloom risk categories. Bloom severity is increasing for multiple individual waterbodies. Significant differences in bloom frequency, severity, and spatial extent are observed between trophic states. The findings of this research highlight the potential of remote sensing as a valuable tool for HAB monitoring and provide insights for developing effective HAB management strategies.

TABLE OF CONTENTS

Chapter Page

I. INTRODUCTION....1

Background....3
HAB Impacts....4
Economic Impacts....8
Legislation....12
Remote Sensing and Cyanobacteria....14

II. LITERATURE REVIEW....17

Historical and Current Sensors....19
Remote Sensing Challenges....22
Algorithms....25
Cyanobacteria Assessment Network....27

III. DATA AND METHODS....34

Satellite Imagery....34
Study Area....36
Trophic Status....36
Frequency....39
Weekly Frequency....40
Maximum Bloom Severity....40
Spatial Extent....41
Trends....41

Chapter Page

IV. RESULTS....45

Frequency....45
Weekly Frequency....56
Severity....66
Spatial Extent....68

V. DISCUSSION....79

Limitations....81
Future Considerations....84
Summary....87

REFERENCES....89

APPENDICES....111

APPENDIX A: Kruskal Wallis Tests....111
APPENDIX B: Dunn's Pairwise Comparisons....113
APPENDIX C: Trend Analysis....116
APPENDIX D: Monthly Spatial Extent High Risk Blooms....146
APPENDIX E: Trophic State Graphs....150
APPENDIX F: Trophic Trend Analysis....155

LIST OF TABLES

Table Page

1. Compounds and rodent 24h intraperitoneal LD50 (ug/kg) 5
2. Cyanobacterial toxins, taxa, and human health impacts..... 6
3. WHO Recreational guidance levels..... 35
4. Lake trophic state categories 36
5. Analysis summary table 43
6. Statewide frequency trends..... 46
7. Waterbody high-risk bloom frequency trends..... 48
8. Waterbody total bloom frequency trends 54
9. Waterbody weekly high-risk bloom frequency trends 56
10. Waterbody weekly total bloom frequency trends..... 64
11. Waterbody maximum severity trends..... 66
12. Statewide monthly spatial extent trends 68
13. Waterbody monthly bloom coverage trends..... 70
14. Waterbody monthly high risk bloom percent cover trends 77

A1. Waterbody bloom frequency Kruskal Wallis tests 111
A2. Trophic state bloom frequency Kruskal Wallis tests..... 111
A3. Waterbody weekly bloom frequency Kruskal Wallis tests..... 112
A4. Trophic state weekly bloom frequency Kruskal Wallis tests 112
A5. Trophic state maximum bloom severity Kruskal Wallis test 112
A6. Trophic state monthly bloom percent cover Kruskal Wallis test 112

B1. Trophic state high risk bloom frequency pairwise comparison..... 113
B2. Trophic state low risk bloom frequency pairwise comparison..... 113
B3. Trophic state no bloom frequency pairwise comparison..... 113
B4. Trophic state total bloom frequency pairwise comparison..... 114
B5. Trophic state weekly high risk frequency pairwise comparison..... 114
B6. Trophic state weekly medium risk frequency pairwise comparison..... 114
B7. Trophic state maximum bloom intensity pairwise comparison..... 114
B8. Trophic state high risk percent cover pairwise comparison..... 115
B9. Trophic state medium risk percent cover pairwise comparison..... 115
B10. Trophic state no bloom percent cover pairwise comparison 115
B11. Trophic state total bloom percent cover pairwise comparison 115

Table Page

C1. Waterbody high risk bloom frequency trends....116
C2. Waterbody medium risk bloom frequency trends....118
C3. Waterbody low risk bloom frequency trends....120
C4. Waterbody no bloom frequency trends....122
C5. Waterbody total bloom frequency trends....124
C6. Waterbody weekly high risk bloom frequency trends....126
C7. Waterbody weekly medium risk bloom frequency trends....128
C8. Waterbody weekly low risk bloom frequency trends....130
C9. Waterbody weekly no bloom frequency trends....132
C10. Waterbody weekly total bloom frequency trends....134
C11. Waterbody maximum bloom severity trends....136
C12. Waterbody monthly high risk percent cover trends....138
C13. Waterbody monthly medium risk percent cover trends....140
C14. Waterbody monthly low risk percent cover trends....142
C15. Waterbody monthly total bloom percent cover trends....144

F1. Trophic state average annual high risk bloom frequency trends....155
F2. Trophic state average annual medium risk bloom frequency trends....155
F3. Trophic state average annual low risk bloom frequency trends....155
F4. Trophic state average annual no bloom frequency trends....155
F5. Trophic state average annual total bloom frequency trends....156
F6. Trophic state average annual weekly high risk bloom frequency trends....156
F7. Trophic state average annual weekly medium risk bloom frequency trends....156
F8. Trophic state average annual weekly low risk bloom frequency trends....156
F9. Trophic state average annual weekly no bloom frequency trends....157
F10. Trophic state average annual weekly total bloom frequency trends....157
F11. Trophic state maximum bloom severity trends....157

LIST OF FIGURES

Figure Page

1. Aspects to consider when assessing the economic impact of blooms 9
2. Electromagnetic Spectrum 15
3. Cyanobacteria spectral curves 16
4. Cyanobacteria Index Validation 32
5. Study Area Map 38
6. Frequency calculation at varying scales 39
7. Average statewide bloom frequency 45
8. Average waterbody high-risk bloom frequency 47
9. Average waterbody medium-risk bloom frequency 49
10. Average waterbody low-risk bloom frequency 51
11. Average waterbody no bloom frequency 53
12. Average waterbody total bloom frequency 55
13. Weekly waterbody high-risk bloom frequency 57
14. Weekly waterbody medium-risk bloom frequency 59
15. Weekly waterbody low-risk bloom frequency 61
16. Weekly waterbody no bloom frequency 63
17. Weekly waterbody total bloom frequency 65
18. Maximum bloom severity 67
19. Statewide monthly spatial extent of high risk blooms 69
20. Monthly distribution of high-risk bloom percent cover 71
21. Statewide monthly spatial extent of medium risk blooms 72
22. Monthly distribution of medium-risk bloom percent cover 73
23. Statewide monthly spatial extent of low-risk blooms 74
24. Monthly distribution of low-risk bloom percent cover 75
25. Statewide monthly total bloom spatial extent 76
26. Monthly distribution of total bloom percent cover 78

Figure Page

D1. Waterbody monthly high risk spatial extent 146

E1. Trophic state average annual bloom frequency 150
E2. Trophic state average annual weekly bloom frequency 151
E3. Trophic state monthly bloom percent cover 152
E4. Trophic state average annual no bloom frequency 153
E5. Trophic state average annual weekly no bloom frequency 153
E6. Trophic state maximum bloom intensity 154

CHAPTER I

INTRODUCTION

Harmful algal blooms (HABs) are a growing national and worldwide concern. HABs occur when algal communities abundance grows exponentially potentially producing toxic or adverse effects to organisms that come into contact with them (NOAA, 2016). HAB occurrences are increasing both nationally and worldwide (Hudnell, 2010). These blooms can comprise microscopic cellular populations, including dinoflagellates, diatoms, and cyanobacteria (Hudnell, 2010). Cyanobacteria are recognized as the leading harmful algal group and pose a fast-emerging worldwide issue threatening both human and ecosystem health (Carmichael, 2008). Monitoring, management, and mitigation of HABs are crucial to lessen their health, ecosystem, and economic impacts.

The impacts of HABs can be varied, including health hazards for humans and animals and degradation of water quality (Lopez, Jewett, Dortch, Walton, & Hudnell, 2008). The majority of the impacts in the United States (US) have included animal deaths, reduced recreational opportunities, and taste-and-odor problems in drinking water and aquaculture (Lopez et al., 2008). Mass die-offs of large algal biomass and the associated decomposition can lead to depleted dissolved oxygen (hypoxia) in the water (Lopez et al., 2008). Many cyanobacteria species produce cyanotoxins with potentially fatal consequences (Hudnell, 2010). The most common cyanotoxins observed in the US include saxitoxins, cylindrospermopsin, anatoxins, and microcystins (US EPA, 2018b).

Traditional methods of HAB sampling include visual assessments and in-situ monitoring. These traditional methods can be both time and cost-intensive. The high number of waterbodies and difficulty reaching remote areas further add to the challenges associated with in-situ monitoring. More recent methods include the use of satellite remote sensing data to help monitor for harmful algal blooms. One of the new systems utilized for HAB detection is known as CyAN (Cyanobacteria Assessment Network).

CyAN was developed with multiple agencies, including the EPA, the National Aeronautics and Space Administration (NASA), the National Oceanic and Atmospheric Administration (NOAA), and the United States Geological Survey (ORD US EPA, 2014a). The goal was to help provide near-real-time data that could act as an early warning system for HAB detection. This will support federal, state, tribal, and local managers in their monitoring efforts (ORD US EPA, 2014a). CyAN continues to be refined since its inception in 2015. It now utilizes satellite data from both the European Space Agency Envisat MERIS and Copernicus Sentinel-3 Ocean and Land Color Imager (OLCI) sensors (US EPA, 2022).

HABs can be characterized in Oklahoma and provide valuable information that managers can utilize regarding monitoring, management, and mitigation through CyAN. Understanding historical HAB trends can help develop better forecasting estimates (J. S. Clark et al., 2001; Urquhart, Schaeffer, Stumpf, Loftin, & Werdell, 2017). The most extensive remote sensing characterization of HAB dynamics in Oklahoma analyzed HAB frequency for blooms above 100,000 cells/mL from 2008-2011 and 2017 as part of the analysis for the Nutrient Scientific Technical Exchange Partnership Support (N-STEPS) program. This thesis expands on the N-STEPS research. It adds five additional years of high-risk bloom frequency and the characterization of the maximum HAB abundance and spatial extent. This additional information can be instrumental in understanding HAB occurrence and behavior in Oklahoma's largest reservoirs.

Background

Harmful algal blooms (HABs) occur when algal community abundance grows exponentially, potentially producing toxic or adverse effects on organisms that come into contact with them or cause water quality degradation (Lopez et al., 2008; NOAA, 2016). HAB occurrences are increasing nationally and worldwide (Hudnell, 2010). It affects most of the US (Lopez et al., 2008). These blooms are microscopic cellular populations, including dinoflagellates, diatoms, and cyanobacteria (Hudnell, 2010). Cyanobacteria, also known as blue-green algae, are recognized as the leading harmful algal group. They are considered a fast-emerging worldwide issue that threatens both human and ecosystem health (Carmichael, 2008).

Harmful algal blooms vary in appearance. Blooms typically range from light green to darker, browner greens. They can also take on reddish hues (Hudnell, 2010). Cyanobacteria HABS (CyanoHABS) can appear as water discolorations, forming dense scums and mats on the water's surface. They can appear as spilled paint slicks (Hudnell, 2010). Harmful effects from HABs are not limited to when they are visible and can occur even when apparent signs of a bloom are missing (Hudnell, 2010). CyanoHABs cause most freshwater HAB problems (Lopez et al., 2008). Cyanobacteria have developed competitive advantages over their long evolutionary timeline (Hudnell, 2010).

Some species of cyanobacteria can fix nitrogen (Latysheva, Junker, Palmer, Codd, & Barker, 2012; Stal, 2015).Nitrogen fixation is a resource-intensive process and requires sunlight as a source of that energy (Stal, 2011). The ability to fix nitrogen provides a competitive advantage over non-nitrogen fixing species when nitrogen is limiting (Chang et al., 2020). Cyanobacteria also have the ability to regulate their buoyancy. They are able to move up and down within the water column (Oliver & Walsby, 1988). Buoyancy regulation helps cyanobacteria access the sunlight necessary for photosynthesis at the surface of the water while also shading out other

species of phytoplankton (Chang et al., 2020). Cyanobacteria have been shown to grow faster than other benign algal species in warm water (Michalak et al., 2013). Buoyancy regulation and increased growth rate in warm waters can trigger a feedback loop where surface algal mats absorb more sunlight leading to yet warmer waters and more cyanobacteria growth (Sturm & Denchak, 2019).

The causes of cyanobacterial blooms are not well understood (Hudnell, 2010). Chemical and physical factors are believed to play a role in forming blooms. Physical conditions promoting growth include light availability, water temperature, flow, and vertical mixing (US EPA, 2018a). Chemical factors include pH, nutrient loading, and the presence of trace metals (US EPA, 2018a).

HABs are often considered one of the most apparent signals of nutrient over-enrichment (H. W. Paerl & Fulton, 2006). These factors can act synergistically, creating optimal growth conditions, though they vary between the species (Lopez et al., 2008). Particular difficulty remains in understanding how these factors affect bloom dynamics and toxin production (Perovich et al., 2008).

Climate change impacts, including increases in temperature and hydrologic changes, have been theorized to impact HAB occurrence. Prolonged droughts followed by more severe storms have been shown to lead to increased runoff and nutrient loading of waterways (Sturm & Denchak, 2019). Prolonged droughts can also reduce water flow. This results in the remaining water becoming more stagnant and warmer. Stagnant and warmer waters are optimal conditions for HABs to propagate.

HAB Impacts

The impacts of HABs are varied. They can include health hazards for humans and animals as well as water quality degradation (Lopez et al., 2008). Impacts in the US include animal deaths, reduced recreational opportunities, and taste-and-odor problems in drinking water and

aquaculture (Lopez et al., 2008). Mass die-offs of large algal biomass resulting in decomposition can lead to depleted dissolved oxygen (hypoxia) in the water (Lopez et al., 2008).

Many cyanobacteria species produce cyanotoxins as secondary metabolites. The results are potentially fatal (Hudnell, 2010). Cyanotoxins are comprised of a group of compounds that are both chemically and toxicologically diverse (Bláha, Babica, & Maršálek, 2009). Cyanotoxins can be classified as hepatotoxins, neurotoxins, cytotoxins, dermatoxins, or irritant toxins (Bláha et al., 2009; Wiegand & Pflugmacher, 2005). Each cyanotoxin is known to be produced by multiple genera of cyanobacteria. Species can produce two or more types of these toxins (Table 2) (Hudnell, 2010; Humpage, 2008; Pegram et al., 2008). The most common cyanotoxins observed in the US include saxitoxins, cylindrospermopsin, anatoxins, and microcystins (US EPA, 2018b).

Cyanotoxins can be potent, with few other toxins being known to be more potent (Hudnell, 2010; Humpage, 2008). A comparison between the lethal dose for 50% of mice with a single intraperitoneal injection (LD_{50}) for common cyanotoxins and more familiar toxins are found in Table 1. The EPA includes certain cyanotoxins on their Contaminant Candidate List (CCL) version CCL 3 (2009) and CCL 4 (2016) (OW US EPA, 2016). EPA has included specific cyanotoxins in their fourth Unregulated Contaminant Monitoring Rule (UCMR 4) (OW US EPA, 2015). The UCMR is a list of a maximum of 30 unregulated contaminants to be monitored in public water systems (OW US EPA, 2016).

Table 1: Compounds and rodent 24h intraperitoneal LD50 (ug/kg). Adapted from "The state of U.S. freshwater harmful algal blooms assessments, policy and legislation", by Hudnell, K., 2010. *Toxicon*, *55*

Cyanotoxins	LD_{50}	EPA priority	Comparison	LD_{50}
Saxitoxins	10	Medium/High	Ricin	22
Anatoxin-a(s)	20	Medium/High	Cobra Venom	185
Microcystin-LR	50	Highest	Sarin	218
Cylindrospermopsin	300	Highest	Strychnine	980

Microcystins are likely the most prevalent cyanotoxin in freshwater HABs (FHABs) (Bláha et al., 2009; OW US EPA, 2013). Microcystin is a hepatoxin, or a toxin that impacts the liver, and evidence of it acting as a tumor promotion factor (Bláha et al., 2009).

Table 2: Cyanobacterial toxins, taxa, and human health impacts. Adapted from "Scientific assessment of freshwater harmful algal blooms" by Lopez, C. 2008. *Interagency Working Group on Harmful Algal Blooms, Hypoxia, and Human Health of the joint Subcommittee on the Ocean Science and Technology*

Toxin	Genera	Short-Term Health Effects	Long-Term Health Effects
Microcystins	Anabaena, Aphanocapsa, Hapalosphon, Microcystis, Nostoc, Oscillatoria, Planktothrix	Gastrointestinal, liver inflammation, and hemorrhage and liver failure leading to death, pneumonia, dermatitis	Tumor promoter, liver failure leading to death
Saxitoxins	Anabaena, Aphanizomenon, Cylindrospermopsis, Lyngbya	Tingling, burning, numbness, drowsiness, incoherent speech, respiratory paralysis leading to death	Unknown
Anatoxins	Anabaena, Aphanizomenon, Oscillatoria, Planktothrix	Tingling, burning, numbness, drowsiness, incoherent speech, respiratory paralysis leading to death	Cardiac arrhythmia leading to death
Cylindrospermopsin	Aphanizomenon, Cylindrospermopsis, Umezakia	Gastrointestinal, liver inflammation and hemorrhage, pneumonia, dermatitis	Malaise, anorexia, liver failure leading to death

Human illnesses and fatalities have been linked to cyanobacteria across the globe. Two fatality events occurred in Brazil, with 88 deaths in 1988 and 52 deaths in 1996 associated with cyanotoxins in drinking water (World Health Organization, 2003). Gastrointestinal issues have been associated with cyanobacteria in Australia, Canada, China, England, Sweden, and the US (World Health Organization, 2003). No cyanotoxins have been solely tied to human deaths in the US (Lopez et al., 2008). Exposure to CyanoHABs and toxins can occur through direct skin

contact, inhalation, and accidental ingestion for those recreating in or around waterbodies (World Health Organization, 2003). The exposure pathway is frequently through ingestion of contaminated water. Long-term effects from chronic low-level exposure are not well understood nor studied (Lopez et al., 2008).

The ecological impacts of CyanoHABs and their associated toxins are varied. Many impacts occur from high biomass blooms. High biomass blooms have the potential to substantially reduce the light entering the water column and inhibit other primary producer growth, benthic algae, and vascular plants (Fournie et al., 2008). High biomass blooms can result in low dissolved oxygen situations, leading to fish and bottom-dwelling organism kills, anoxia of sediments, increases in ammonium in the water, and the associated pH changes (Fournie et al., 2008; Lopez et al., 2008; H. W. Paerl, Fulton, Moisander, & Dyble, 2001; Rao, Howell, Watson, & Abernethy, 2014). These impacts can lead to food web alterations and subsequent crashes, as cyanobacteria are often unpalatable and of low quality, potentially starving consumers and their predators (Lopez et al., 2008; H. W. Paerl et al., 2001).

These impacts can further be stressed if a bloom has associated toxicity. The relative impact of cyanotoxins when compared to the other stressors remains unclear (Lopez et al., 2008; H. W. Paerl et al., 2001). Cyanotoxins have been shown to accumulate in primary consumers (Prepas, Kotak, Campbell, & Evans, 1997).,This can result in transfers up the food chain (Ferrão-Filho & Kozlowsky-Suzuki, 2011; Lopez et al., 2008).

Cyanotoxins have been deemed responsible for mass fish kills (Landsberg et al., 2020; Rodger, Turnbull, Edwards, & Codd, 1994; Tencalla, Dietrich, & Schlatter, 1994) and bird kills (Stewart, Seawright, & Shaw, 2008). Cyanobacteria were eventually found to be the cause of vacuolar myelinopathy in Bald Eagles in 2021, 25 years after it was first observed in the US. Vacuolar myelinopathy is a neurological diseases that causes brain lesions and had been killing Bald Eagles

after exposure(Breinlinger et al., 2021). Pet deaths have been associated with cyanotoxin exposure across the US ("Dog Days of Summer," 2020). Livestock and cattle have been reported as victims of cyanotoxin exposure. The results include 72 cows out of 170 dying within 24 hours of ingesting cyanobacteria from their water source (Carmichael, 1992; Odriozola, Ballabene, & Salamanco, 1984).

Economic Impacts

Freshwater HABs can result in severe economic costs. The full magnitude of these costs has yet to be well quantified in the US (Lopez et al., 2008). Less than 5% of publications centered on cyanotoxins focus on the economy, public health, or epidemiology (Merel et al., 2013). The economic impacts of HABs arise from "public health costs, commercial fishery and aquaculture closures and fish kills, insurance costs, possible medium and long-term declines in tourism, and the costs of monitoring, management and mitigation" (Figure 1) (Berdalet, 2017). Estimates of HAB economic impacts rarely consider all of these factors together (Morgan, Larkin, & Adams, 2010). Aggregating the economic impacts is problematic in part due to the methodologies of estimating these costs (Berdalet, 2017; Hoagland, Anderson, & Kaoru, 2002). Estimates that include additional drinking water treatment, loss of recreational use, and decline in property values result in an estimated cost of $64 million in the US (Boyer, Danniels, & Melstrom, 2017).

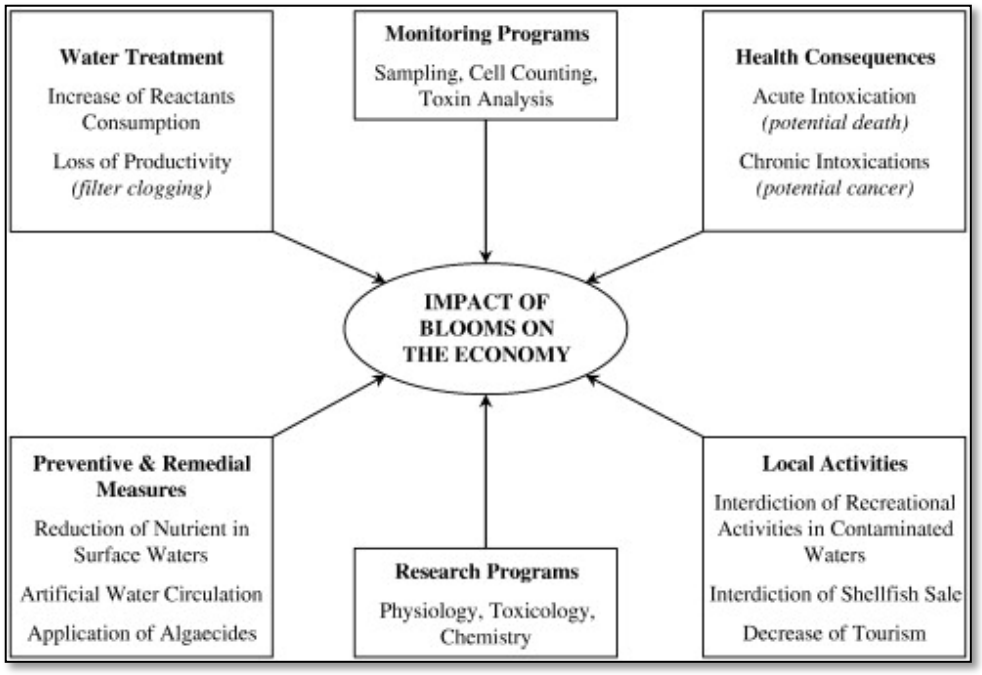

Figure 1: Aspects to consider when assessing the economic impact of blooms. Reprinted from "State of knowledge and concerns on cyanobacterial blooms and cyanotoxins" by Merel, S. 2013. *Environmental International, 59*

Public health impacts comprise the most significant economic losses caused by HABs (Hoagland & Scatasta, 2006), estimated to be approximately 42% of the total impact (Anderson, Hoagland, & Kaoru, 2009; Hoagland et al., 2002). Public health impacts include medical costs, lost wages and work days, and reduced quality of life (Kouakou & Poder, 2019). Healthcare and medication costs associated with respiratory and gastrointestinal impacts following exposure can cost upwards of $12,000-14,000 per incident (Kouakou & Poder, 2019). Lost wages and work days can also result from HAB exposure (Kouakou & Poder, 2019).

HABs can result in fishing and aquaculture losses. Areas surrounding Lake Erie were estimated to lose up to $5.58 million in lost fishing expenditures during summers that experience long-term cyanobacteria blooms (Fisheries, 2021; Wolf, Georgic, & Klaiber, 2017). Thirty four million fish were killed in 33 Texas waterbodies from toxic algae between 1981-2008. They were valued at $14 million (Fisheries, 2021; Southard, Fries, & Barkoh, 2010). Catfish farming in the US is the

largest aquaculture industry valued at over $450 million annually (Lopez et al., 2008). Cyanobacteria can produce compounds resulting in an off-flavor in catfish (Tucker, 2000). Off-flavor fish is the industry's second largest cause of economic loss (Lopez et al., 2008). Estimates show that economic losses due to cyanobacteria could range to $60 million in 1998 prices (Tucker, 2000). Direct mortality of catfish due to toxic microcystins have been documented in the most extreme examples (Zimba, Khoo, Gaunt, Brittain, & Carmichael, 2001).

Cyanobacterial blooms affect tourism detrimentally. The associated costs are often not calculated (Merel et al., 2013). Blooms can result in restrictions on recreational activities, even if they are not toxic. A bloom of *Anabaena* occurred in the Darling River in Australia in 1991. This *Anabaena* bloom was not neurotoxic. The tourism industry still faced an estimated loss of approximately $1.5 million (Steffensen, 2008). Another bloom that same year in New South Wales resulted in a total estimated tourism loss of $6.7 million compared to the previous year, which did not experience a bloom (Steffensen, 2008).

Losses of tourism can also directly impact business demand and property values. A publicized HAB event can lead to reduced tourism, reducing the revenue of local businesses such as restaurants, hotels, and boat tours (Bingham, Kinnell, Bingham, & Kinnell, 2020). These impacts can continue up the supply chain if local businesses buy fewer supplies or employ fewer workers and even impact property values.

An analysis of Lake Erie's HABs on local tourism estimated that Ohio had $66-305 million tourist dollars at risk from HABs. It estimated that Michigan had approximately $25 million in tourism dollars at risk from HABs (Bingham et al., 2020). A 2014 bloom resulted in Toledo, Ohio issuing a do not drink order for 500,000 residents for three days due to the levels of microcystin present (Fisheries, 2021). It was estimated that this resulted in over $10 million (2015 dollars) in losses to shoreline property value services, including drinking water, recreation, and

wildlife habitat (Fisheries, 2021). Lake Erie experienced blooms in 2011 and 2014 estimated to have an average economic loss of $70 million (Berdalet, 2017). The 2011 bloom covered more than 2,000 square miles leading to fouled beaches, a larger anoxic zone, and impacted fish populations (Erickson, 2013). Economists have estimated that if the 67 beaches on Lake Erie had to close due to HABs, over $2 million would be lost each day (Fisheries, 2021)., Home prices were shown to increase by 2% or roughly $2,000 based on median home price when algal levels (chlorophyll-a used as a proxy) were reduced in Lake Erie (Fisheries, 2021).

HAB advisories alone have been shown to impact tourism in Oklahoma. A survey of Grand Lake visitors in 2015 revealed that 25% of respondents would have canceled a visit if a "no bodily contact" warning was issued prior to their trip. Twenty percent of those indicated that they would not visit at a later date after the advisory (Boyer, Danniels, et al., 2017). A study of Oklahoma state parks showed a 19% decrease in visitation to lakes during the month that a blue-green algae (BGA) warning was issued (Boyer, Danniels, et al., 2017). Analysis of the impacts of the 2011 BGA advisories for Lake Texoma estimated a loss of $45 million in lost sales and tourism-related activities (Boyer, Danniels, et al., 2017). This loss equates to roughly 8% or almost one month of tourism business for the lake.

Complete analysis of the economic impacts of HABs in Oklahoma is difficult to capture, particularly when events such as the 2013 HAB event wiping out the fishery at Altus-Lugert Lake occur (Boyer, Danniels, et al., 2017). Estimating the total loss is difficult because it is hard to place a value on sport fish. The Oklahoma Secretary of the Environment in 2011 created a committee that determined monitoring once a month at just the 100 largest reservoirs across the state would cost over $3.5 million a year (Smithee, Cauthron, Wright, Armstrong, & Gillilans, 2012).

Legislation

Initial government focus on HABs was centered on oceans, estuaries, and the Great Lakes. Legislation led to the creation of the National Research Plan for Coastal Harmful Algal Blooms in 1998. There was no national research plan for freshwater HABs (FHABs). Most of the research came from individual projects without a concerted effort (Lopez et al., 2008). Federal policy and guidelines have yet to be developed for FHABs. Many states and localities rely on guidance from the World Health Organization concerning risk management and control of FHABs (Lopez et al., 2008).

There has been more focus on FHAB research across the nation in recent years. Congress reauthorized the Harmful Algal Bloom and Hypoxia Research and Control Act with amendments to include freshwater HABs in 2004 (HABHRCA, 2004). The new legislation required the creation of a report titled, *Scientific Assessment of Freshwater Harmful Algal Blooms*. This report aspired to 1) examine the causes, consequences, and economic costs of freshwater HABs, 2) establish priorities and guidelines for a research program on freshwater HABs, and 3) make recommendations to improve coordination among Federal agencies with respect to research on HABs in freshwater environments (Lopez et al., 2008).

The reauthorized legislation required a National Research Plan to reduce HAB occurrence and impacts to be developed (Hudnell, 2010). The HAB Research, Develop, Demonstrate and Technology Transfer Plan was created. It was designed to prevent, control, and mitigate blooms within the US ("HABHRCA," 2017; Hudnell, 2010). Additional programs funded under the HABHRCA include the Ecology and Oceanography of Harmful Algal Blooms (ECOHAB); Monitoring and Event Response for Harmful Algal Blooms (MERHAB); Prevention, Control, and Mitigation of Harmful Algal Blooms (PCMHAB); Gulf of Mexico Ecosystems and Hypoxia Assessment (NGOMEX); and the Coastal Hypoxia Research (CHRP) ("HABHRCA," 2017).

The Congressional committees involved with HABHRCA did not have the authority to authorize funding for EPA or to mandate that the EPA create a research plan focused on FHABs (Hudnell, 2010). This presented a problem for implementing such plans, as the EPA is the agency that oversees all US freshwaters under the Clean Water Act (2002) and Safe Drinking Water Act (2002) (Hudnell, 2010). Recent HABHRCA amendments in 2014 and 2017 required NOAA and the EPA to "advance the scientific understanding and ability to detect, monitor, assess, and predict HAB and hypoxia events" in freshwaters (US EPA, 2021b). The amendments also granted the EPA the statutory authority to declare if a HAB or hypoxia event in freshwater is an event of national significance (OW US EPA, 2021). A 2019 amendment required the EPA HAB task force to conduct a scientific assessment of HABs in the US at least every five years. The first report is due in 2024 (US EPA OIG, 2021).

Nationwide standards and guidance were still missing despite these amendments. An assessment by the EPA's Office of Inspector General in 2021 found that the EPA still lacked an agency-wide strategic action plan to address HABs (US EPA OIG, 2021). The assessment determined, that while the EPA is working on HABs on many fronts,EPA must coordinate the efforts across the whole agency at national, regional, and local levels to avoid duplication of efforts, facilitate information exchange, and further advance Agency efforts to address HABs (US EPA OIG, 2021). The EPA's OIG recommended that any agency-wide strategic plan should incorporate strategies for (1) closing identified knowledge gaps; (2) monitoring and tracking HABs; (3) enhancing the EPA's leadership role in addressing freshwater HABs; (4) coordinating EPA activities internally and with states; and (5) establishing additional criteria, standards, and advisories, as the scientific information allows (US EPA OIG, 2021). The Agency responded with an expected completion date of April 2023 for an agency-wide strategic plan (US EPA, 2021).

Remote Sensing and Cyanobacteria

Remote sensing (RS) is the process of detecting and monitoring the physical characteristics of an area by measuring it's reflected and emitted radiation at a distance, most often from satellite or aircraft (USGS, 2015). Sensors detect emitted or reflected light from the target object. Earth features can reflect, absorb, transmit, and emit electromagnetic (EM) energy ("Geospatial Technology," 2023). A sensor can then measure that feature's radiance, or the amount of light the sensor captures.

The electromagnetic spectrum is comprised of the range of frequencies, wavelengths, and energy of electromagnetic radiation. The sun produces energy across the full spectrum (NASA, 2016). Humans can only see a small portion of the spectrum. This is termed visible light (Figure 2). All objects produce a unique spectral response curve which is the magnitude of EM energy reflected or emitted from an object across a range of wavelengths (DiBiase, 2018). These patterns and their relationship to each other allow objects to be accurately identified from RS techniques. Variables including atmospheric absorption, atmospheric scattering, sun glint, and others can impact what the sensors detect and lead to erroneous data. Attempts to mitigate these impacts are often required. This includes atmospheric and radiometric corrections and the proper understanding of the sensors' characteristics and capabilities.

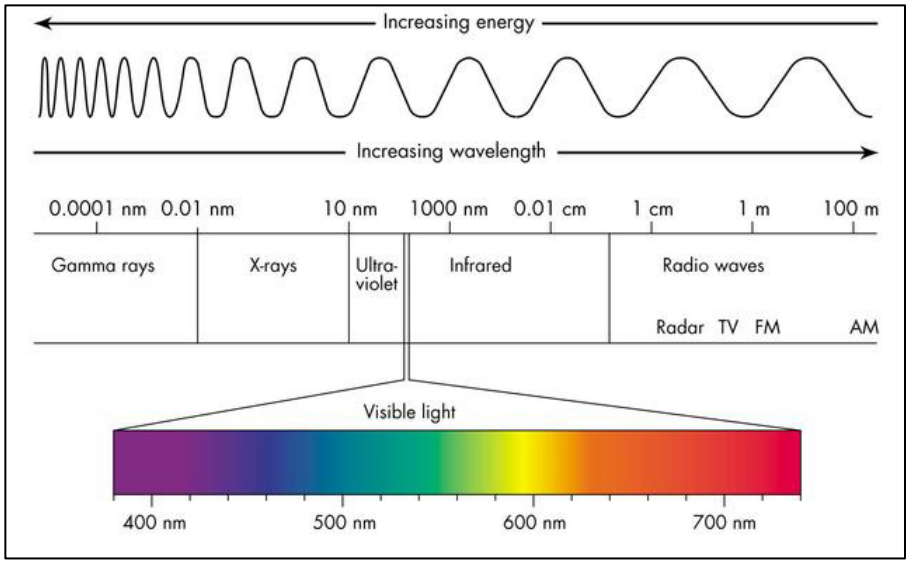

Figure 2: Electromagnetic Spectrum. Reprinted from Electromagnetic Spectrum by Franson, J. 2017. Principals of Structural Chemistry.

Cyanobacteria produce a unique spectral response curve which is used for detection and monitoring purposes. Most RS methods for detecting and estimating bloom biomass utilize algorithms that rely on chlorophyll-a (Chl-a) and phycocyanin (PC) (Kutser, 2004; L. Li, Li, Shi, Li, & Song, 2012; S. Mishra, Mishra, Lee, & Tucker, 2013; Shi, Zhang, Qin, & Zhou, 2019). Chlorophyll-a has long been used as one of the primary phytoplankton pigments for bloom indication. It is present in all phytoplankton communities and not just cyanobacteria. Chl-a exhibits noticeable peaks at approximately 440 nm (blue light) and 675 nm (red light) (Figure 3) (Shi et al., 2019). Chl-a can be derived accurately from the absorption peak in the blue wavelengths in ocean waters (Shi et al., 2019). This approach can fail in inland waters due to impacts from colored dissolved organic matter (CDOM) and detritus that interfere with the necessary spectral region (Gitelson et al., 2008; Shi et al., 2019; Stumpf et al., 2016a). Alternative approaches to Chl-a estimation have been developed leveraging the red and near-infrared (NIR) wavelengths (Gitelson et al., 2008; Kudela et al., 2015; Matthews, Bernard, & Robertson, 2012).

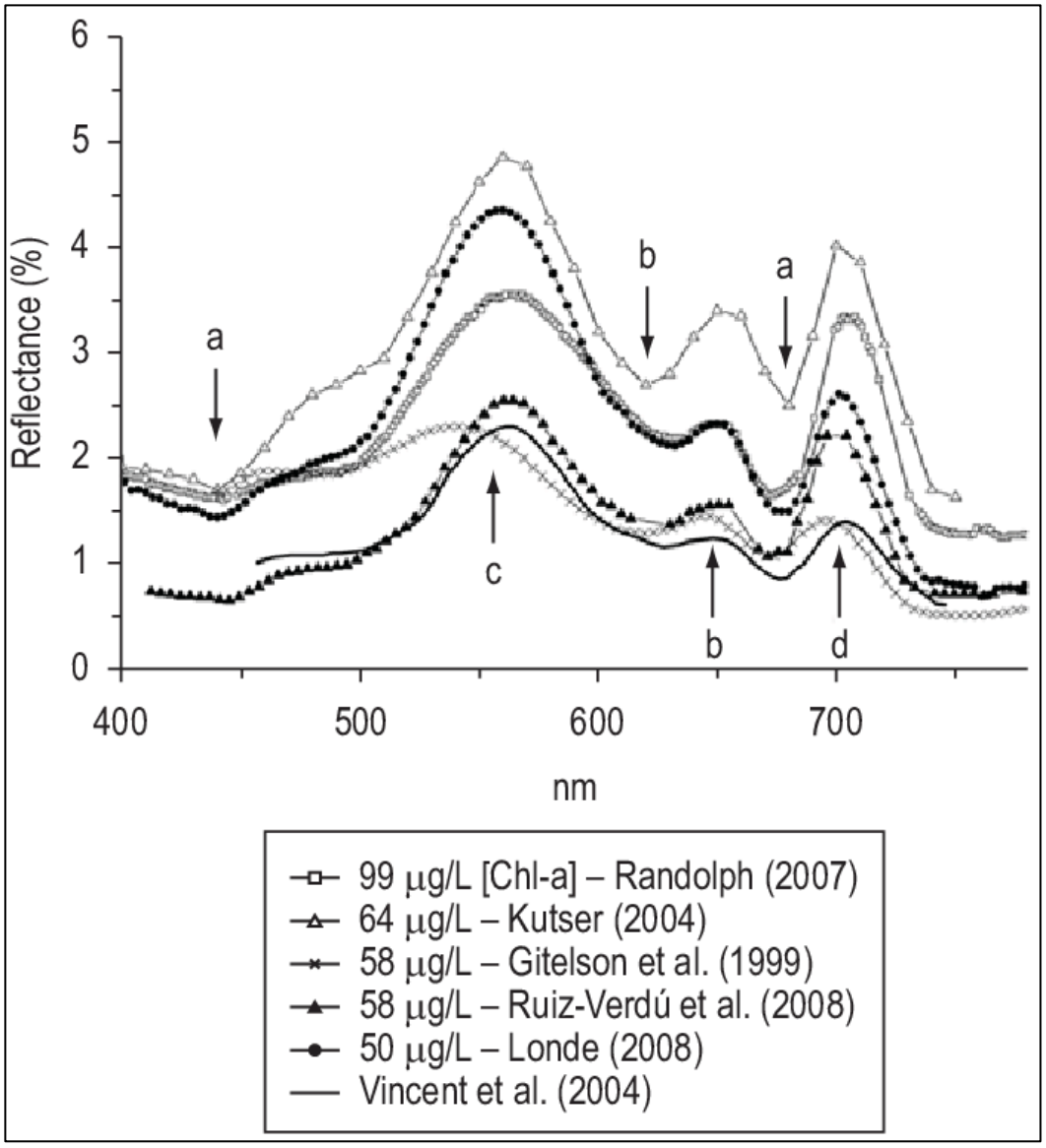

Figure 3: Spectral curves obtained at different regions and with several methods presented common cyanobacteria features: a) Chl-a absorption at 440 and 675 nm; b) phycocyanin absorption at 620 nm and fluorescence at 650 nm; c) scattering in the green region; d) near-infrared scattering by phytoplankton cells. Reprinted from "Mapping potential cyanobacterial bloom using Hyperion/E)-1 data in the Patos Lagoon estuary" by Lobo, F. 2009.

Chl-a-only algorithms are limited as Chl-a cannot differentiate between all phytoplankton communities and those specific to cyanobacteria. PC is unique to freshwater cyanobacteria (Shi et al., 2019). PC exhibits a distinct absorption signature at approximately 620 nm (Figure 3) that a spectral band centered around 615-630nm can quantify (L. Li et al., 2012; S. Mishra et al., 2013; Randolph et al., 2008; Ruiz-Verdú, Simis, de Hoyos, Gons, & Peña-Martínez, 2008)

CHAPTER II

LITERATURE REVIEW

The 1970s marked the beginning of remote sensing (RS) applications in regards to water (Yang et al., 2022). The increased spatial and temporal coverage offered through remote sensing technologies has dramatically increased our ability to evaluate the dynamic nature of many water quality parameters (Yang et al., 2022). Standard water quality parameters assessed with remote sensing include total suspended matter (TSM) or turbidity; Secchi disk depth (SDD); colored dissolved organic matter (CDOM); chlorophyll-a (Chl-a); water temperature; sea surface salinity (SS); dissolved oxygen (DO); biochemical oxygen demand (BOD); nutrients including total nitrogen (TN) and phosphorous (TP); and land use changes that may impact waterbodies (Gholizadeh, Melesse, & Reddi, 2016; Lee, Orne, & Schaeffer, 2014; Ritchie, Zimba, & Everitt, 2003; Yang et al., 2022).

Focus was placed on the remote sensing of HABs in line with the development of RS technologies and algorithms for water quality parameters (Y. Li, Zhou, Zhang, Li, & Shi, 2021). The first use of satellite observations to detect HABs came after the launch of the Coastal Zone Color Scanner (CZCS) in 1978. They were able to detect a bloom in the Gulf of Mexico (L. Shen, Xu, & Guo, 2012). Only a few published studies existed using CZCS until the 21st century (Khan et al., 2021). The launch of the Sea-viewing Wide Field-of-view Sensor (SeaWiFS) in 1997 significantly contributed to the increase in HAB studies and monitoring capabilities that arose in the early 2000s (L. Shen et al., 2012).

Marine remote sensing has seen significant financial contributions from international organizations and varying space agencies (Stephanie C. J. Palmer, Kutser, & Hunter, 2015). This resulted in robust programs. One such program includes the International Ocean Color Coordinating Group (IOCCG). This program helps to coordinate and synthesize worldwide efforts and establish research agendas (S. C. J. Palmer et al., 2015). Inland remote sensing of freshwater HABs received much less attention and coordination until more recently (Lopez et al., 2008). FHABs were considered more of a local or regional problem. They were susceptible to falling through gaps in regards to funding (Stephanie C. J. Palmer et al., 2015). A bibliometric analysis of approximately 1,300 peer-reviewed articles published between 1999-2019 revealed that 85% of publications were marine focused (60% coastal, 25% open ocean), with inland environments comprising 14% of the research (Sebastiá-Frasquet et al., 2020).

The trajectory of RS applications in inland waters differs from that of ocean and terrestrial RS advancements (Topp, Pavelsky, Jensen, Simard, & Ross, 2020). A bibliometric analysis of the patterns and trends of RS studies was conducted in 2020. This analysis illustrated that the method development of oceanic and terrestrial RS that occurred in the 1970s led to publications focused on understanding spatially expansive, complex processes as early as the mid-1980s (Topp et al., 2020). Inland waters did not show such a progression. Inland water RS experienced a 30-year period where the majority of the publications focused primarily on developing models and validating those efforts (Topp et al., 2020). The early 2000s marked the start of rapid increases in RS publications (Y. Li et al., 2021). This increase included the advancement from a model and algorithm focus for inland waters to research that attempted to address spatiotemporal trends, drivers, and the impacts of altered water quality in regard to human and ecosystem health and functioning (Y. Li et al., 2021; Topp et al., 2020).

The past 10-15 years have seen significant advances in computing resources, longer and more frequently obtained datasets, and improved operational RS algorithms (Topp et al., 2020). This

has led to an increased understanding of the complicated and varied nature of inland water systems (Topp et al., 2020). Inland water RS studies have exhibited increasing trends since 2010 (Sebastiá-Frasquet et al., 2020).

Initial uses of remote sensing for HAB detection were limited to coastal and ocean uses (Stephanie C. J. Palmer et al., 2015). These ocean sensors typically had such a large spatial resolution that they were considered unsuitable for monitoring most inland waterbodies except for the largest (Stephanie C. J. Palmer et al., 2015). Ocean color sensors such as Moderate Resolution Imaging Spectroradiometer (MODIS), Medium Resolution Imaging Spectrometer (MERIS), SeaWiFS, and CZCS were initially used for inland waters (Topp et al., 2020). Sensors designed for terrestrial applications were incorporated more into inland water RS later and continue to be used (Stephanie C. J. Palmer et al., 2015). Each sensor has its own applicability based on the sensors' spatial, temporal, spectral, and radiometric resolutions (Topp et al., 2020). Ocean sensors typically have a coarse spatial resolution (300-1000m), but a finer temporal resolution (~1 day) (Olmanson, Brezonik, & Bauer, 2011; Topp et al., 2020). These resolutions can make them more suitable for large-scale processes that change quickly. Terrestrial sensors typically offer a much finer spatial resolution (10-30m), but a much more infrequent return interval (1-2 weeks) (Olmanson et al., 2011). All sensor choices involve tradeoffs. A relatively small subset of researchers have leveraged commercial sensors, including IKONOS and Worldview 2, that offer high spatial resolution (Dvornikov et al., 2018; Sawaya, Olmanson, Heinert, Brezonik, & Bauer, 2003; Topp et al., 2020).

Historical and Current Sensors

Research designed to analyze HABs has utilized a variety of satellite sensors from their inception to present. The first sensor used was the CZCS. CZCS was operational from 1978-1986 (IOCCG, 2023). CZCS had a spatial resolution of 825m and six spectral bands (443nm, 520nm, 550nm,

670nm, 750nm, and 11.5μm) (IOCCG, 2023). Five of these bands resided in the most common HAB spectral region. This resulted in the first chance to detect HABs (Topp et al., 2020). CZCS's delayed data collection and processing capabilities reduced its HAB applicability due to the ephemeral nature of blooms.

The next generation of ocean sensors included NASA's Sea-viewing Wide Field of View Sensor (SeaWiFS). SeaWiFS was operational from 1997-2010 (Shen et al., 2012). SeaWiFS significantly improved HAB detection by adding four spectral bands. These bands included bands more sensitive to chlorophyll variation and those better suited for atmospheric correction (L. Shen et al., 2012). SeaWiFS was better suited to capturing bloom dynamics due to its fine temporal frequency capturing daily imagery (NASA, 2020).

SeaWiFS data has been used for many studies. These studies include chlorophyll-a estimation, dissolved organic carbon (DOC), and total suspended sediment estimates (Dvornikov et al., 2018; Heim, Oberhaensli, Fietz, & Kaufmann, 2005; Korosov, Pozdnyakov, Pettersson, & Grassl, 2007; Stephanie C. J. Palmer et al., 2015; D. Pozdnyakov, Korosov, Grassl, & Pettersson, 2005; D. V. Pozdnyakov, Korosov, Petrova, & Grassl, 2013). SeaWiFS was the most used satellite sensor from 2000-2015. It used in 49% of RS studies during this timeframe (Sebastiá-Frasquet et al., 2020).

SeaWiFS still had its limitations. SeaWiFS lacked a spectral band in the 683nm range where chlorophyll florescence peaks (Shen et al., 2012). SeaWiFS also suffered from a lack of in-situ validation, limiting its potential accuracy of HAB detection (L. Shen et al., 2012). Reinart and Kuster (2006) examined the limitations of the applications of SeaWiFS data. Those limitations include its coarse temporal resolution which was greater than 1000m (Reinart & Kutser, 2006). This spatial resolution primarily limited it to coastal applications.

MODIS represented the third generation of sensors. MODIS was first launched in 1999 on the Terra satellite (NASA, 2023a). MODIS was launched again on the Aqua satellite in 2002. MODIS remains operational today (NASA, 2023a). It collects 36 spectral bands with varying spatial resolutions (L. Shen et al., 2012). Bands 8-16 (405-877nm) are the most suitable for HAB detection. These bands have a spatial resolution of 1,000m (NASA, 2023a). MODIS data has been consistently used for HAB detection (Bergamino et al., 2010; Chavula, Brezonik, Thenkabail, Johnson, & Bauer, 2009; Hu et al., 2010; Moradi, 2014; Y. Zhang et al., 2015). It was the second most used sensor between 2005-2017 (Sebastiá-Frasquet et al., 2020). This sensor is known to suffer from solar flare influence, as it does not tilt the sensor track. MODIS does not tilt the sensor track because it was designed for observations including the atmosphere and land, not just the ocean (L. Shen et al., 2012).

MERIS was launched in 2002 by the European Space Agency (IOCCG, 2023). It is a third generation ocean sensor (IOCCG, 2023; L. Shen et al., 2012) that remained operational through 2012. It collected 15 spectral bands (350nm-1,040nm) (L. Shen et al., 2012) and had a much finer spatial resolution of 300m (European Space Agency, 2021). The finer spatial resolution of MERIS significantly improved the number of waterbodies that could be observed. This improved the observation of temporal and spatial water quality and HAB patterns (Tyler et al., 2016). MERIS has been shown capable of extracting more fluorescence information than MODIS (L. Shen et al., 2012). MERIS had spectral bands more suitable for HAB detection and identification than MODIS (Koponen et al., 2007; Reinart & Kutser, 2006). It was a commercial satellite. These commercial costs limited the data availability for HAB studies and researchers (L. Shen et al., 2012).

The Ocean Land Colour Imager (OLCI) sensor is part of the newest generation of ocean sensors. OLCI was first launched in 2016 on the Sentinel-3A platform (NASA Ocean Biology Processing Group, 2020). Its key mission driver was the continuation of MERIS instrument capabilities

(European Space Agency, 2023b). Key advancements were made between these sensors. OLCI captures 21 spectral bands (European Space Agency, 2023b). This is an increase from the 15 bands MERIS captured. These bands are suitable for inland waters (400-1020nm) (Topp et al., 2020). OLCI retains a finer spatial resolution of 300m and a significantly finer temporal frequency. OLCI initially offered a less than three-day return interval. This was shortened to a roughly one-day return interval with the launch of an additional OLCI sensor aboard Sentinel-3B in 2018 (European Space Agency, 2023b). This contrasts with MERIS's return time of approximately 15 days. OLCI added a spectral band at 673nm. This band was chosen to improve chlorophyll fluorescence measurements (European Space Agency, 2023b). OLCI reduced sun-glint contamination by tilting its cameras. The OLCI sensors now represent one of the primary sensors used for inland water remote sensing (M. Shen et al., 2017).

Sensor selection involves weighing the tradeoffs between sensors. These tradeoffs are associated with sensors varying spectral, temporal, and spatial resolution. The spectral band locations and widths are typically the most crucial aspect for HAB detection. Spectral band location and width control the detection algorithms that can be chosen (Liu, Glamore, Tamburic, Morrow, & Johnson, 2022). Comparisons of applicability and limitations between sensors have been conducted for many scenarios. These include bloom detection in the Baltic Sea (Reinart & Kutser, 2006) and southern Caspian Sea (Moradi, 2014), lake water quality assessments (Olmanson et al., 2011), and HAB detection in small-medium waterbodies (Liu et al., 2022).

Remote Sensing Challenges

Detecting and characterizing HABs offers several challenges in marine and freshwater environments. HABs can exhibit significant spatial heterogeneity (Kutser, 2009). A pixel size of 300-1,000m likely captures an area that has variation in HAB abundance. This is likely not represented in the data. Satellite sensors can only detect blooms roughly two meters into the water

column in clear water (D. R. Mishra, Narumalani, Rundquist, & Lawson, 2005). Detection depth is greatly reduced with increasing turbidity (Coffer, Schaeffer, Foreman, et al., 2021; T. Wynne, Stumpf, Tomlinson, & Dyble, 2010). Cyanobacteria species, including *Microcystis,* have the mechanisms to control their buoyancy (Mishra et al., 2019). They will be found near the surface when there is minimal water column mixing (S. Mishra et al., 2019; Timothy T. Wynne & Stumpf, 2015). Mixing of the water column can greatly increase the uncertainty around abundance and biomass estimates (S. Mishra et al., 2019; Stumpf, Wynne, Baker, & Fahnenstiel, 2012). Wind-driven mixing is a significant contributor. Water column mixing can result in the majority of a blooms biomass failing to get captured (S. Mishra et al., 2019; Stumpf et al., 2012).

Inland water remote sensing contains challenges not present in the marine environment. Inland waters are considered to be dynamic, highly optically-complex systems (Morel & Prieur, 1977; Tyler et al., 2016). Water quality parameters including suspended particles and detritus and colored dissolved organic matter (CDOM) further contribute to this complexity (Mouw et al., 2015; Stephanie C. J. Palmer et al., 2015; Shi et al., 2019). Terrestrial impacts including bottom reflectance, and land adjacency effects play a role (Mouw et al., 2015; Palmer, Kutser, et al., 2015). These factors rarely co-vary over space and time (Mouw et al., 2015; Stephanie C. J. Palmer et al., 2015; Shi et al., 2019). This makes them significantly more difficult to consistently correct for in the imagery. Inland waters require more challenging atmospheric corrections (Tyler et al., 2016). Atmospheric impacts can further impact the operation and performance of selected in-water algorithms (Stephanie C. J. Palmer et al., 2015).

Suspended particulate matter (SPM) in inland waters can complicate RS algorithm performance. SPM reduces the light passing through a water column. This leads to decreasing transparency as SPM concentrations increase (Dörnhöfer & Oppelt, 2016). It also increases the water leaving radiance through its scattering of light (Giardino et al., 2015).

CDOM is a product of decaying material ("Chromophoric Dissolved Organic Matter," 2022). It may come from allochthonous or autochthonous sources (Brezonik, Olmanson, Finlay, & Bauer, 2015). This material strongly absorbs shorter wavelengths of light (blue and ultraviolet) (Nguy-Robertson, Li, Tedesco, Wilson, & Soyeux, 2013). It alters the spectral distribution of the radiation in the water while also causing light attenuation with increasing concentration (Nguy-Robertson et al., 2013). CDOM can impact accurate estimations of Chl-a (Zhu et al., 2014). This is a particular problem when ocean algorithms utilizing a blue spectral band are used (Zhu et al., 2014).

Bottom reflectance can impact the quantity and spectral nature of the light being reflected from a waterbody (Cannizzaro & Carder, 2006). It is impacted by depth and substrate composition (Mouw et al., 2015). Bottom reflectance can pose a particular problem in optically shallow waters. Many bloom detection algorithms were primarily developed in ocean environments where bottom reflectance does not factor in. This makes many of those algorithms unsuitable for inland waters (Mouw et al., 2015). The contamination from bottom reflectance has been shown to produce drastically overestimated chlorophyll concentrations (Barnes et al., 2013; Cannizzaro & Carder, 2006; Carder, Cannizzaro, & Lee, 2005). It often varies within and between waterbodies (Mouw et al., 2015). Work has been done to help mitigate bottom reflectance impacts by utilizing spectral bands between 600-650nm (Barnes et al., 2013).

Atmospheric corrections over inland waters require more complicated correction algorithms than those applied to marine environments. Nearby land can produce adjacency effects. This occurs when light reflected from land surfaces is scattered by atmospheric components and enters a sensor's field of view (Paulino et al., 2022; Richter, Bachmann, Dorigo, & Muller, 2006). Scattered light can alter the water's spectral reflectance. It is particularly a problem in smaller waterbodies (Paulino et al., 2022). The impact from adjacency effects and their magnitude can vary wildly between waterbodies. They depend on surrounding land cover, shape and size of the

waterbody, sensor characteristics, and the atmosphere composition, including aerosols (Paulino et al., 2022). This often results in pixels near land being masked (Mouw et al., 2015). Masking pixels can help reduce erroneous information but results in a loss of observations about a critical portion of many inland waterbodies.

Aerosols around inland waters include smoke, dust, and emissions (e.g. NO_2 and CO_2) (Dörnhöfer & Oppelt, 2016). They further complicate atmospheric corrections (Dörnhöfer & Oppelt, 2016; Mouw et al., 2015). No reasonable means for correcting aerosol effects have been developed (Mouw et al., 2015). This is due to a lack of aerosol vertical distribution information (Gordon, 1997). Aerosols such as NO_2 have been demonstrated to vary significantly over the span of less than a day (Fishman et al., 2012). This would require almost simultaneous in situ sampling to apply to atmospheric corrections (Fishman et al., 2012; Herman et al., 2009; Mouw et al., 2015). Work is being conducted to further the development of algorithms that account for atmospheric corrections and adjacency effects (Kiselev, Bulgarelli, & Heege, 2015; Sterckx, Knaeps, Kratzer, & Ruddick, 2015).

Algorithms

HAB detection algorithms are developed based on the bio-optical factors related to HABs. These bio-optical factors include Chl-a, phycocyanin, and CDOM (Liu et al., 2022; Tao et al., 2013). Bio-optical algorithms can range widely in complexity. The most common algorithms in use today for inland waters include empirical and semi-empirical algorithms, semi-analytical algorithms, and the rising use of machine learning algorithms (Liu et al., 2022; Topp et al., 2020).

Empirical algorithms are most commonly used in inland remote sensing (Topp et al., 2020). Empirical models fit a standard linear regression between the spectral bands and in-situ water samples. These empirical models can struggle with increasing spatial and temporal scales that exhibit large variability in spectral patterns of the bio-optical factors (Topp et al., 2020).

Empirical algorithms perform best within the range of input data (Topp et al., 2020). They are typically simplistic, easy to understand, and have minimal computation requirements (Topp et al., 2020). This leads them to be chosen often for use in these applications.

Semi-empirical models utilize multi-band index values (Topp et al., 2020). These are designed to reduce confusion from non-interest constituents while enhancing the spectral properties of the parameter of interest (Topp et al., 2020). Common semi-empirical indexes include the normalized difference chlorophyll index (NDVI) (S. Mishra & Mishra, 2012), maximum chlorophyll index (MCI) (Gower, King, Borstad, & Brown, 2005), and the floating algal index (FAI) (Hu, 2009; Topp et al., 2020). Semi-empirical models are generalizable, but require the measurement of specific wavelengths to capture the absorption peaks (Topp et al., 2020). This restricts their application to sensors with appropriately located bands and spectral resolution (Topp et al., 2020).

Semi-analytical models are physics-based (Topp et al., 2020; Tyler et al., 2016). They are driven by the relationships between the water's and atmosphere's inherent optical properties (IOPs) (Topp et al., 2020; Tyler et al., 2016). Semi-analytical models incorporate in-situ measurements for model parameterization (Topp et al., 2020). They are the most used physics-based algorithm for inland waters (Topp et al., 2020). Theoretical absorption and scattering features are modeled in relation to the apparent optical properties. These include illumination conditions, field of view, and sensor orientation (Topp et al., 2020). Inversion techniques can then be utilized to estimate the water quality constituents (Tyler et al., 2016). Full analytical models are rarely used for complex inland waters (Topp et al., 2020). The number of water constituents in inland waters becomes increasingly difficult to model (Topp et al., 2020).

Machine learning methods have been developed as computational capacity and available data have increased over the past several years (Liu et al., 2022; Topp et al., 2020). The use of machine learning algorithms in optically complex waters has primarily utilized neural network

techniques (Doerffer & Schiller, 2007; González Vilas, Spyrakos, & Torres Palenzuela, 2011; Liu et al., 2022; Tyler et al., 2016). Other machine learning techniques include support vector machines (Matarrese et al., 2008), mixture density networks (Pahlevan et al., 2020), random forest/boosted regression trees (Lin, Novitski, Qi, & Stevenson, 2018), and hybrid active learning models (Taheri Shahraiyni et al., 2009; Tyler et al., 2016).

Machine learning models have shown good prediction and detection capabilities (Odermatt, Giardino, & Heege, 2010; Tyler et al., 2016). They are still limited as they require extensive and representative training sets and validation (Liu et al., 2022; Stephanie C. J. Palmer et al., 2015; Tyler et al., 2016). Their algorithms can fail to provide accurate results in local and non-typical systems (Liu et al., 2022; Stephanie C. J. Palmer et al., 2015; Tyler et al., 2016).

Availability of in-situ measurements temporally coincident with satellite overpasses remains one of the biggest challenges to algorithm development and validation for optically complex waterbodies (L. Shen et al., 2012). Traditional in-situ monitoring typically only encompasses a limited spatial coverage and frequency for many inland waters (Stephanie C. J. Palmer et al., 2015). In-situ data is entirely absent for many inland waterbodies (Stephanie C. J. Palmer et al., 2015). Access to in-situ data restrained to a handful of lakes can bias algorithm development and validation studies (Stephanie C. J. Palmer et al., 2015). This can bias algorithms to the optical properties of those specific waterbodies that have available in-situ data (Stephanie C. J. Palmer et al., 2015). Increased coordination to compare algorithms and clarification of the strengths and limitations of the different algorithms are still needed (Mouw et al., 2015).

Cyanobacteria Assessment Network (CyAN)

CyAN represents a multi-agency collaboration between the United States Environmental Protection Agency (EPA), the National Aeronautics and Space Administration (NASA), the National Oceanic and Atmospheric Administration (NOAA), and the United States Geologic

Survey (USGS) (ORD US EPA, 2014b). The agencies' goals were to develop a consistent nation-wide remote sensing system for the identification of harmful cyanobacteria blooms. The CyAN project officially started in October 2015.

CyAN was designed to support the management and public use of lakes and reservoirs (ORD US EPA, 2014b; Werdell, 2015). The CyAN project characterizes the exposure and human health impacts from recreational and drinking waters. It also helps identify surrounding landscape factors hypothesized to impact cyanobacterial blooms in freshwater systems (ORD US EPA, 2014b).

Management of cyanobacterial blooms varies between states (Werdell, 2015). Certain states have their own monitoring programs. Vermont has a Cyanobacteria tracking program ("Cyanobacteria (Blue-Green Algae) Tracker," 2016). Indiana monitors cyanobacteria across the state through Indiana's Department of Environmental Management (Algae, 2021).

Some states conduct only sporadic, or deemed as needed, sampling and monitoring. This results in a patchwork of detection and response strategies across the US (Werdell, 2015). Access to frequent and consistent data is considered one of the most significant issues facing water resource managers (Werdell, 2015).

One of CyAN's goals is to provide user-friendly data structures that non-specialists are able to analyze and act upon (Schaeffer et al., 2018; Werdell, 2015). Past methods for disseminating satellite imagery to water resource managers were often cumbersome (Werdell, 2015). CyAN offers data in an easy-to-use format. This increases the ability of managers to identify waterbodies experiencing a bloom and analyze annual and seasonal patterns (Werdell, 2015).

CyAN data are provided to managers after post-processing. This removes a challenging step for many non-specialists. CyAN data is processed through NOAA's automated satellite processing system (ORD US EPA, 2014b). This system incorporates the NASA standard ocean color

satellite processing software found in NASA's SeaWiFS data analysis system (SeaDAS) (ORD US EPA, 2014b). SeaDAS is a free, open-source software designed for the processing, display, analysis, and quality control of a wide array of satellite data (Schaeffer et al., 2018).

Initial CyAN algorithm development utilized the MERIS archive of imagery from 2002-2012 (ORD US EPA, 2014b). These algorithms were based on the cyanobacteria monitoring program for Lake Erie (Lunetta et al., 2015). Lake Erie has the longest-running monitoring program in the US (Lunetta et al., 2015). It primarily uses the Cyanobacterial Index (CI) (Wynne et al., 2010).

The CI utilizes a second derivative spectral shape algorithm centered on the 68nm band in MERIS imagery (T. Wynne et al., 2010; T. T. Wynne et al., 2008). Second derivative algorithms have been shown to function well even with subpar or minimal atmospheric corrections (Philpot, 1991). Validation efforts were undertaken to evaluate the algorithms applicability across the US (CyAN, 2022). These efforts started in the eastern US (Lunetta et al., 2015).

The algorithm for cyanobacteria detection that utilizes a spectral shape (SS) equation is:

$$SS(\lambda) = R(\lambda) - R(\lambda^{-}) + \{R(\lambda^{-}) - R(\lambda^{+})\} * \frac{(\lambda - \lambda^{-})}{(\lambda^{+} - \lambda^{-})}$$

where λ=681nm, λ^{-}=665nm, and λ^{+} = 709nm following Wynne et. al., 2008. R is the Rayleigh-corrected reflectance (Lunetta et al., 2015). This results in a Cyanobacterial Index (CI) = -SS(681) (Lunetta et al., 2015). Cyanobacteria have been observed to have negligible fluorescence (Seppälä et al., 2007). This results in a dip at 681nm due to strong chlorophyll absorption that results in the negative SS(681) (Binding, Greenberg, Jerome, Bukata, & Letourneau, 2011; Lunetta et al., 2015). This CI algorithm provided strong cell count estimates of the primarily *Microcystis* spp. cyanobacterial blooms in Lake Erie (Wynne et al., 2010).

The algorithm was updated to include exclusionary criteria (CI_{cyano}) (US EPA, 2022). This was done to help remove other erroneously identified blooms that were not cyanobacteria, such as

chlorophytes (T. Wynne et al., 2013). Updates include using spectral bands centered around λ=665nm, λ^-=620nm, and λ^+=681nm to exclude non-cyanobacterial blooms producing the SS(665) (Lunetta et al., 2015). The band centered at 620 nm is sensitive to phycocyanin. Increased phycocyanin reduces the reflectance at 620nm (Simis, Peters, & Gons, 2005) producing a positive SS(665) (Lunetta et al., 2015). Cyanobacteria are presumed absent when the CI SS(665)<0 and present when SS(665)>0 (Lunetta et al., 2015).This helps to reduce non-cyanobacteria bloom detection (Lunetta et al., 2015).

CI validation efforts occurred in Ohio, Florida, Rhode Island, Massachusetts, New Hampshire, Maine, New York, and Vermont (Lunetta et al., 2015). In-situ cyanobacterial cell counts were broken down into four categories: Low(10,000-109,999), Medium (110,000-299,999), High (300,000-1,000,000), and Very High (>1,000,000) (Lunetta et al., 2015). CyAN estimated cell counts were derived from the CI using the following equation (T. Wynne et al., 2010):

$$Cyanobacteria\ Abundance\ \left(\frac{cells}{mL}\right) = CI * 10^8$$

A total of 2,068 independent in situ samples were selected from lakes in the region between 2009 and 2012 from several existing monitoring programs (Lunetta et al., 2015). Participating agencies are detailed in Lunetta et al., 2015. All data sources utilized different field sampling and cell count enumeration methodologies (Lunetta et al., 2015). Samples collected from greater than 2.0m depth were excluded. The majority of samples were a single surface measurement no lower than 2m in depth (Lunetta et al., 2015).

These were matched with MERIS derived cell counts (Lunetta et al., 2015). Only 579 of the matches corresponded with a temporal window +/- 7 days from sample collection. Eight-two percent of the matched in-situ samples corresponded with the “Low” cell count range (Lunetta et al., 2015). Comparisons of correspondence between the in situ measurements and MERIS-derived estimates were analyzed for temporal windows including <1 day, and +/- 1, 3, 5, and 7 days.

Insufficient samples sizes for the Medium, High, and Very High categories were found in the <1 day temporal window (Lunetta et al., 2015). Correspondence results had very minimal variability for temporal windows ranging from 3 to 15 days indicating that the cyanobacterial bloom events tended to have a relatively long and typically stable duration (Lunetta et al., 2015).

The results indicated that the algorithm had correspondence levels of 90% for the Low (10,000-109,999) category and 83% for the Very High (>1,000,000) category. The Medium and High categories performed poorly with only 28% and 40% correspondence, respectively (Lunetta et al., 2015). This result is important in the context that the reference data was heavily skewed towards the Low range category. Seventy-two percent of the reference data was associated with the Low category (Lunetta et al., 2015). These correspondence values account for the errors present within both the satellite derived estimates and the in situ cell counts from the reference data (Lunetta et al., 2015). The correspondence values represent a conservative estimate of the performance of the algorithm (Lunetta et al., 2015).

Wynne et al. (2010) also highlighted that cyanobacterial blooms may exhibit a high degree of spatial variability. This illustrates that a 300m pixel size may contain many different cell densities across its area (Lunetta et al., 2015). Inter-pixel variability cannot be captured. Clark et al. (2017) presents the CyAN validation efforts with revisions in Figure 4. Those revisions include presenting the data in log space, the inclusion of mean absolute percent error (MAPE), and coefficient of determination when non-detect and minimum detect values were excluded (Figure 4) (Clark et al., 2017; Lunetta et al., 2015).

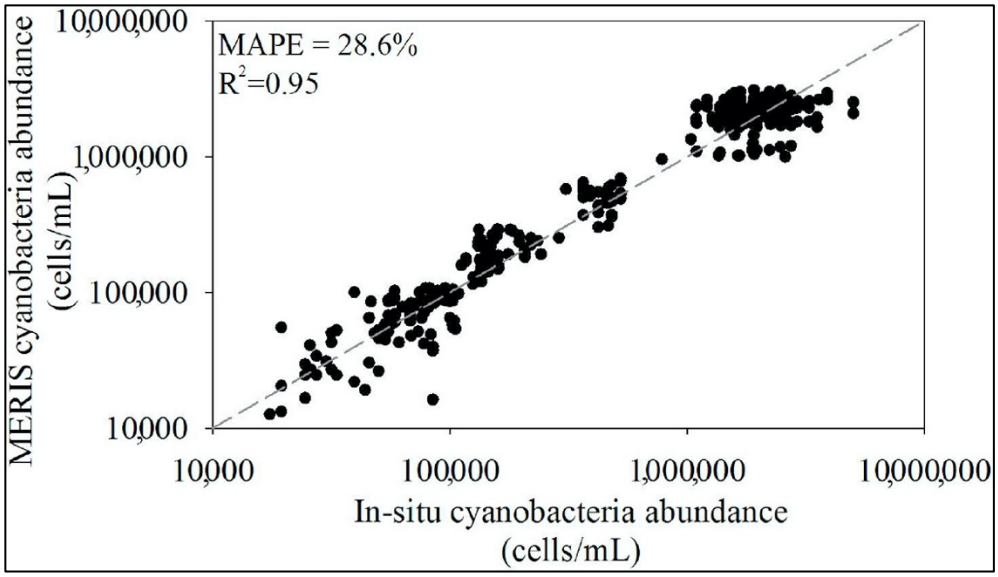

Figure 4: Validation of CI algorithm using all cyanobacterial cell count available in situ data within +- 7 days of the satellite overpass from Florida, Ohio, and New England states. Reprinted from "Satellite monitoring of cyanobacterial harmful algal bloom frequency in recreational waters and drinking water sources" by Clark, J. 2017. *Ecological Indicators, 80*

CyAN data is available through NASA's Ocean Color direct data download source or on their mobile or web app. Managers accessing and downloading the data directly can choose 7-day maximum composites from MERIS (2002-2012) and OLCI (2016-present) sensors. They can otherwise choose daily data products from OLCI sensors (2019-present) (NASA, 2023b). Data is provided as a GeoTIFF with digital numbers (DN). Land, cloud, and no data pixels are already flagged.

The CyAN app is available as both a web and mobile app. The app provides CyAN data for over 2,000 lakes across the US (ORD US EPA, 2019). This app was developed to help managers make faster and better-informed management decisions related to cyanobacterial blooms (ORD US EPA, 2019). This app offers a customizable interface. Users can determine their own cyanobacterial abundance thresholds. This allows for easy use across states and localities that may set their own risk thresholds. Lake managers can use this app to monitor their region on a

daily or weekly basis. They can pinpoint potential problem areas and focus their attention and resources (ORD US EPA, 2019).

CHAPTER III

DATA AND METHODS

Satellite Imagery

Satellite imagery was obtained from NASA's Ocean Biology Processing Group (OBPG) CyAN project data page (https://oceancolor.gsfc.nasa.gov/projects/cyan/). The imagery was obtained from the European Space Agency's (ESA's) Ocean and Land Colour Instrument (OLCI). OLCI has been operational aboard the Sentinel-3A platform since May 2016 (*NASA Ocean Color*). A second OLCI sensor has been aboard the Sentinel-3B platform since April 2018 (*NASA Ocean Color*). The addition of Sentinel-3B allowed for a higher temporal resolution and a shorter revisit time between image captures. This led to the production of daily CyAN data products.

OLCI sensors collect 21 spectral bands ranging between 400-1020 nanometers (nm) (European Space Agency, 2023a). OLCI sensors have a spatial resolution of 300m per pixel. The Cyanobacteria Index product (CI-cyano) utilizes a spectral shape algorithm centered on the 681nm band (Lunetta et al., 2015).

Imagery was collected for the years 2017-2022. The imagery was 7-day maximum value composites and delivered as GeoTIFF files. These composites preserved the maximum value for each pixel over the 7-day period.

The number of images per 7-day composite increased with the launch of Sentinel-3B in 2019. Average number of images per week increased from approximately 3-4 to approximately 5-7. All 7-day composites were analyzed the same regardless of the average number of images. Pixels were removed if flagged as land, clouds, or mixed (T. Wynne, Andrew, Briggs, Litaker, & Stumpf, 2020).

Digital Numbers (DNs) were converted to CI-cyano using the following equation:

$$CI_{cyano} = 10^{\left(\frac{3.0}{250.0}\right)*DN-4.2}$$

Cyanobacteria abundance was derived using the following equation from Wynne et al. (2010):

$$Cyanobacteria\ Abundance\ \left(\frac{cells}{mL}\right) = CI * 10^8$$

Detected blooms were considered for any pixels where cyanobacterial abundance was greater than the sensors lower detection limit. The sensors estimated lower detection limit is around 10,000 cells/ml (CyAN, 2022). Detected blooms were separated into four categories. These categories are low-risk blooms (<20,000 cell/ml), medium-risk blooms (20,000-100,000 cell/ml), high-risk blooms (>100,000 cell/ml), and total blooms. Total blooms represent any level of bloom detection above the sensor detection limit. Low, medium, and high-risk blooms are based on the WHOs recreational guidance and action levels (Table 3) (WHO, 2003).

Table 3: Recreational Guidance/Action Levels for Cyanobacteria, Chlorophyll a, and Microcystin. Adapted from "Guidelines for safe recreational water environments. Volume 1, Coastal and freshwaters" by the World Health Organization. 2003.

Relative Probability of Acute Health Effects	Cyanobacteria (cells/mL)	Chlorophyll *a* (µg/L)	Estimated Microcystin Levels (µg/L)
Low	<20,000	<10	<10
Medium	20,000-100,000	10-50	10-20
High	>100,000	>50	>20

Study Area

A total of 69 waterbodies were selected in Oklahoma (Figure 5). These waterbodies align closely with the National Hydrography Dataset (NHDplus v2) of lakes that are resolvable by the satellite. Resolvable lakes within CONUS require at least three adjacent, water-only pixels (Seegers et al., 2021). Waterbodies were designated based on their unique Oklahoma Water Resource Board (OWRB) Waterbody ID. This results in certain lakes and reservoirs having multiple sections. Lakes with multiple sections are analyzed independently in this analysis. All waterbodies had an area greater than 1,000 acres. These lakes and reservoirs represent the largest waterbodies across the state.

Trophic Status

Waterbody trophic status is classified by OWRB. They utilize the Carlson's Trophic State Index (TSI). Carlson's TSI uses Chl-a concentrations to classify trophic status (OWRB, 2018). Carlson's TSI is calculated as:

$$TSI = 9.81 * \ln Chl - a\left(\frac{\mu g}{L}\right) + 30.6$$

Lakes larger than 250 surface acres require a minimum of 20 samples for classification purposes (OWRB, 2018). All TSI evaluations have been based on annualized Chl-a values since 2001 (OWRB, 2018). Samples are collected over four sampling quarters. Carlson's TSI includes four main trophic categories (Table 4).

Table 4: Lake trophic state categories. Reprinted from "2017 Oklahoma Lakes Report: Beneficial Monitoring Program" by the Oklahoma Water Resource Board. 2018.

Carlson TSI	Trophic State	Definition
≤ 40	Oligotrophic	Low primary productivity and/or low nutrient levels
41-50	Mesotrophic	Moderate primary productivity with moderate nutrient levels
51-60	Eutrophic	High primary productivity and nutrient rich
≥ 60	Hypereutrophic	Excessive primary productivity and excessive nutrients

Twenty-five waterbodies are hypereutrophic, 31 are eutrophic, 12 are mesotrophic, and 1, Stanley Draper, is oligotrophic of the selected 69 waterbodies.

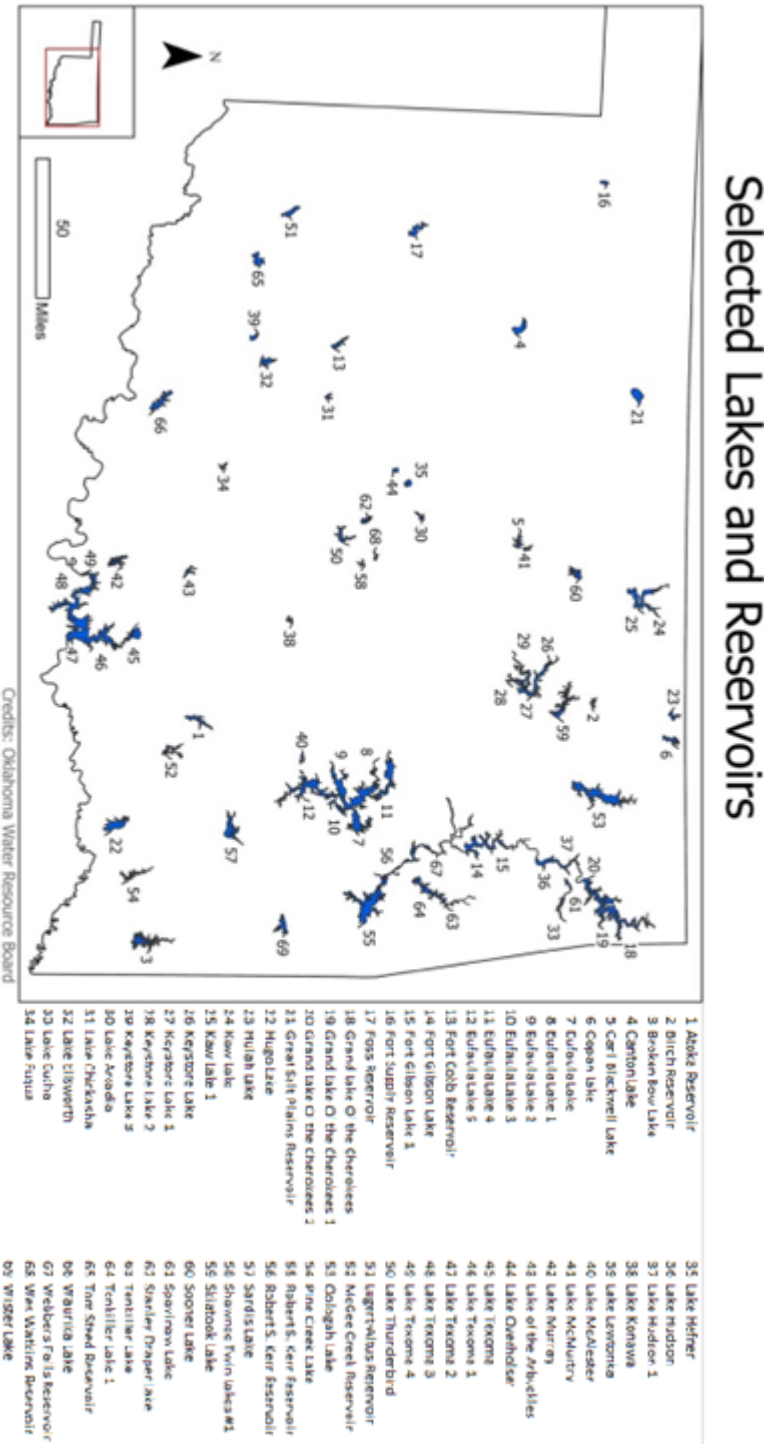

Figure 5: Study area and selected lakes and reservoirs for HAB characterization. Data sourced from Oklahoma Water Resource Board Open Data Access Portal. “Surface Water- Lake”.

Frequency

Frequency is defined as the number of bloom occurrences out of the total number of potential bloom occurrences comprised within the 52 weekly composites (Coffer et al., 2021). Pixel frequency was calculated first for every resolvable pixel within a waterbody (Figure 6). Pixel frequency was calculated as the number of weeks a bloom was occurring in each bloom category, divided by the number of weeks of satellite observation for that pixel. Pixel frequencies were then averaged to obtain lake scale frequencies (Figure 6). Lake frequencies were calculated as the average of all pixel frequencies inside the waterbody. Statewide frequency is calculated as the average of all lake scale frequencies. Frequencies were calculated annually for the six-year study period.

$$Annual\ pixel\ scale\ frequency = 100 * \frac{n\ of\ pixels\ with\ detectable\ HAB}{n\ of\ all\ valid\ pixels}$$

$$Annual\ lake\ scale\ frequency = 100 * \frac{\sum annual\ pixel{-}scale\ frequenceis\ within\ lake}{n\ of\ pixels\ within\ lake}$$

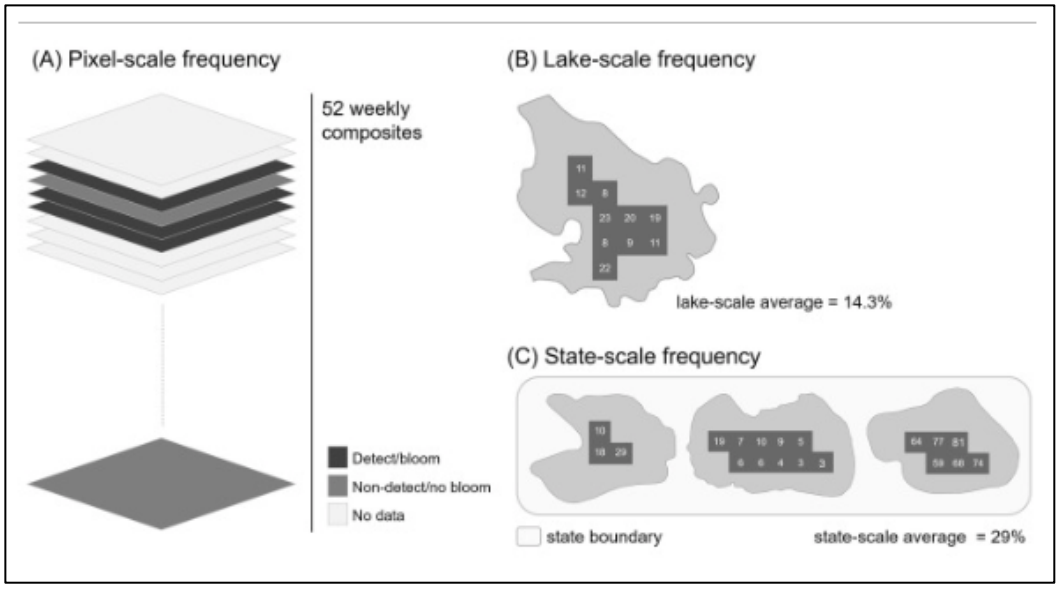

Figure 6: Display of frequency values at different scales. Reprinted from "Assessing cyanobacterial frequency and abundance at surface waters near drinking water intakes across the United States" by Coffer, M. 2021. *Water Research, 201*

Weekly Frequency

There is no standard regarding the minimum area of a harmful algal bloom for a waterbody to be characterized as experiencing a bloom (Coffer, Schaeffer, Darling, Urquhart, & Salls, 2020). Some studies have characterized a waterbody as experiencing a bloom as soon as the satellite detects cyanobacteria in a single pixel (Zhang et al., 2012). This would be analogous to ground sampling at a single point to classify a bloom. Other studies have used thresholds on the percent of a waterbody experiencing a bloom (Coffer et al., 2020; Davis et al., 2019; Hu et al., 2010; Qin et al., 2015). A waterbody is classified as experiencing a bloom if one pixel is above the threshold for the purpose of this analysis.

Weekly frequency was computed as the fraction of weeks that had a bloom occurring in at least one pixel of the waterbody during the 7-day composite in each bloom category. Weekly frequency represents an easily understandable metric illustrating how frequently a bloom may occur in at least one pixel in a waterbody over the year. They represent the worst bloom

experienced by a lake each week. This means that if a waterbody experiences a low and medium-risk bloom, the medium-risk bloom is reported for that week. This results in high-risk blooms exhibiting a much greater weekly frequency than low and medium-risk blooms. This does not indicate that low and medium-risk blooms aren't occurring at a similar rate. This indicates that most waterbodies frequently experience high-risk blooms.

Maximum Bloom Severity

Maximum bloom severity is calculated as the most severe bloom. The most severe bloom is calculated as the pixel with the highest cyanoHAB abundance within each waterbody, per lake, per year.

Spatial Extent

The spatial extent of blooms was calculated monthly for each risk category. Monthly composites represent the total area of a waterbody that experienced a bloom at least once in that month. The spatial extent of blooms was characterized in two ways: 1) the area in km^2 and 2) the percent coverage of a waterbody that experienced a bloom for a given month. Monthly maximum composites were created, retaining the max value that each pixel exhibited over the month. Weekly composites were assigned to each month. They were assigned to whichever month the majority of days fell in. All months had at least 4 weekly observations. Some months had five weekly observations. Maximum composites, rather than mean composites, were computed to reduce the potential effect of wind and clouds reducing bloom detection. This is in line with Urquhart et al. (2017).

Bloom spatial extent is calculated as the number of the pixels experiencing a bloom multiplied by the pixel size, 300m or $0.09km^2$. Percent coverage of blooms was calculated as the number of

pixels with detectable cyanoHAB divided by the total number of valid pixels for the month. The number of valid pixels per waterbody varied each month with the removal of quality flagged pixels due to cloud cover or some other reason.

$$Bloom\ Coverage\ (\%) = \frac{n\ of\ pixels\ with\ detectable\ CIcyano}{n\ of\ valid\ pixels} * 100\%$$

$$Spatial\ Extent\ (km^2) = n\ of\ valid\ pixels * 0.09\ km^2$$

Trends

Non-parametric tests were used to identify trends in cyanoHAB bloom frequency, maximum severity, and spatial extent. Non-parametric slope estimation is required due to the limited study period. The Theil-Sen slope estimator and Mann-Kendall (MK) test were used for assessing the direction and strength of trends for bloom frequency and severity. A seasonal MK test and Thiel-Sen estimator were used for assessing trends in monthly bloom spatial extent. The seasonal MK (SMK) test assesses for trends over seasons (Coffer et al., 2020). The SMK further accounts for heterogeneity and serial dependence of observations (Coffer et al., 2020; Hirsch & Slack, 1984). Each month represents its own season in this analysis.

The MK test produces Kendall's *tau* (τ) as its test statistic. Kendall's τ is an extension of Spearman's rho (Akoglu, 2018). Kendall's τ indicates the strength of the monotonic changes (Schaeffer et al., 2022a). Tau values of $|\tau| < 0.2$ or $0.2 \leq |\tau| < 0.3$ indicate negligible and weak changes over time. Higher values of $0.3 \leq |\tau| < 0.5$, $|\tau| \geq 0.5$, are considered moderate and strong changes over time (Schaeffer et al., 2022b).

The Thiel-Sen slope estimator is calculated by taking the median of slopes between all points (Sen, 1968; Theil, 1992). Thiel-Sen can estimate the change per unit in time. Short time series, comparable to our study period, have previously been used for trend detection (Coffer, Schaeffer,

Foreman, et al., 2021). Trends in air quality were assessed using three and five years of data (Kim et al., 2009). Water quality trends were assessed over a three year period (Psilovikos, Margoni, & Psilovikos, 2006). Coffer et al. (2021) assessed trends for cyanobacterial frequency over a five year study period using remote sensing data whilr utilizing MK and Theil-Sen. Thiel-Sen was determined to be an appropriate test based on previous peer-reviewed use.

A Kruskal Wallis test was conducted to determine if individual waterbodies and trophic-grouped waterbodies were significantly different from each other. The Kruskal Wallis test is a non-parametric test that determines whether the medians of two or more groups differ (Glen, 2015; S. C. J. Palmer et al., 2015). A Kruskal Wallis test is considered the non-parametric version of a one-way ANOVA test. A significant Kruskal Wallis test does not indicate which groups significantly differ. Dunn's test and pairwise comparison indicates which groups are significantly different from each other (Zach, 2020). A Bonferroni adjustment is applied to control the family-wise error rate that can arise from multiple comparisons (Zach, 2020).

All analysis, image processing, and trend detection was performed in R version 4.2.1 ("R: The R Project for Statistical Computing," 2023). Trend detection was analyzed using the *trend* and *Kendall* package (McLeod, 2022; Pohlert, 2020).

Table 5 summarizes the spatial scale, bloom risk group, and type of analysis conducted in this research.

Table 5: CyanoHAB characterization of frequency, spatial extent, and intensity, by spatial scale, and bloom risk thresholds and their associated type of trend and significant difference analysis to characterize OK HABs. MK: Mann-Kendall, SMK: Seasonal Mann-Kendall, TS: Thiel-Sen, KW: Kruskal-Wallis, PWC: Dunn's Pairwise Comparison

Metrix	Level of Analysis	Analysis Groups	Type of Analysis
Frequency	State Scale	Total	MK, TS
		High Risk	MK, TS
		Medium Risk	MK, TS
		Low Risk	MK, TS

		No Bloom	MK, TS
	Individual Waterbodies	Total	MK, TS, KW, PWC
		High Risk	MK, TS, KW, PWC
		Medium Risk	MK, TS, KW, PWC
		Low Risk	MK, TS, KW, PWC
		No Bloom	MK, TS, KW, PWC
	Trophic Grouped Waterbodies	Total	MK, TS, KW, PWC
		High Risk	MK, TS, KW, PWC
		Medium Risk	MK, TS, KW, PWC
		Low Risk	MK, TS, KW, PWC
		No Bloom	MK, TS, KW, PWC
Weekly Frequency	Individual Waterbodies	Total	MK, TS, KW, PWC
		High Risk	MK, TS, KW, PWC
		Medium Risk	MK, TS, KW, PWC
		Low Risk	MK, TS, KW, PWC
		No Bloom	MK, TS, KW, PWC
	Trophic Grouped Waterbodies	Total	MK, TS, KW, PWC
		High Risk	MK, TS, KW, PWC
		Medium Risk	MK, TS, KW, PWC
		Low Risk	MK, TS, KW, PWC
		No Bloom	MK, TS, KW, PWC
Spatial Extent	State Scale	Total	SMK, TS
		High Risk	SMK, TS
		Medium Risk	SMK, TS
		Low Risk	SMK, TS
	Individual Waterbodies	Total	SMK, TS, KW, PWC
		High Risk	SMK, TS, KW, PWC
		Medium Risk	SMK, TS, KW, PWC
		Low Risk	SMK, TS, KW, PWC
	Trophic Grouped Waterbodies	Total	SMK, TS, KW, PWC
		High Risk	SMK, TS, KW, PWC
		Medium Risk	SMK, TS, KW, PWC
		Low Risk	SMK, TS, KW, PWC
Severity	Individual Waterbodies	NA	MK, TS, KW, PWC
	Trophic Grouped Waterbodies	NA	MK, TS, KW, PWC

CHAPTER IV

RESULTS

FREQUENCY

High Risk Bloom Frequency

Harmful algal bloom frequency shows an upward trend for all bloom risk categories over the period of the study (Figure 7). High-risk blooms have experienced the largest increase in cyanoHAB frequency of the WHO risk categories. All bloom risk categories have a significant positive, monotonic trend (Table 6). The frequency of observable pixels with no-bloom did not show a significant trend over the study period.

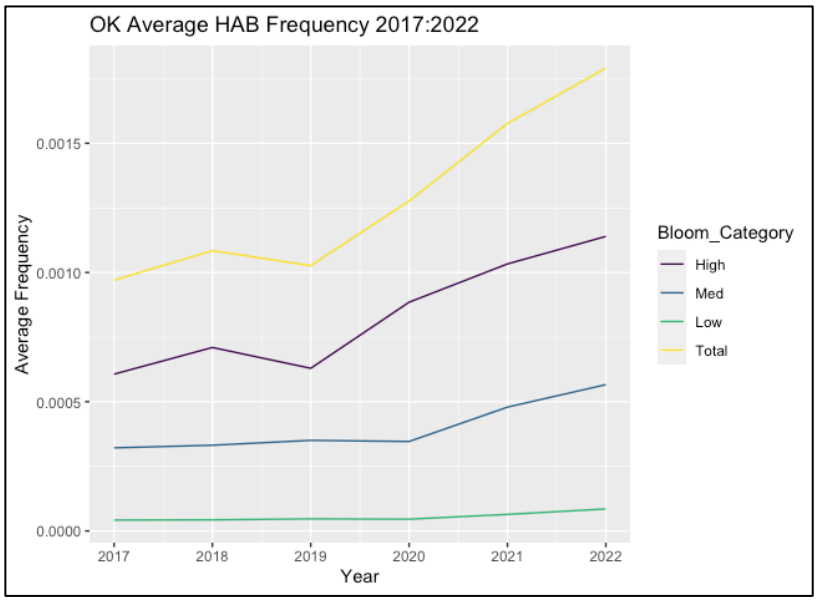

Figure 7: Average statewide bloom frequency by bloom risk categories for the years 2017 through 2022

Table 6: Mann Kendall tests for monotonic trends and Sen's slope estimator for trends in average statewide HAB frequency by bloom risk category from 2017-2022. Significant trends are bolded.

Bloom Category	Tau	MK P value	Sen's Slope	Sen's P value
Total	**0.86667**	**0.02417052**	**0.00016412**	**0.02417055**
High	**0.86667**	**0.02417052**	**0.00010662**	**0.02417055**
Medium	**0.86667**	**0.02417052**	**4.89E-05**	**0.02417055**
Low	**0.86667**	**0.02417052**	**7.07E-06**	**0.02417055**
No Bloom	0.199999	0.70711422	4.11E-05	0.70711423

High-risk bloom frequency varies considerably across the 69 waterbodies (Figure 8). These differences are statistically significant (Table A1). Over half of the waterbodies never have a high-risk bloom frequency above 10%. Lake Murray, Lake Eucha, and Broken Bow Lake exhibit the lowest high-risk bloom frequency. Lake Overholser, Fort Supply Reservoir and Lake Chickasha exhibit the highest high-risk bloom frequency. Lakes with a higher bloom frequency also exhibit more variation in bloom frequency between the years (Figure 8).

Tom Steed Reservoir, Sooner Lake, and Robert S Kerr Reservoir 1 exhibited significant trends in high-risk bloom frequency over the study period (Table 7). Tom Steed Reservoir exhibited the highest rate of increase in high-risk bloom frequency with a Sen's slope of 0.0855 (P value = 0.0241). The Kendall tau (0.8667) indicates a strong trend in high-risk bloom frequency for this reservoir. It should be noted that Robert S Kerr Reservoir exhibited no trend in high-risk bloom frequency, but had one of the largest high-risk bloom frequencies among any of the waterbodies.

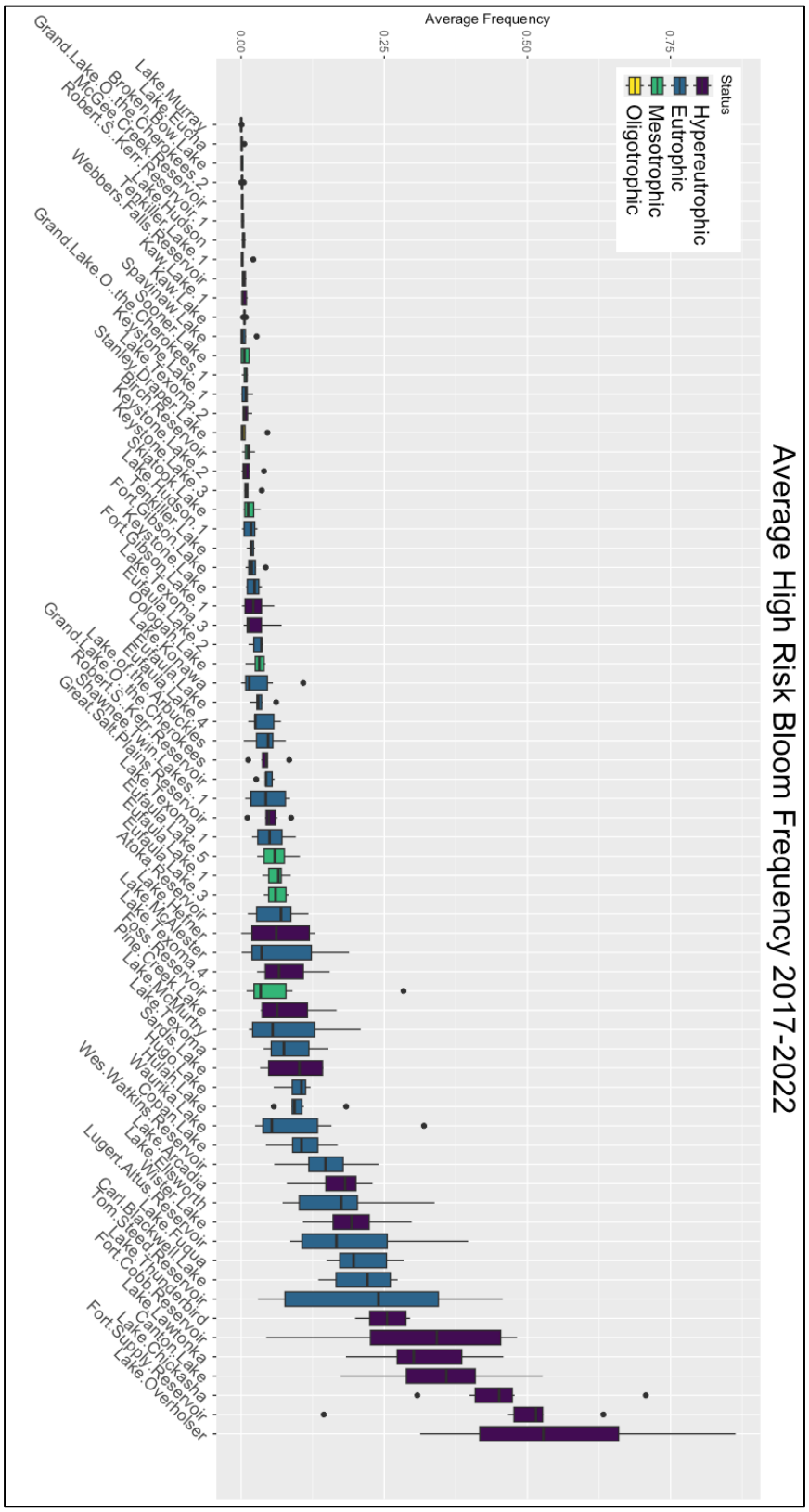

Figure 8: Average high-risk bloom frequency for each lake between 2017-2022. Lakes are colored based on their trophic status reported by the OWRB.

Table 7: Mann Kendall and Sen's Slope to assess for trends in lake high-risk bloom frequency. Significant trends are shown. Refer to table C1 for full analysis.

Waterbody	Tau	MK P value	Sen's Slope	Sen's p.value
Robert.S.Kerr.Reservoir.1	**0.86667**	**0.02417**	**0.00090**	**0.02417**
Sooner.Lake	**0.86667**	**0.02417**	**0.00305**	**0.02417**
Tom.Steed.Reservoir	**0.86667**	**0.02417**	**0.08548**	**0.02417**

The waterbodies with the greatest high-risk bloom frequency were classified as hypereutrophic and eutrophic (Figure E1). Hypereutrophic and eutrophic waterbodies had significantly greater bloom frequencies compared to mesotrophic and oligotrophic waterbodies (Table B1). Eutrophic waterbodies showed a significant upward trend in high-risk bloom frequency with a Sen's slope of 0.0119 (P value <0.05) (Table F1).

Medium Risk Bloom Frequency: Medium-risk bloom frequency across the different waterbodies exhibited a similar shape distribution as high-risk bloom frequency (Figure 9). The Kruskal-Wallis test indicates a significant difference between waterbodies (Table A1), though less significant than high-risk bloom frequency.

Lake Murray, Lake Eucha, and Broken Bow Lake had the lowest medium-risk bloom frequencies. Lake Lawtonka, Sardis Lake, and Fort Supply Reservoir had the greatest medium-risk bloom frequencies. Sooner Lake, Grand Lake O the Cherokees 1, and Lake Thunderbird showed significant trends in medium-risk bloom frequency (Table C2). Sooner Lake exhibited the most significant trend with an increase in medium-risk bloom frequency with a Sen's slope of 0.0022 (P value <0.05). Grand Lake O the Cherokees 1 also exhibited a positive trend in frequency. Lake Thunderbird was the only waterbody to show a significant downward trend in medium-risk bloom frequency.

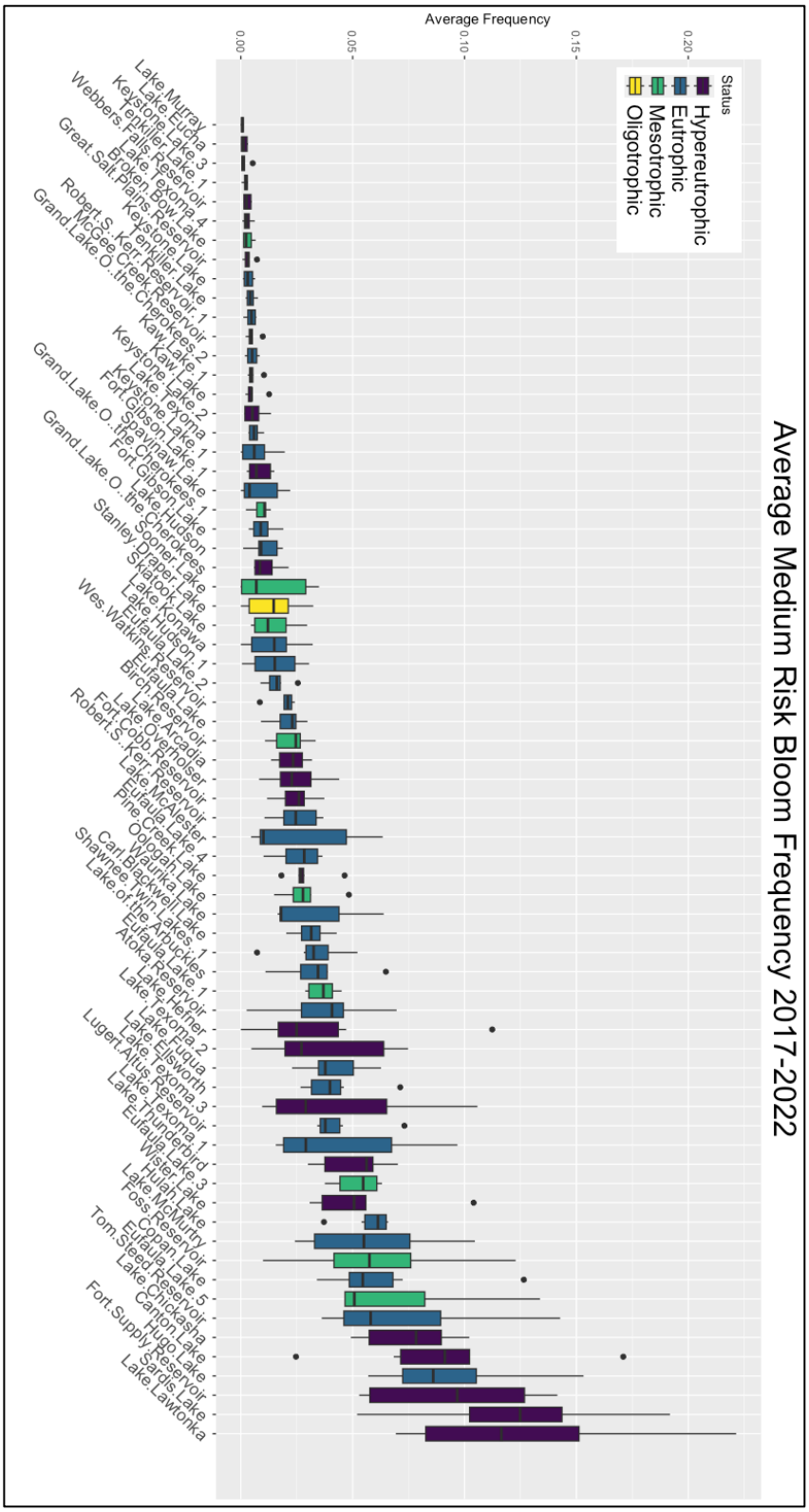

Figure 9: Average Medium risk bloom frequency for each lake between 2017-2022. Lakes are colored based on their trophic status reported by the OWRB.

The waterbodies with the highest medium-risk bloom frequency were often hypereutrophic and eutrophic (Figure 9). Multiple mesotrophic waterbodies had high medium-risk bloom frequencies. No significant difference between trophic states was found when comparing medium-risk bloom frequency (Fig E1, Table A2). Eutrophic and mesotrophic waterbodies exhibited a significant positive trend in medium-risk bloom frequency (Table F2).

Low Risk Bloom Frequency: Low-risk bloom frequency exhibited little variation across the waterbodies (Figure 10). The Kruskal-Wallis test indicated a significant difference between waterbodies (Table A1). Low-risk blooms had the smallest Kruskal-Wallis effect size of the risk categories at 0.689 (Table A1). Six waterbodies exhibited a significant positive trend over time (Table C3). These waterbodies included Lake Konawa, Eufaula Lake, Lake Texoma 1 and 2, Sooner Lake, and McGee Creek Reservoir.

The pattern between low-risk bloom frequency and trophic state is much less apparent (Figure E1). The results of the Kruskal-Wallis test indicate there was a significant difference between trophic states (Table A2). The oligotrophic waterbody, Stanley Draper Lake, was significantly different from all other trophic states in terms of low-risk bloom frequency (Table B2). No other pairwise comparisons were significant. No trophic states showed significant trends for low-risk bloom frequency (Table F3).

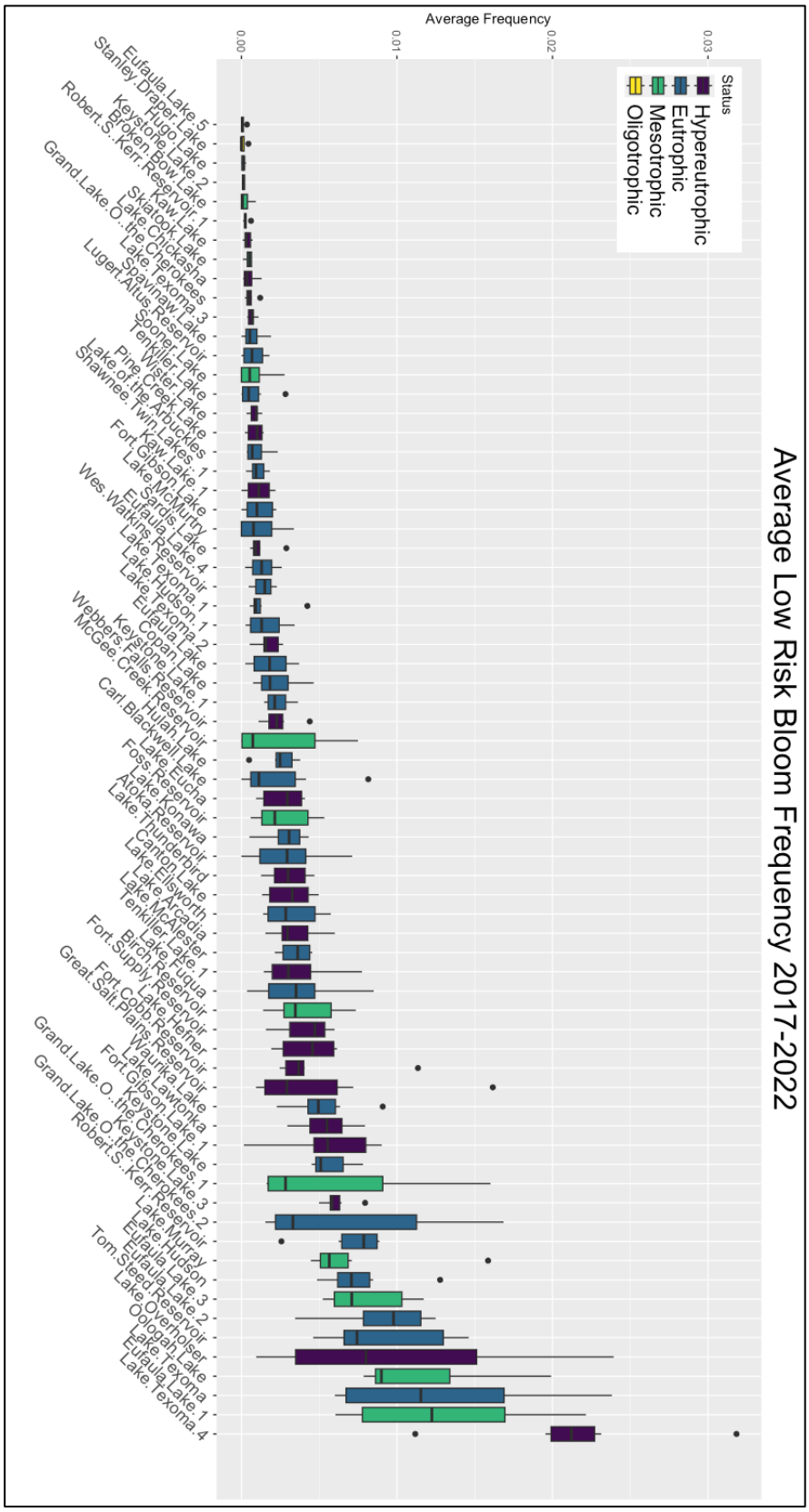

Figure 10: Average annual low-risk bloom frequency for each lake between 2017-2022.

No Bloom Frequency: The average no-bloom frequency of the waterbodies exhibited a different distribution than the other bloom risk categories (Figure 11). Fort Supply Reservoir, Lake Overholser, and Lake Chickasha experienced some of the lowest average no-bloom frequencies. Great Salt Plains Reservoir, Kaw Lake 1, and Lake Texoma 2 experienced some of the highest no-bloom frequencies. Average no-bloom frequencies significantly differ between waterbodies (Table A1). Lugert Altus Reservoir and Tom Steed Reservoir exhibit a significant downward trend over time (Table C4).

Differences in no-bloom frequency between trophic states were slight (Fig E4, Table A2). The difference in no-bloom frequency was significant only between the eutrophic and hypereutrophic waterbodies (Table B3). No trophic states exhibit a significant trend in no-bloom frequency (Table F4).

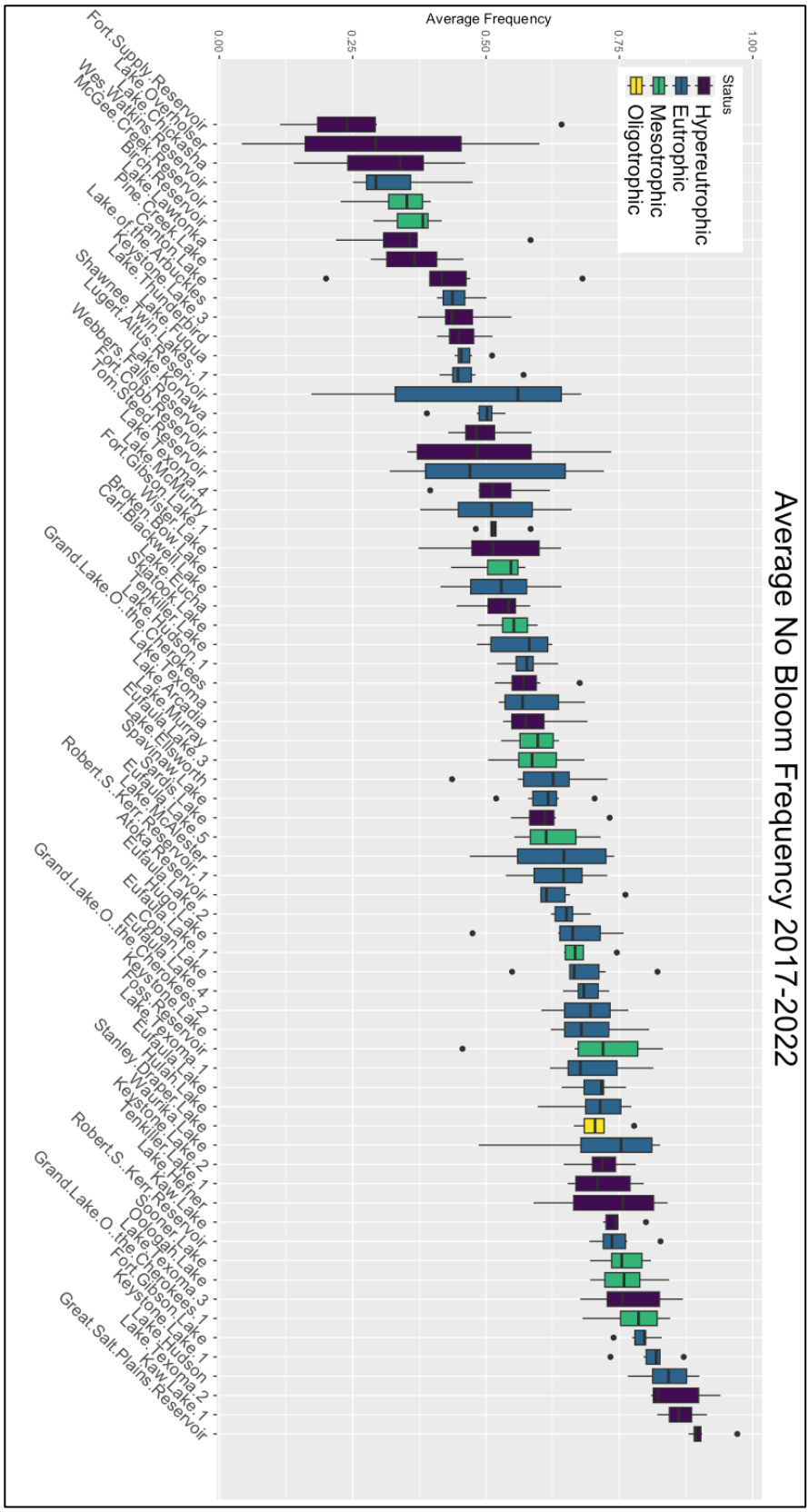

Figure 11: Average no bloom frequency for waterbodies between 2017-2022

Total Bloom Frequency: The average total bloom frequency represents any bloom above the sensor's detection limit of approximately 10,000 cells/ml (Fig 6). Total bloom frequency is statistically significant between waterbodies (Table A1). Lake Murray, Lake Eucha, and Broken Bow Lake had some of the lowest total bloom frequencies. Lake Overholser, Fort Supply Reservoir, Lake Chickasha, and Lake Lawtonka have some of the highest total bloom frequencies.

Four waterbodies showed significant trends in total bloom frequency (Table A1). Lugert Altus Reservoir and Sooner Lake exhibit the largest positive trend with a Sen's slope of 0.05877 and 0.01218 respectively. Kaw Lake and Keystone Lake 1 also exhibited a significant positive trend (Table 8).

Table 8: Significant average annual total bloom frequency trends. Complete total bloom trend analysis can be found in Table C5.

Waterbody	Tau	MK P value	Sen's Slope	Sen's p.value
Kaw.Lake	**0.86667**	**0.02417**	**0.00244**	**0.02417**
Keystone.Lake.1	**0.86667**	**0.02417**	**0.00656**	**0.02417**
Lugert.Altus.Reservoir	**0.86667**	**0.02417**	**0.05877**	**0.02417**
Sooner.Lake	**0.86667**	**0.02417**	**0.01218**	**0.02417**

The differences in total bloom frequency between trophic states (Fig E1) were significant (Table A2). Hypereutrophic waterbodies exhibited significantly greater total bloom frequency than mesotrophic waterbodies ($p<0.001$) (Table B4). Eutrophic waterbodies were also significantly higher than mesotrophic waterbodies ($p<0.005$). Only eutrophic waterbodies exhibit a significant positive trend with a Sen's slope of 0.0151 (Table F5).

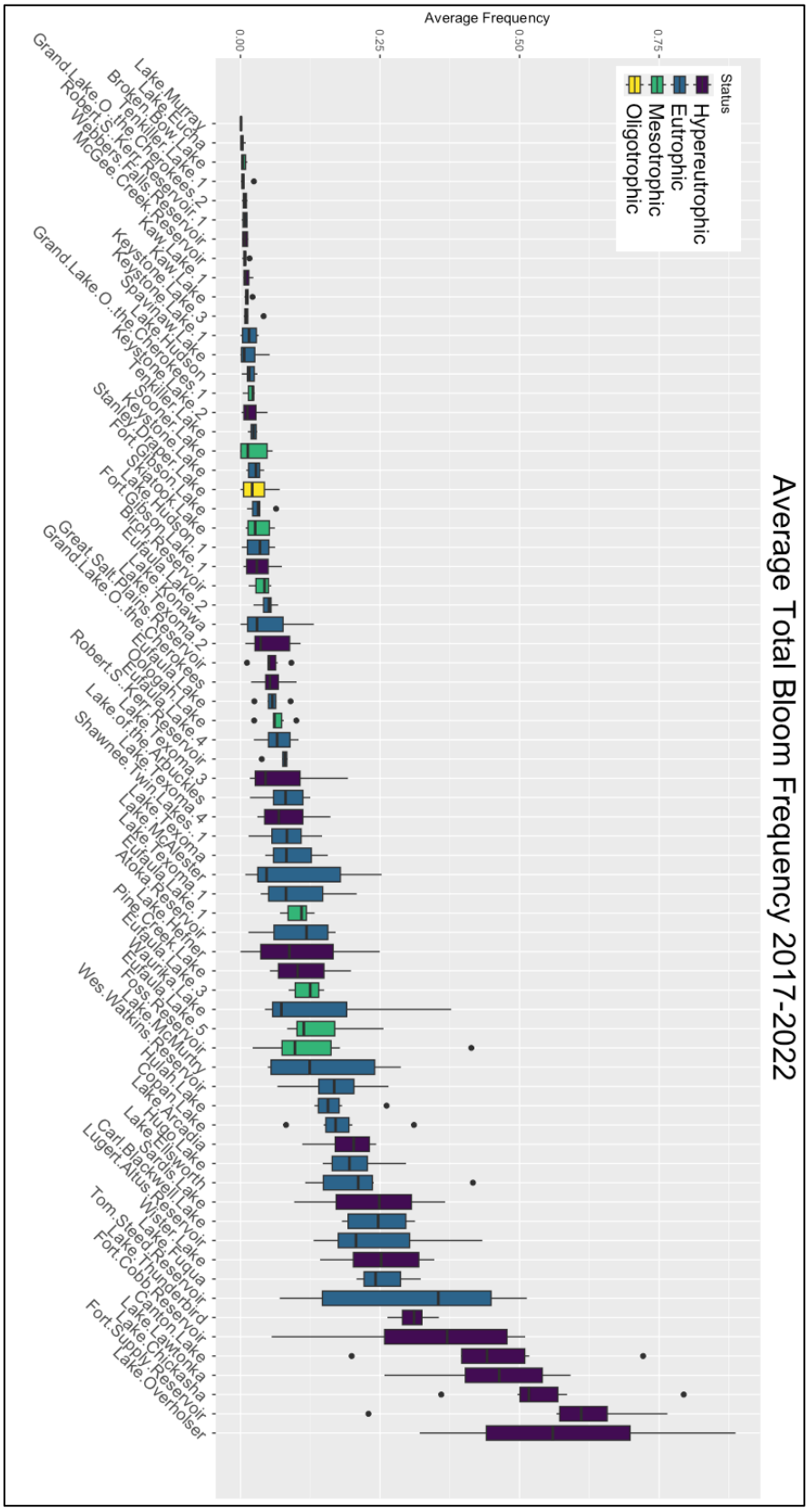

Figure 12: Average annual total bloom frequency for waterbodies between 2017-2022

WEEKLY FREQUENCY

High Risk Blooms: Weekly high-risk bloom frequency represents the weekly frequency of at least one pixel having a bloom in the corresponding risk category. High-risk weekly bloom frequency exhibited a wide range between the waterbodies (Figure 13). Approximately one-third of the waterbodies experienced a high-risk bloom over half of the year.

Eight waterbodies exhibited a significant positive trend in high-risk weekly bloom frequency (Table 9). All were positive trends with Lake Ellsworth, Great Salt Plains Reservoir, and Lake Arcadia experiencing the largest increase in trend over time. The Sen's slope of 0.072 for Lake Ellsworth's equated to an increase in the number of weeks with high-risk blooms by approximately 3.5 weeks per year.

Table 9: MK and Sen's slope trend detection for the weekly frequency of high-risk blooms

Waterbody	Tau	MK P value	Sen's Slope	Sen's p.value
Eufaula.Lake	**0.86667**	**0.02417**	**0.05769**	**0.02417**
Great.Salt.Plains.Reservoir	**0.86667**	**0.02417**	**0.06923**	**0.02417**
Lake.Chickasha	**0.86667**	**0.02417**	**0.04311**	**0.02417**
Lake.Ellsworth	**0.86667**	**0.02417**	**0.07231**	**0.02417**
McGee.Creek.Reservoir	**0.86667**	**0.02417**	**0.04082**	**0.02417**
Hulah.Lake	**0.82808**	**0.03538**	**0.03846**	**0.03538**
Lake.Arcadia	**0.82808**	**0.03538**	**0.05897**	**0.03538**
Lake.Texoma.3	**0.82808**	**0.03538**	**0.02525**	**0.03538**

High-risk bloom weekly frequency by trophic states showed a significant difference between groups (Table A4). High-risk bloom weekly frequency for hypereutrophic lakes was significantly higher than eutrophic waterbodies (Table B5). No trophic groups showed significant trends over time (Table F6).

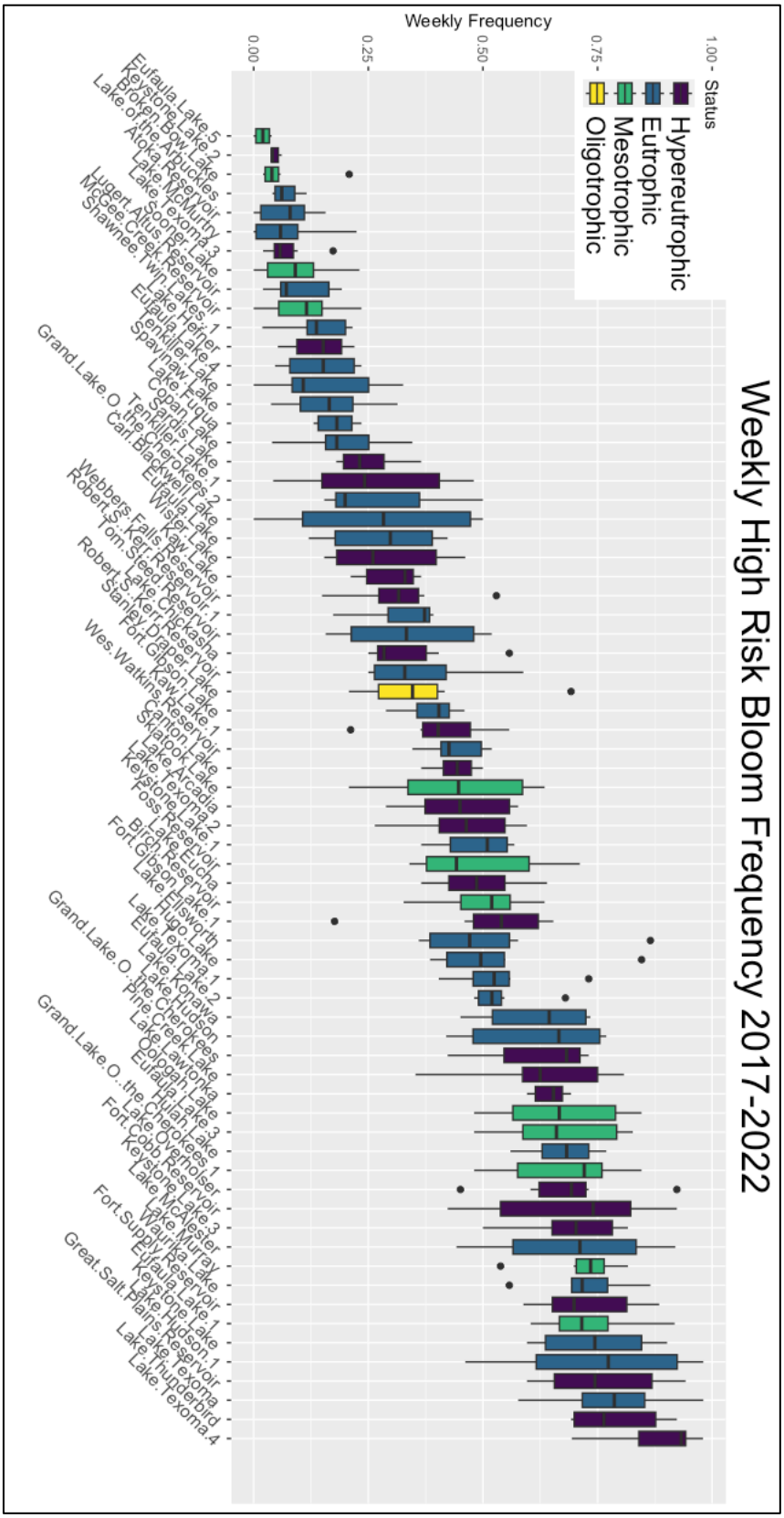

Figure 13: Annual weekly high-risk bloom frequency

Medium Risk Blooms: Two waterbodies showed a significant positive trend in weekly medium-risk bloom frequency over time (Figure 14, Table C7). Lake Texoma 4 showed a significant negative trend over time with a Sen's slope of -0.0249. This decrease indicated that medium-risk bloom frequency was decreasing roughly 1 week per year over the study period. Eufaula Lake experienced the opposite. Eufaula Lake exhibited a significant positive trend of a roughly one-week increase in medium-risk bloom frequency per year over the study period.

The differences between trophic state's weekly medium-risk bloom frequency (Figure E2) were significant (Table A3). Oligotrophic weekly medium-risk bloom frequency was significantly lower than all other trophic states (Table B6). No trophic states showed significant trends over time (Table F7).

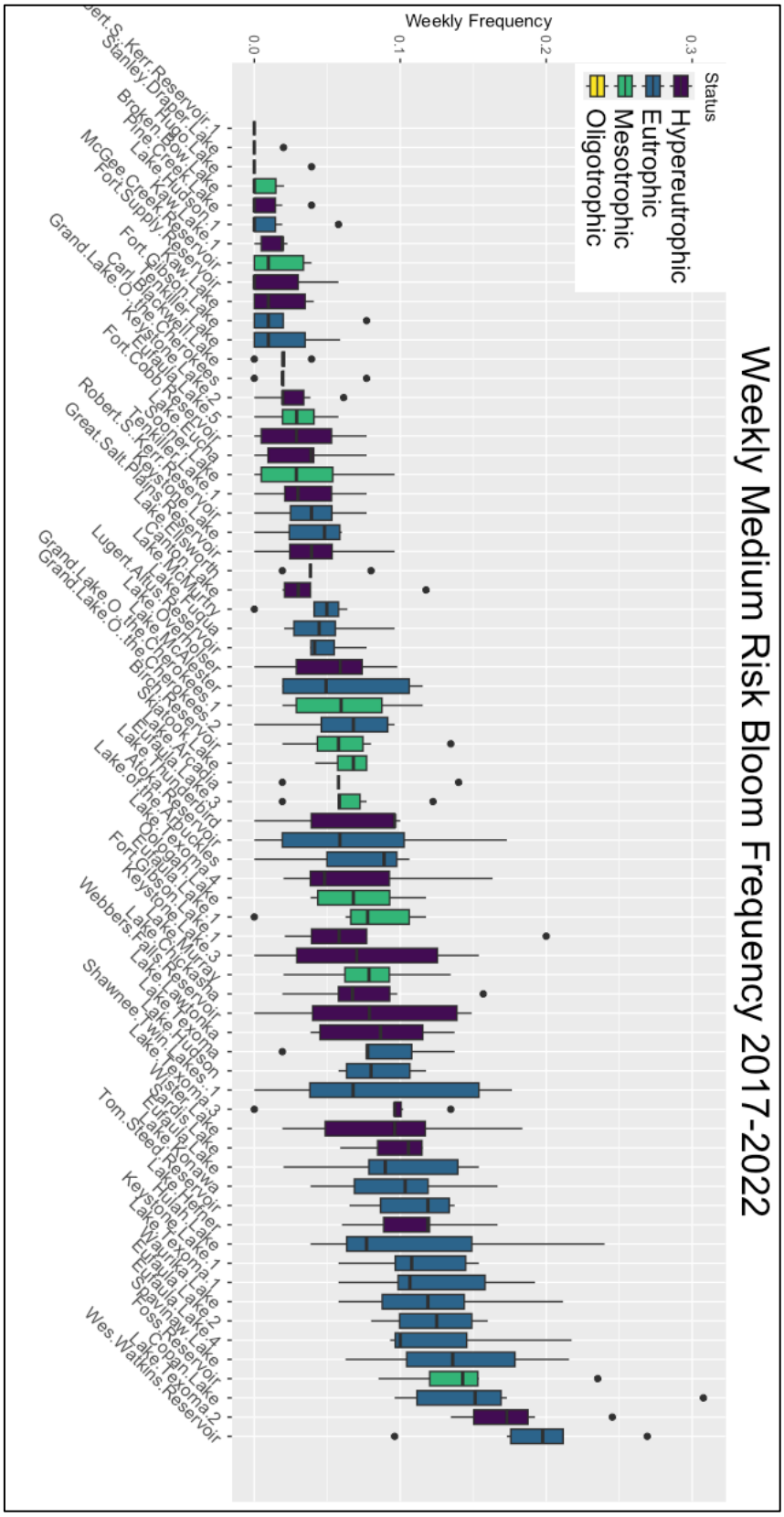

Figure 14: Annual weekly medium-risk bloom frequency

Low Risk Blooms: Slightly over half of the waterbodies experienced no weeks or only one week with a maximum low-risk bloom over the study period (Figure 15). Lake Thunderbird exhibited a significant downward trend in weekly low-risk bloom frequency (Table C8).

No significant differences in weekly low-risk bloom frequency by the trophic state were observed (Figure E2, Table A3). No trophic states showed significant trends in weekly low-risk bloom frequency (Table F8).

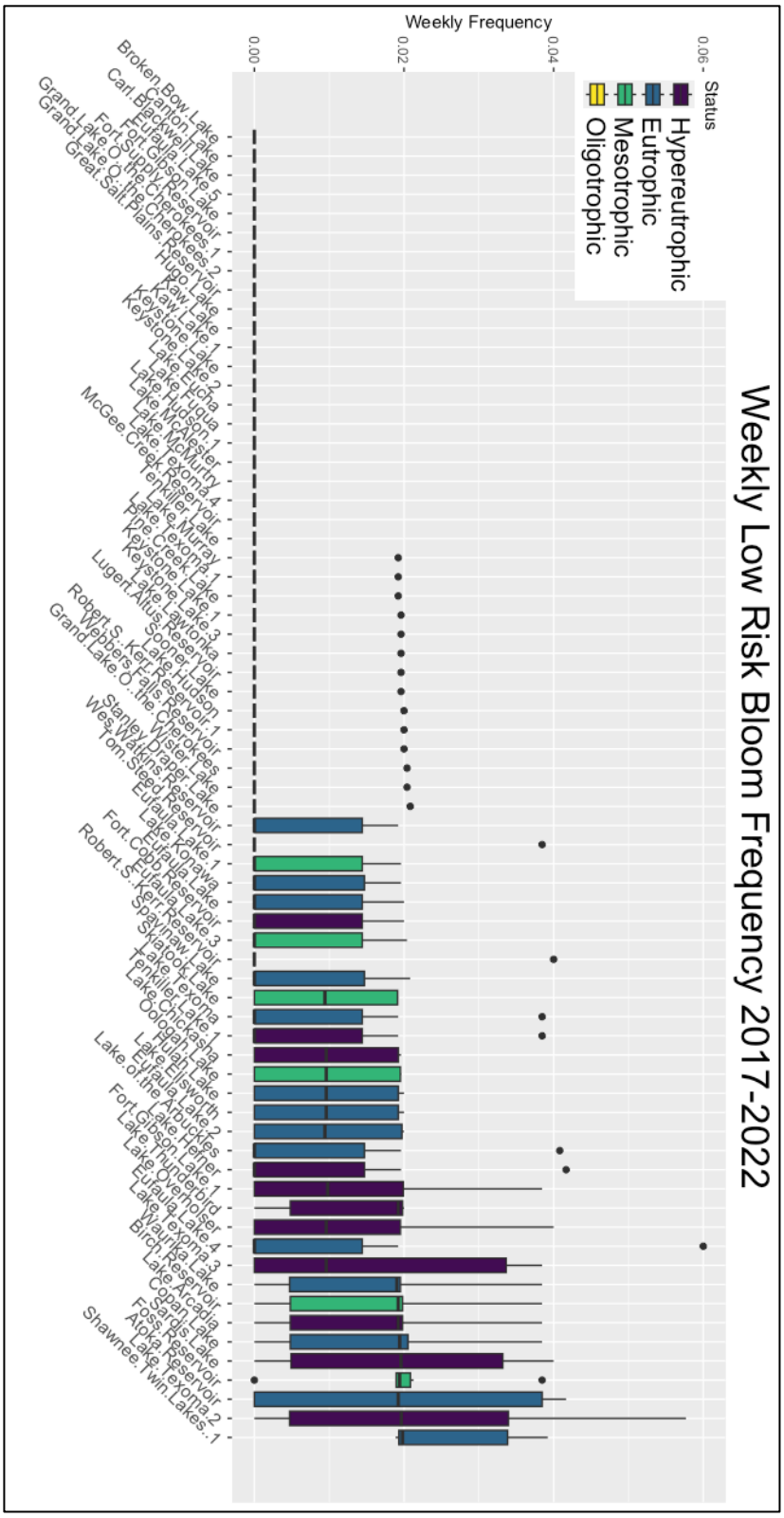

Figure 15: Annual weekly low-risk bloom frequency

No Bloom Detection: The waterbodies show a wide range in the number of weeks not experiencing any bloom (Figure 16). Lake Texoma 4, Lake Texoma, Lake Thunderbird, and Eufaula Lake 1 frequenctly had blooms occurring in more than 35 weeks a year. Some lakes experienced most years with only a handful of weeks experiencing any type of bloom. These include Eufaula Lake 5, Broken Bow Lake, and Keystone Lake 2. Nine waterbodies showed a significant downward trend over time (Table C9). These include Grand Lake O the Cherokees 2, Lake Ellsworth, Lake Texoma 3, Great Salt Plains Reservoir, Lake Chickasha, Shawnee Twin Lakes 1, Lake Texoma 2, Eufaula Lake, and McGee Creek Reservoir.

No significant differences between trophic states were observed in weekly no-bloom frequency (Figure E5, Table A4). Eutrophic lakes were the only trophic state to show a significant trend of roughly an average 1.5-week reduction in weeks with no blooms per year (Table F9).

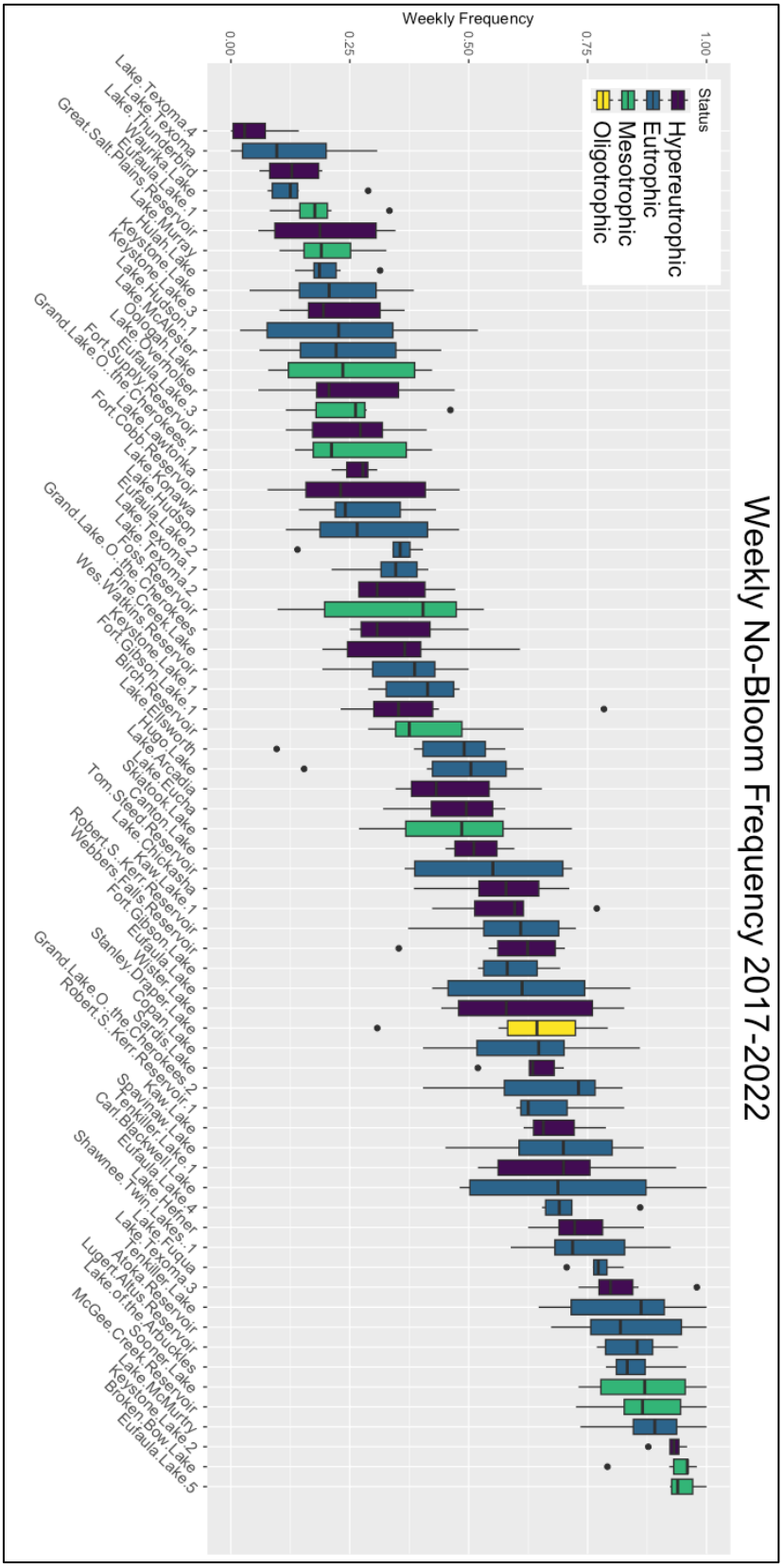

Figure 16: Annual weekly no-bloom frequency

Total Bloom: Weekly total bloom frequency varies significantly between waterbodies (Figure 17). Waterbodies with the lowest weekly total bloom frequency include Eufaula Lake 5, Broken Bow Lake, Keystone Lake 2, and Lake McMurtry. Waterbodies with the highest total bloom frequency include Lake Texoma 4, Lake Texoma, Lake Thunderbird, and Waurika Lake.

Nine waterbodies show a significant positive trend over time (Table 10). Grand Lake O the Cherokees 2, Eufaula Lake, Shawnee Twin Lakes 1, and Lake Chickasha exhibited the largest positive trend, ranging from roughly four to three-week increases in weeks with a bloom per year.

Table 10: MK and Sen's Slope for trend detection of weekly total bloom frequency

Waterbody	Tau	MK P value	Sen's Slope	Sen's p.value
Grand.Lake.O.the.Cherokees.2	**1.00000**	**0.00853**	**0.08047**	**0.00853**
Lake.Ellsworth	**1.00000**	**0.00853**	**0.05769**	**0.00853**
Lake.Texoma.3	**1.00000**	**0.00853**	**0.03434**	**0.00853**
Great.Salt.Plains.Reservoir	**0.86667**	**0.02417**	**0.05618**	**0.02417**
Lake.Chickasha	**0.86667**	**0.02417**	**0.06071**	**0.02417**
Shawnee.Twin.Lakes...1	**0.86667**	**0.02417**	**0.07127**	**0.02417**
Lake.Texoma.2	**0.89443**	**0.02677**	**0.04313**	**0.02677**
Eufaula.Lake	**0.82808**	**0.03538**	**0.08338**	**0.03538**
McGee.Creek.Reservoir	**0.82808**	**0.03538**	**0.04409**	**0.03538**

No significant differences in weekly total bloom frequency were evident between trophic states (Fig E2, Table A4). Hypereutrophic waterbodies exhibited a significant positive trend in weekly total bloom frequency of a roughly 1.5 week increase per year (Table F10). No other trophic states exhibited a significant trend.

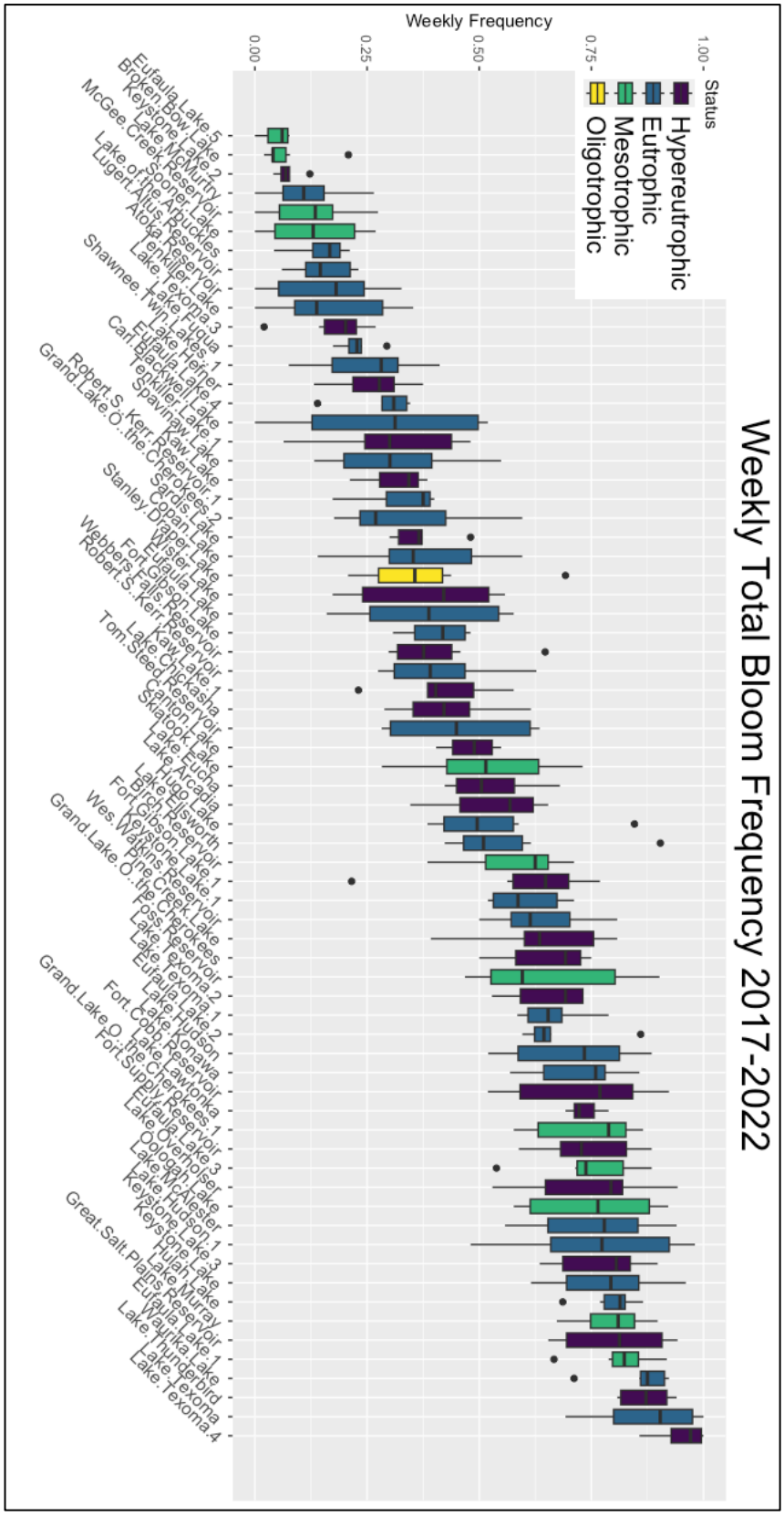

Figure 17: Weekly total bloom frequency

SEVERITY

All waterbodies experienced a bloom above the WHO high-risk threshold of 100,000 cells/ml (red dashed line) during most years (Figure 18). The Kruskal-Wallis test indicated that there were significant differences between waterbodies' max bloom severity (Table A5). Lakes with the lowest max bloom severity included Lake Murray, Birch Reservoir, Grand Lake O the Cherokees 2, Lake Hudson, Robert S Kerr Reservoir, Lake Eucha, and Spavinaw Lake. The waterbodies with some of the highest severity blooms included Eufaula Lake 1, Lake Texoma 4, and Keystone Lake 3. Grand Lake O the Cherokees 1 showed a significant positive trend of max bloom severity increasing by approximately 45,000 cells/ml/yr. (Table 11).

Table 11: MK and Sen's slope for trend detection of max bloom severity. See C11 for complete trend analysis

Waterbody	Tau	MK P value	Sen's Slope (cells/mL/year)	Sen's p.value
Grand.Lake.O.the.Cherokees.1	**0.82808**	**0.03538**	**45237**	**0.03538**

Max bloom severity by trophic status showed a significant difference between groups (Figure F6, Table A6). Hypereutrophic waterbodies were significantly higher in maximum bloom severity compared to mesotrophic and oligotrophic waterbodies (Table B7). Eutrophic waterbodies exhibited a significantly higher maximum bloom intensity than mesotrophic waterbodies. Eutrophic and mesotrophic waterbodies exhibit strong upward trends with an estimated average increase in maximum bloom severity of approximately 80,000 cells/ml/year and 45,000 cells/ml/year, respectively (Table F11).

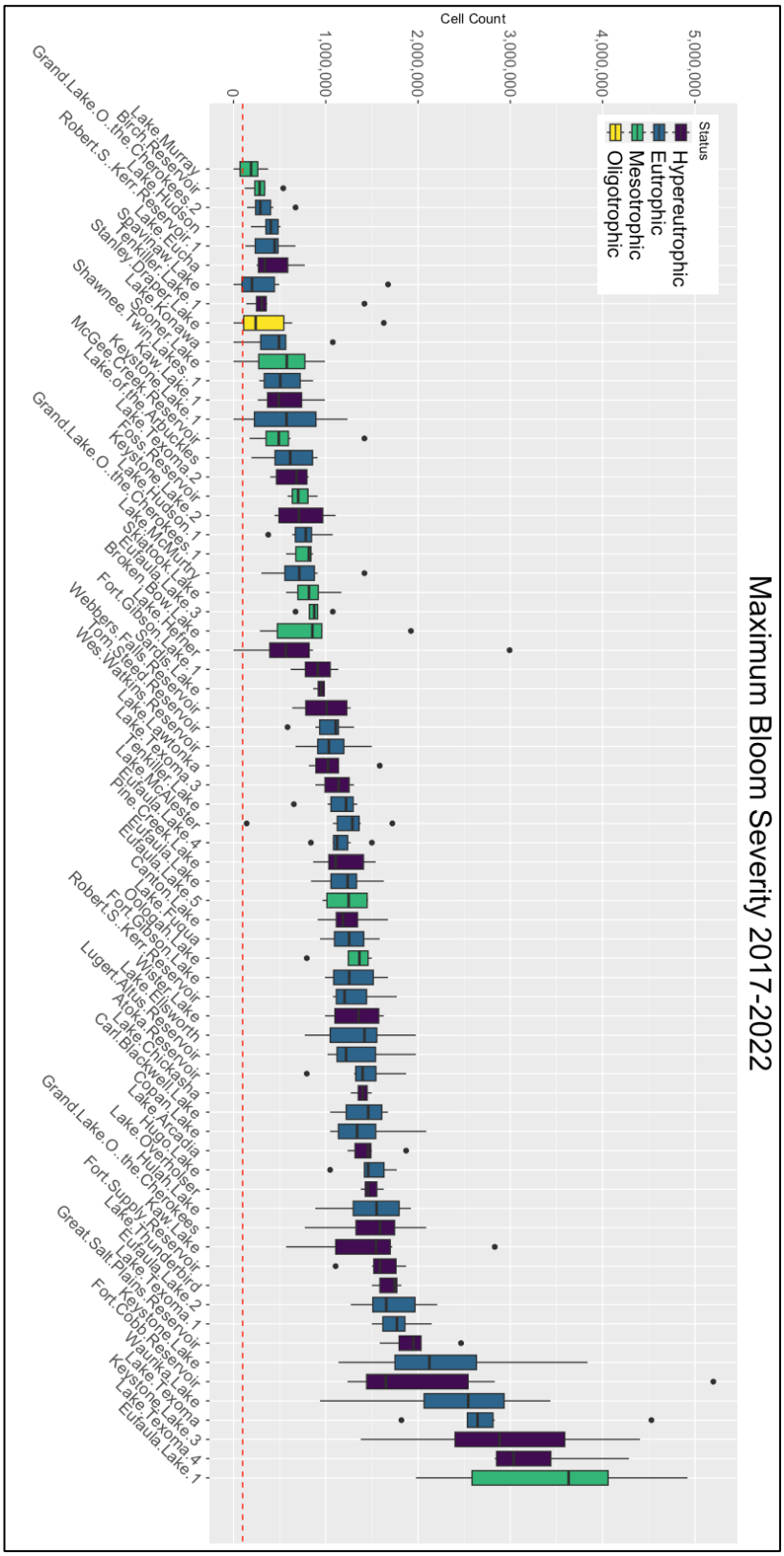

Figure 18: Maximum bloom severity (cells/ml). The red dashed line indicates the WHO high-risk threshold of 100,000 cells/ml.

SPATIAL EXTENT

High Risk Blooms: The statewide monthly high-risk bloom extent showed a significant positive trend over the study period. High-risk bloom extent increased by approximately 2 km^2 /season/year across the state (Table 12). The seasonality of bloom spatial extent can be observed in Figure 19. Half of the waterbodies showed a significant upward trend for high-risk spatial bloom extent (Table 13). Individual waterbody high-risk monthly bloom extent can be seen in Appendix D. The distribution of the waterbody's monthly high-risk bloom percent coverage can be seen in Figure 20. Multiple lakes including Lake Overholser, Fort Supply Reservoir, Lake Chickasha, and Lake Lawtonka spent many months with complete or near-complete coverage of a high-risk bloom. The monthly high-risk bloom percent coverage significantly differed between tropic states (Figure E3, Table A7). All trophic states are significantly different from each other, with hypereutrophic waterbodies exhibiting the highest monthly percentage of high bloom coverage (Table B8).

Table 12: Seasonal Mann-Kendall and Sens Slope for State Extent Trends

Bloom Risk Level	Tau	SMK p value	Sen's Slope (km^2/year)	Sen's p value
High Extent State	**0.4444444**	**1.43E-05**	**2.13675**	**0.01298803**
Medium Extent State	**0.3555555**	**0.00051874**	**1.351452**	**0.00120528**
Low Extent State	**0.3464021**	**0.00074528**	**0.18**	**0.00326559**
Total Extent State	**0.4222222**	**3.76E-05**	**3.806572**	**0.00891278**

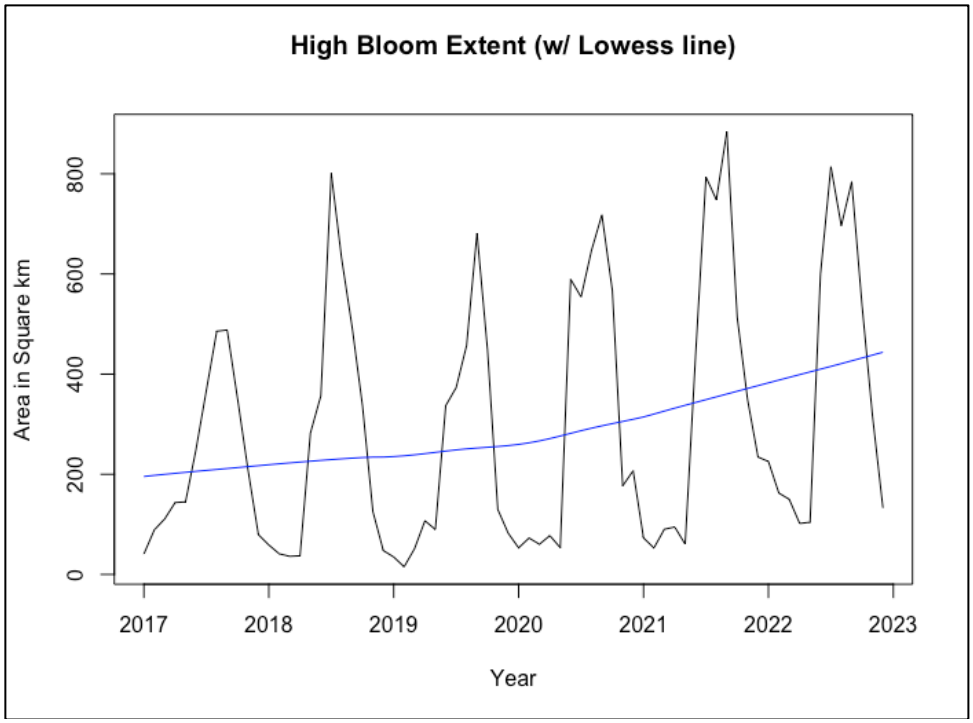

Figure 19: Statewide Extent of High Risk Blooms

Table 13: Seasonal Mann-Kendall and Sen's Slope for High Risk Bloom Extent. See Table C12 for full trend analysis.

Waterbody	tau	SMK P value	Sen's Slope(% coverage)	Sen's p.value
Tom.Steed.Reservoir	**0.55446**	**0.00000**	**0.00703**	**0.00004**
Lake.Texoma.3	**0.51219**	**0.00000**	**0.00037**	**0.00006**
Skiatook.Lake	**0.47173**	**0.00001**	**0.00059**	**0.00442**
Lugert.Altus.Reservoir	**0.43829**	**0.00002**	**0.00758**	**0.00001**
Waurika.Lake	**0.40645**	**0.00015**	**0.00140**	**0.00034**
Canton.Lake	**0.37997**	**0.00028**	**0.00189**	**0.00126**
Lake.Texoma.4	**0.37585**	**0.00030**	**0.00165**	**0.00288**
Keystone.Lake.3	**0.37542**	**0.00050**	**0.00018**	**0.00782**
Lake.Hudson.1	**0.37256**	**0.00093**	**0.00000**	**0.00714**
Eufaula.Lake.4	**0.36218**	**0.00094**	**0.00012**	**0.02656**
Lake.Texoma.2	**0.40236**	**0.00107**	**0.00000**	**0.00068**
Webbers.Falls.Reservoir	**0.33144**	**0.00176**	**0.00013**	**0.01135**
Lake.of.the.Arbuckles	**0.33055**	**0.00230**	**0.00000**	**0.01660**
Pine.Creek.Lake	**0.31193**	**0.00253**	**0.00116**	**0.03799**
Eufaula.Lake.5	**0.30714**	**0.00298**	**0.00151**	**0.02830**
Keystone.Lake	**0.31066**	**0.00311**	**0.00020**	**0.02916**
Lake.Texoma.1	**0.30171**	**0.00331**	**0.00116**	**0.00788**
Lake.Hudson	**0.33126**	**0.00351**	**0.00000**	**0.00553**
Robert.S.Kerr.Reservoir.1	**0.34756**	**0.00395**	**0.00000**	**0.00228**
Fort.Gibson.Lake.1	**0.31894**	**0.00491**	**0.00000**	**0.02577**
Keystone.Lake.1	**0.35932**	**0.00531**	**0.00000**	**0.00954**
Keystone.Lake.2	**0.32696**	**0.00609**	**0.00000**	**0.00903**
Broken.Bow.Lake	**0.42410**	**0.00669**	**0.00000**	**0.15414**
Grand.Lake.O.the.Cherokees.1	**0.28394**	**0.00699**	**0.00014**	**0.01167**
Sardis.Lake	**0.26185**	**0.01069**	**0.00197**	**0.01026**
Sooner.Lake	**0.40188**	**0.01785**	**0.00000**	**0.02923**
Eufaula.Lake.1	**0.23333**	**0.02274**	**0.00141**	**0.04725**
Eufaula.Lake.2	**0.24958**	**0.02315**	**0.00001**	**0.13336**
McGee.Creek.Reservoir	**0.25400**	**0.02389**	**0.00000**	**0.05618**
Kaw.Lake	**0.25145**	**0.02464**	**0.00000**	**0.04315**
Copan.Lake	**0.23112**	**0.02494**	**0.00330**	**0.02342**
Lake.Ellsworth	**0.24721**	**0.02716**	**0.00000**	**0.11762**
Carl.Blackwell.Lake	**0.25870**	**0.03329**	**0.00000**	**0.12301**
Eufaula.Lake	**0.21859**	**0.03346**	**0.00027**	**0.13168**
Birch.Reservoir	**0.26405**	**0.04700**	**0.00000**	**0.04095**

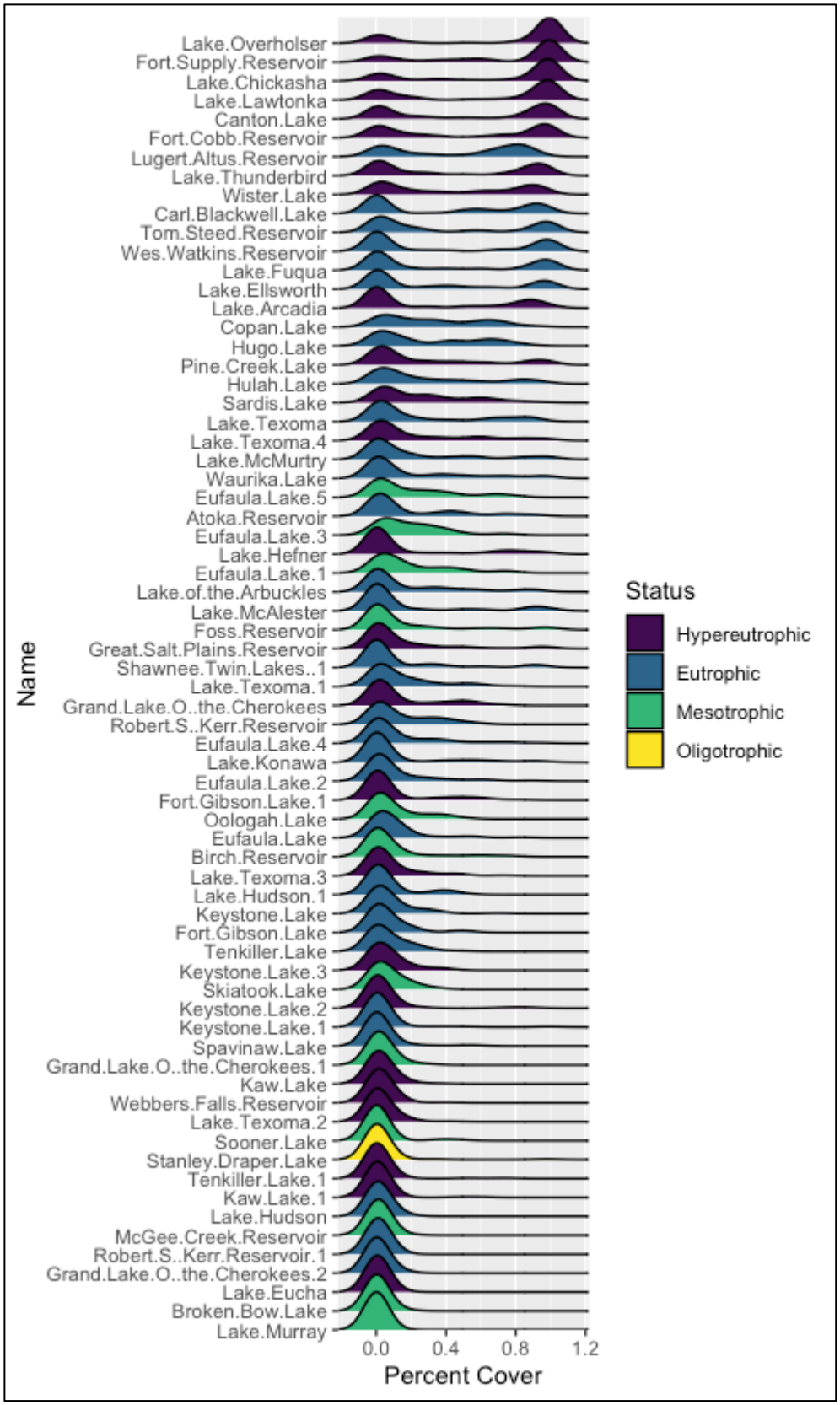

Figure 20: Distribution of monthly high-risk bloom percent cover

Medium Risk Blooms: Statewide monthly medium-risk bloom extent showed an upward trend of approximately 1.3 km^2 /season/year (Table 12). Medium-risk bloom extent exhibited a seasonal pattern (Figure 21). Twenty-one waterbodies showed a significant trend in medium-risk bloom extent, all positive (Table C13). Many lakes exhibited very few months with a medium-risk bloom covering more than 25% of the waterbody (Figure 22). Significant differences in monthly medium-risk bloom coverage were found between all trophic states except eutrophic and mesotrophic waterbodies (Figure E3, Table B9).

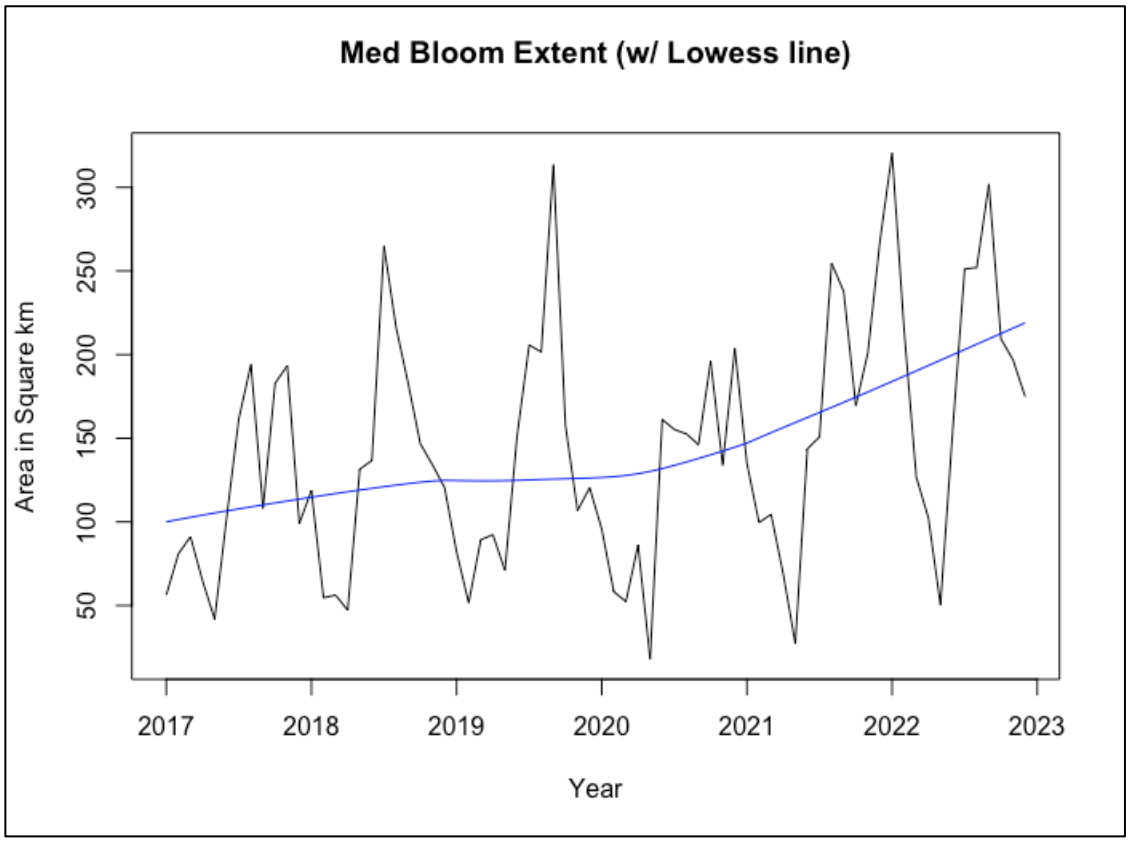

Figure 21: State extent of medium-risk blooms

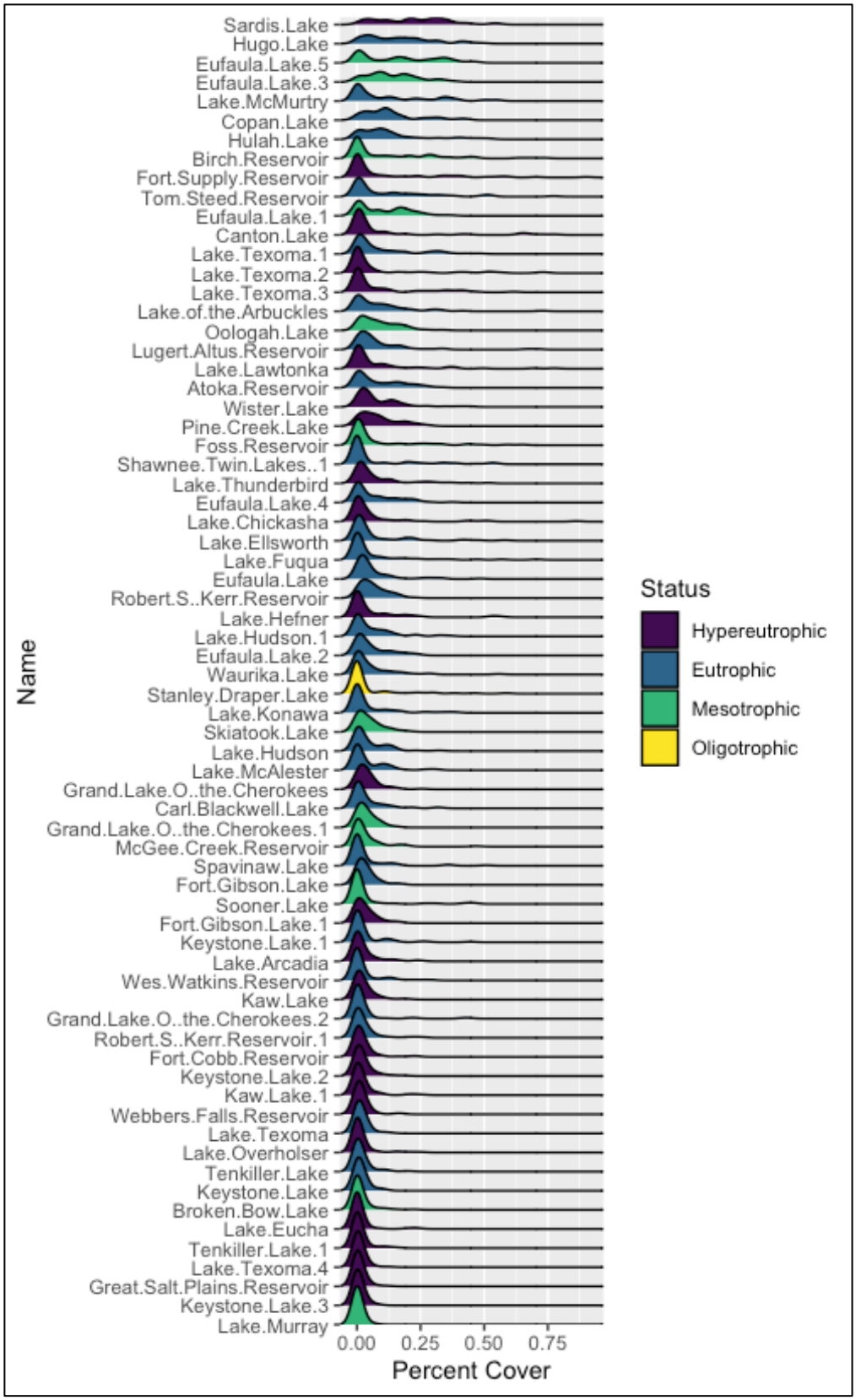

Figure 22: Distribution of monthly medium-risk bloom percent coverage of waterbody

Low Risk Bloom: Statewide monthly low-risk bloom extent exhibited a significant positive trend over time (Table 12). Statewide low-risk bloom extent appeared to peak in late 2021 and early 2022 (Figure 23). Seventeen waterbodies exhibited a significant trend. All trending lakes except Lake Chickasha showed a positive trend (Table C13). Sardis Lake and Hugo Lake showed some of the highest low-risk bloom percent coverage distribution, similar to medium-risk bloom percent coverage distribution (Figure 24). Significant differences between trophic states were found in monthly low-risk bloom percent coverage (Figure E3, Table A7). Mesotrophic waterbodies were considered significantly different from all other trophic groups with a greater low-risk bloom extent (Table B10).

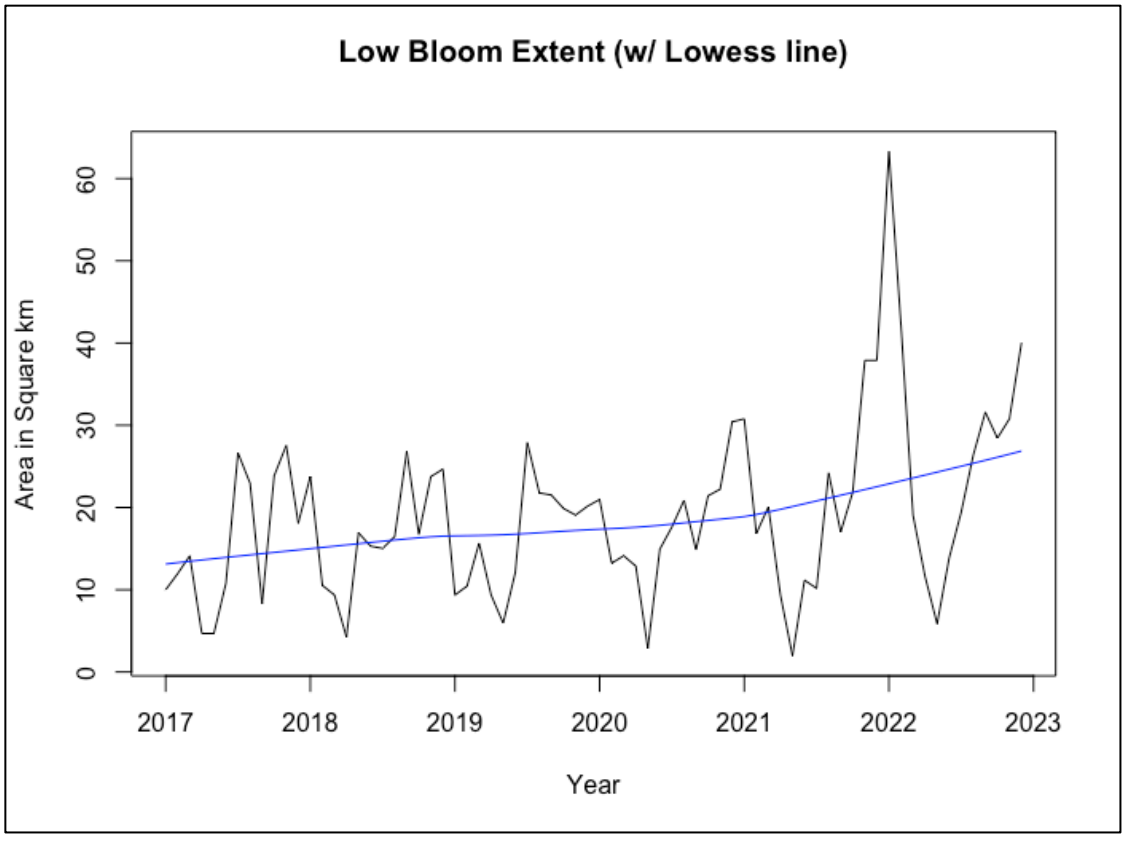

Figure 23: State extent for monthly low-risk blooms

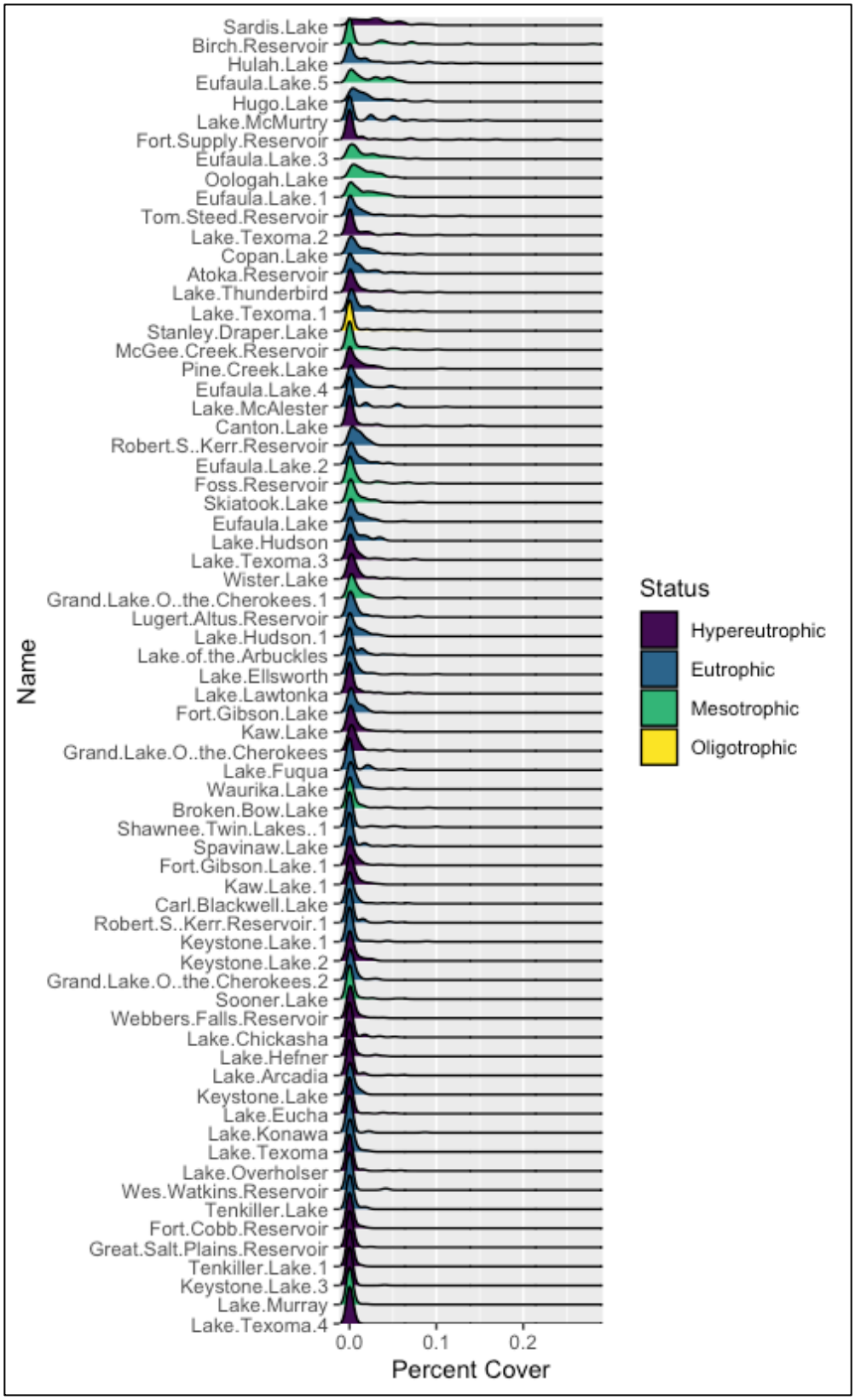

Figure 24: Monthly distribution of low-risk bloom percent coverage

Total Bloom: Statewide monthly total bloom extent showed a significant positive trend over time. Statewide monthly total bloom extent increased by almost 4 km^2/season/year (Table 12). The years 2017 and 2020 experienced lower peak total bloom extent (Fig 25). Thirty-six waterbodies showed a significant trend in total bloom extent over time, all positive (Table 14). Significant differences were found in monthly total bloom percent coverage between waterbodies (Figure 26, Table A7). All trophic states were significantly different from each other with hypereutrophic waterbodies exhibiting the greatest total bloom coverage followed by eutrophic, mesotrophic, and oligotrophic waterbodies, respectively (Figure E3, Table B11).

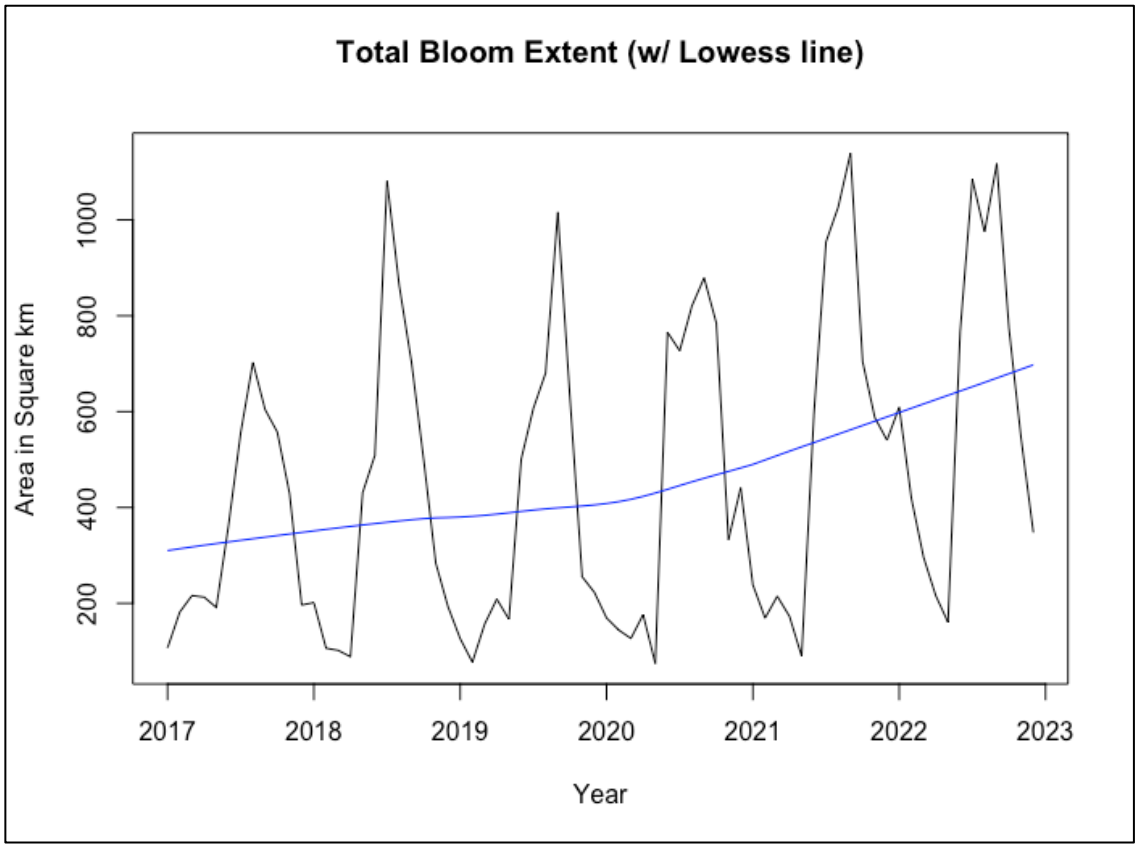

Figure 25: State Total Bloom Extent

Table 14: Seasonal Mann-Kendall and Sen's slope for monthly total bloom extent

Waterbody	Tau	MK P value	Sen's Slope (% coverage)	Sen's p.value
Skiatook.Lake	**0.49042**	**0.00000**	**0.00219**	**0.00021**
Lake.Texoma.3	**0.47635**	**0.00001**	**0.00103**	**0.00012**
Waurika.Lake	**0.44843**	**0.00002**	**0.00335**	**0.00025**
Tom.Steed.Reservoir	**0.43213**	**0.00003**	**0.00937**	**0.00003**
Lake.Texoma.1	**0.40670**	**0.00007**	**0.00272**	**0.00095**
Canton.Lake	**0.40134**	**0.00012**	**0.00178**	**0.00010**
Lake.Texoma.4	**0.38915**	**0.00017**	**0.00206**	**0.00221**
Lake.Texoma.2	**0.40109**	**0.00038**	**0.00010**	**0.00060**
Grand.Lake.O.the.Cherokees.1	**0.36213**	**0.00042**	**0.00114**	**0.00058**
Lugert.Altus.Reservoir	**0.35758**	**0.00050**	**0.00532**	**0.00030**
Keystone.Lake.1	**0.40095**	**0.00050**	**0.00000**	**0.00041**
Lake.Hudson	**0.36169**	**0.00053**	**0.00080**	**0.00139**
Grand.Lake.O.the.Cherokees	**0.35912**	**0.00054**	**0.00138**	**0.00884**
Lake.Hudson.1	**0.37774**	**0.00058**	**0.00138**	**0.00045**
Keystone.Lake.3	**0.35812**	**0.00082**	**0.00040**	**0.00677**
Lake.Ellsworth	**0.34565**	**0.00093**	**0.00113**	**0.01735**
Kaw.Lake.1	**0.35387**	**0.00098**	**0.00016**	**0.00038**
Eufaula.Lake.2	**0.34483**	**0.00137**	**0.00065**	**0.05827**
Eufaula.Lake.4	**0.33730**	**0.00182**	**0.00063**	**0.02519**
Eufaula.Lake.5	**0.31937**	**0.00190**	**0.00371**	**0.01437**
Keystone.Lake	**0.31952**	**0.00212**	**0.00079**	**0.00963**
Fort.Gibson.Lake.1	**0.31001**	**0.00332**	**0.00057**	**0.00594**
Pine.Creek.Lake	**0.30000**	**0.00341**	**0.00252**	**0.05237**
Robert.S.Kerr.Reservoir.1	**0.31844**	**0.00503**	**0.00000**	**0.00236**
Eufaula.Lake	**0.27778**	**0.00670**	**0.00072**	**0.07441**
Broken.Bow.Lake	**0.31557**	**0.00821**	**0.00000**	**0.04419**
Webbers.Falls.Reservoir	**0.27177**	**0.00928**	**0.00062**	**0.00404**
Sooner.Lake	**0.37501**	**0.00955**	**0.00000**	**0.00343**
Atoka.Reservoir	**0.26668**	**0.01044**	**0.00169**	**0.03403**
Keystone.Lake.2	**0.25822**	**0.01361**	**0.00035**	**0.00721**
Grand.Lake.O.the.Cherokees.2	**0.26523**	**0.01376**	**0.00000**	**0.00314**
StanleyDraperLake	**0.29677**	**0.02064**	**0.00000**	**0.01654**
Sardis.Lake	**0.22222**	**0.03006**	**0.00408**	**0.04022**
Lake.of.the.Arbuckles	**0.22614**	**0.03127**	**0.00152**	**0.03386**
Copan.Lake	**0.21852**	**0.03363**	**0.00379**	**0.02696**
Birch.Reservoir	**0.24549**	**0.03618**	**0.00000**	**0.01623**
Lake.Chickasha	**0.24838**	**0.04589**	**0.00000**	**0.03009**

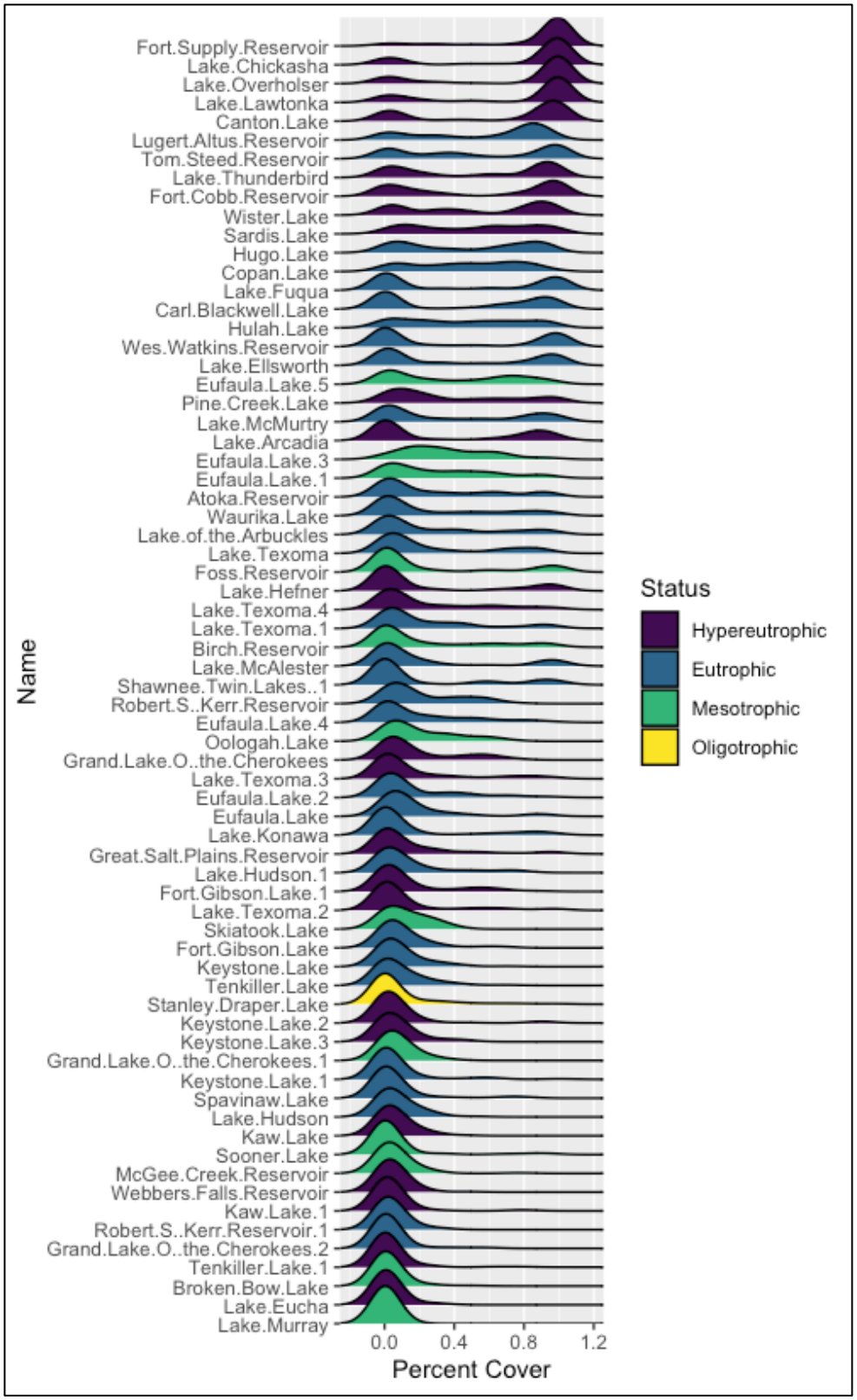

Figure 26: Total Bloom monthly percent coverage

CHAPTER V

DISCUSSION

Harmful algal blooms endanger human health and ecosystem services and lead to significant economic costs. Proper management of HABs is bolstered with increased information about their bloom dynamics, frequency, intensity, and spatial extent. Understanding bloom dynamics can help prioritize which waterbodies need nutrient criteria or adaptive management interventions (Coffer, Schaeffer, Salls, et al., 2021). This analysis supports HABHRCA's recommendations to strengthen long-term HAB monitoring (Urquhart et al., 2017).

Oklahoma HAB frequency is increasing statewide for all bloom risk categories. This is consistent with trends observed elsewhere. It was observed that the waterbodies with the strongest trends are not necessarily those with the highest average frequency. This potentially indicates that those moderate HAB frequency waterbodies pose the most significant risk of worsening over time. Eutrophic and hypereutrophic lakes experience the highest high-risk bloom frequency. They are significantly different from mesotrophic and oligotrophic waterbodies. This is consistent with our understanding of trophic status and bloom formation. These waterbodies often have higher nutrient loadings and other conditions favorable to HAB formation. Weekly frequencies exhibited similar trends to the average frequency for both waterbodies and trophic states. Weekly frequency is a more immediately understandable metric but lacks the spatial component factored into the average frequency.

The most severe blooms often occurred in eutrophic and hypereutrophic lakes. They are frequently found on the waterbodies with the highest bloom frequencies. The combination of most frequent and severe blooms indicates that those waterbodies likely pose some of the highest human exposure and health risks. Almost all waterbodies experienced a bloom above the WHO's highest risk threshold. This further illustrates the importance of real-time access to data, as public health risks frequently occur across the state.

Grand Lake shows a significant trend in worsening severity over time, with an average increase in max HAB abundance by approximately 45,000 cells per year. Grand Lake had the famous HAB outbreak in 2011 that resulted in people becoming sick, including Sen. Jim Inhofe (Meyers, 2011). Grand Lake is characterized as one of the lakes with the most severe blooms. Grand Lake experienced a toxic outbreak in July 2022 (Wheeler, 2022).

One of the more recent notorious Oklahoma blooms occurred in 2021. Lake Hefner experienced a severe bloom prior to Fourth of July weekend in 2021 (Briones, 2021). This bloom is reflected in the satellite imagery. Lake Hefner's max severity bloom in 2021 was nearly 3,000,000 cells/mL. This max severity is six times greater than the average severity of approximately 500,000 cells/mL observed in Lake Hefner over the other five years.

Many of the waterbodies have positive trends in the monthly spatial extent of HABs. Increasing spatial extent is consistent with increasing frequency as frequency takes into account the fraction of blooming to non-blooming pixels for the waterbody. Lake Hefner's severe 2021 bloom is reflected in its seasonal spatial extent graph (Appendix D). Almost the entire lake was experiencing a bloom during July 2021. Increased spatial extent could pose a greater risk for exposure as more of the lake is affected. A larger spatial extent could also indicate an increasing HAB biomass. This is important if a bloom is producing cyanotoxins. Florida and Ohio have similarly seen increases in the spatial extent of HABs over time (Urquhart et al., 2017).

The spatial extent of blooms is highly varied between waterbodies. Some waterbodies exhibit consistent seasonal patterns that increase through the summer before decreasing through the winter. Lake Thunderbird and Lake Fuqua exhibit such a pattern. Others may exhibit low coverage year-round with the exception of one or two spikes in extent in the summer. Sooner Lake exhibits such a pattern with three comparatively major blooms occurring throughout the entire study period. Others may exhibit a spike in spatial extent only once or twice throughout the study period. The high level of stochasticity found in lake's spatial extent indicates that other factors may have a higher relative importance in driving those blooms than solely climatic conditions. Lake McMurtry is an example of a lake with a highly stochastic monthly bloom spatial extent.

Sooner Lake exhibited the most trending bloom dynamics of any of the waterbodies. Sooner Lake exhibited significant positive frequency trends for all bloom risk categories. Sooner Lake also exhibited significant positive trends in monthly bloom spatial extent for all risk categories. A sharp increase occurs after 2019 for the high-risk spatial extent on Sooner Lake. Investigation into any potential surrounding changes could help indicate the potential driver of these blooms. These changes could include land use or non-point source discharge changes. Identifying local scale drivers of bloom formation could help shape management choices. These findings highlight the importance of continued monitoring and management efforts to mitigate the impact of HABs on aquatic ecosystems and human health.

Limitations

Limitations of this study include the natural error and uncertainty associated with remote sensing data. The CI has been validated to have a total mean absolute percent error (MAPE) of approximately 29%. Blooms can be highly ephemeral and there is limited validation data for temporally coincident (<1day) satellite overpasses (Lunetta et al., 2015). This increases the level

of uncertainty in regards to the validation of CyAN for ephemeral blooms. There is a level of uncertainty as to the true HAB abundance. HABs can exhibit heterogeneous spatial distribution, so a 300m pixel likely includes many different cell densities throughout its area. These impacts are reduced through the use of bloom risk categories. All of the analysis, with the exception of severity, is calculated based on the bloom risk categories. Exact biomasses of blooms are less crucial when examining trends than it would be for the purposes of issuing health advisories. Additional sensor limitations include the ability to only capture cyanobacteria in the top 1-2m of the water column (Coffer et al., 2020; D. R. Mishra et al., 2005). Blooms that are occur below 2m in depth may result in underestimates of HAB abundance.

The use of maximum weekly composites impacts the conclusions that can be drawn regarding differences between bloom risk categories. More low and medium-risk blooms may be occurring throughout the week that are overshadowed by a higher risk bloom. This holds true with the monthly spatial extents that are maximum monthly composites. This helps account for the high-risk blooms having a much larger spatial extent than medium-risk and low-risk blooms.

The blooms of most concern for health and ecological reasons are high-risk blooms. These blooms are being fully represented in the data. Daily data was not available until 2019. Its use in the future could overcome some of these limitations when a long enough time series becomes available. The imagery can only report the state of the bloom at the time of the satellite overpass. There is a chance that a bloom is characterized as medium-risk even if it develops into a high-risk bloom hours later or vice versa based solely on satellite overpass timing.

Additional limitations centered around the imagery resolution include its inability to capture the littoral zone or small dendritic coves of waterbodies. Littoral zones can be where blooms may first occur. Frequency and extent may be underrepresented as a result with their exclusion. Littoral zones can also be where scum and algal mats accumulate. This potentially

underrepresents the maximum severity of blooms. Waterbody edges also pose some of the highest exposure risks to those recreating, pets, and livestock. The larger spatial resolution of the sensor also results in only the largest lakes being able to be analyzed by this method. A more comprehensive analysis of trends and patterns could be conducted as data availability increases with finer resolution sensors.

Only one waterbody is classed as oligotrophic. Conclusions about the differences in bloom dynamics between the oligotrophic waterbody and other trophic states should be limited due to this limited sample size. Certain waterbodies have multiple sections and multiple trophic states including Lake Texoma, Eufaula Lake, Grand Lake, and Keystone. While these sections may be classified differently, they do not necessarily have a hard and fast separation between them. This results in pixels that lie near another section potentially representing a mix of the trophic states. This can thereby reduce observed differences between trophic states.

Weekly frequency was calculated based off of one pixel for the purpose of this analysis. This one-pixel threshold could lead to erroneous pixel errors impacting conclusions. Larger lakes have been shown to be overclassified and smaller lakes to be under classified when a 1 pixel threshold is used (Coffer et al., 2020). An analysis of bloom frequency that compared single pixel, 10%, 20%, and 30% area thresholds for classifying a bloom found that a 10% threshold reduced the most variability between thresholds and appeared most appropriate (Coffer et al., 2020). Future analysis could utilize a 10% or even 5% threshold to have a higher level of confidence in weekly frequency conclusions.

The 6 year length of the study period limited the types of analysis and strength of conclusions that could be drawn. The study period is comprised of every full year of data available from the OLCI sensors. Maximum weekly composites were chosen because daily data did not become available until 2019. The use of daily data could reduce the limitations that result from max composites

when a longer time series of it becomes available. A suggested ten years of observations would help account for short term trends that may be observed versus long-term, persistent trends that may be present.

CyAN is still limited in its ability to produce consistently accurate cell counts. CyAN is still limited in its applicability for issuing health and safety advisories based on cyanobacteria abundance estimates. CyAN does provide a consistent product for detecting presence and absence of cyanobacteria and for analyzing long term trends and patterns. This information can still be incredibly beneficial for management decisions and inform future prediction models.

Future Considerations

This analysis is targeted at characterizing some aspects of HAB dynamics in the largest waterbodies in the state. This analysis does not attempt to answer why different waterbodies exhibit different trends and what factors may be driving those trends, with the exception of observing trends by trophic state.

Factors of particular interest include potential patterns and trends by ecoregion. Ecoregions are areas that are ecologically and geographically similar. They are based on climate, temperature, soil type, precipitation, vegetation, and other environmental parameters (ORD US EPA, 2015). Oklahoma is comprised of 12 level III ecoregions. These ecoregions represent a diverse range of climate conditions, terrain, geology, soil, and land use (ORD US EPA, 2016). Analysis of cyanoHAB occurrence has occurred for Level 1 ecoregions across CONUS (Coffer et al., 2020) but never for finer-scale ecoregions in Oklahoma. This indicates a current gap in knowledge that could be filled.

Analysis of the lakes' water quality parameters could provide more context about Oklahoma bloom dynamics. Nutrient loading, particularly nitrogen and phosphorous, are known drivers of HABs. Physical parameters including water temperature are known to contribute to bloom

formation. These relationships are not always clear or consistent. HABs have been shown to occur even below ice sheets (Bertilsson et al., 2013; Vincent & Quesada, 2012) and in low nutrient lakes (Reinl et al., 2021). Nutrient limitation impacts on bloom formation have been shown to change seasonally (J. Li, Hansson, & Persson, 2018). Inclusion of lake morphology and bathymetry data could potentially lead to improved biomass estimates, particularly in lakes with high vertical water column mixing (Bosse et al., 2019). Hydrodynamic regimes such as water residence time has also appeared to be a significant factor in bloom biomass across a range of latitudes (Giani, Taranu, von Rückert, & Gregory-Eaves, 2020; Richardson et al., 2018). Water residence time was shown as a consistent driver in varying waterbody types, such as lakes and reservoirs (Giani et al., 2020).

Climatic drivers could be paired with this analysis. Climate change is the most immediately obvious climatic driver. It has been implicated as a key driver (Alex Elliott, Thackeray, Huntingford, & Jones, 2005; Briand, Leboulanger, Humbert, Bernard, & Dufour, 2004; O'Neil, Davis, Burford, & Gobler, 2012; Hans W. Paerl, Hall, & Calandrino, 2011; Hans W. Paerl & Paul, 2012). Warming temperatures lead to increased stratification and provide a competitive advantage to cyanobacteria allowing them to dominate the system (O'Neil et al., 2012). The impact of altered precipitation regimes including intense precipitation events followed by prolonged droughts is not entirely understood. It is expected that these conditions will favor cyanobacteria through increased nutrient loadings and stable physical conditions (Hans W. Paerl & Huisman, 2008; Richardson et al., 2018). The spatial variability of rainfall around Oklahoma could be investigated to see if that plays a driving role in local bloom formation.

Land use changes have been considered important drivers for HAB formation worldwide (Kakouei et al., 2021; Liao et al., 2016; Weber, Mishra, Wilde, & Kramer, 2020). Analysis of surrounding land use of the different waterbodies could help identify if any of those factors are contributing to bloom formation. Characterizing the surrounding land use of those waterbodies

identified to have severe or worsening HABs could help support management actions. These actions could include the installation of infrastructure designed to reduce runoff and sediment from entering the waterbodies.

While remote sensing can provide cost-effective data on the frequency, extent, and severity of HABs, it cannot determine toxicity (Stumpf et al., 2016b). There is limited data on how frequently HABs in Oklahoma produce cyanotoxins. Remote sensing techniques aimed at identifying toxigenic strains of cyanobacteria are being developed (Legleiter et al., 2022), but actual toxicity information still relies on ground sampling. In-situ sampling that includes genera ID and enumeration as well as toxicity assessments could improve management decisions regarding bloom outbreaks, particularly when paired with remote sensing data.

HAB frequency and severity could be examined in the context of public and private water systems (PPWS) and recreationally exposure risks. All but a handful of the selected waterbodies are considered a PPWS or emergency water supply system (EWS). It is estimated that statewide public water systems (PWS) serve approximately 3.7 million customers (OK DEQ, 2023). Additional water treatment can be required if extracellular toxins are present (Coffer, Schaeffer, Foreman, et al., 2021). Previous assessments have shown that Oklahoma has 71 water intakes resolvable by CyAN (Coffer et al., 2021). Applying an area threshold around these intakes could identify which drinking water systems are most at risk and prioritize management needs.

An assessment of HAB frequency and severity based on recreation and exposure risks could highlight the potential human health concerns. Millions of people utilize Oklahoma lakes for recreation and fishing opportunities each year. Blooms occurring near boat ramps, public beaches, and public access points could pose a higher human health risk. Lakes with the highest public use may benefit from increased monitoring. Lakes with the highest public use may also be the most economically affected when blooms, or even just bloom advisories, are issued. The

quality of the environment and recreational opportunities has been shown to matter to the people of Oklahoma (Boyer, Sanders, Melstrom, Stoecker, & Ferrell, 2017). BGA advisories have been shown to keep people, and their tourism dollars away (Boyer, Danniels, et al., 2017). One study showed that campers at Lake Tenkiller would pay an average of $13.08 per visit if they could receive assurances that there would be no harmful algal blooms during their trip (Boyer, Sanders, et al., 2017). A prioritization of the bloom management strategies available based on the environmental, economic, and social needs could provide the framework for addressing HABs in Oklahoma in the most cost-effective and impactful way.

Summary

This study characterized OK HAB dynamics relating to frequency, extent, and severity for 69 waterbodies in OK utilizing the Cyanobacteria Assessment Network. Cyanobacterial frequency, extent, and severity varied seasonally, with summer (June-August) accounting for the highest frequency, extent, and bloom severity. Statewide, bloom frequency and spatial extent exhibit increasing trends between 2017-2022. Individual waterbodies exhibit varied bloom dynamics, both between individual years as well as between different waterbodies, illustrating the complex nature of cyanoHAB bloom formation. Hypereutrophic and eutrophic waterbodies bloom more frequently, severely, and cover more of the waterbody. Nutrient loadings are likely one of the largest drivers for bloom formation in these waterbodies.

This analysis takes a large scale view at Oklahoma HAB dynamics while also characterizing trophic-grouped and individual waterbodies. It further provides a framework for highlighting which waterbodies may be of most concern. Managers can identify reservoirs of interest and proceed to investigate bloom dynamics at a finer scale. A pixel-scale analysis of bloom frequency and severity would illustrate exactly which areas of the waterbody experiences the most frequent and severe blooms. This information could help target management and mitigation activities to

where they are most needed. The results from this analysis can help inform management decisions in regards to water quality management and recreational guidelines across Oklahoma.

REFERENCES

Akoglu, H. (2018). User's guide to correlation coefficients. *Turkish Journal of Emergency Medicine*, *18*(3), 91–93. https://doi.org/10.1016/j.tjem.2018.08.001

Alex Elliott, J., Thackeray, S. J., Huntingford, C., & Jones, R. G. (2005). Combining a regional climate model with a phytoplankton community model to predict future changes in phytoplankton in lakes. *Freshwater Biology*, *50*(8), 1404–1411. https://doi.org/10.1111/j.1365-2427.2005.01409.x

Algae, B.-G. (2021, February 18). Blue-Green Algae. Retrieved February 27, 2023, from Blue-Green Algae website: https://www.in.gov/idem/algae/

Anderson, D., Hoagland, P., & Kaoru, Y. (2009). *Estimated Annual Economic Impacts from Harmful Algal Blooms (HABs) in the United States*. NOAA. Retrieved from NOAA website: https://apps.dtic.mil/sti/citations/ADA386861

Barnes, B. B., Hu, C., Schaeffer, B. A., Lee, Z., Palandro, D. A., & Lehrter, J. C. (2013). MODIS-derived spatiotemporal water clarity patterns in optically shallow Florida Keys waters: A new approach to remove bottom contamination. *Remote Sensing of Environment*, *134*, 377–391. https://doi.org/10.1016/j.rse.2013.03.016

Berdalet, E. (2017). *Global Harmful Algal Blooms, Science and Implementation Plan* (p. 64). Delaware and Paris: SCOR and IOC.

Bergamino, N., Horion, S., Stenuite, S., Cornet, Y., Loiselle, S., Plisnier, P.-D., & Descy, J.-P. (2010). Spatio-temporal dynamics of phytoplankton and primary production in Lake Tanganyika using a MODIS based bio-optical time series. *Remote Sensing of Environment*, *114*(4), 772–780. https://doi.org/10.1016/j.rse.2009.11.013

Bertilsson, S., Burgin, A., Carey, C. C., Fey, S. B., Grossart, H.-P., Grubisic, L. M., … Smyth, R. L. (2013). The under-ice microbiome of seasonally frozen lakes. *Limnology and Oceanography*, *58*(6), 1998–2012. https://doi.org/10.4319/lo.2013.58.6.1998

Binding, C. E., Greenberg, T. A., Jerome, J. H., Bukata, R. P., & Letourneau, G. (2011). An assessment of MERIS algal products during an intense bloom in Lake of the Woods. *Journal of Plankton Research*, *33*(5), 793–806. https://doi.org/10.1093/plankt/fbq133

Bingham, M., Kinnell, J., Bingham, M., & Kinnell, J. (2020). The Tourism Impacts of Lake Erie Hazardous Algal Blooms. In *Inland Waters—Dynamics and Ecology*. IntechOpen. https://doi.org/10.5772/intechopen.93625

Bláha, L., Babica, P., & Maršálek, B. (2009). Toxins produced in cyanobacterial water blooms – toxicity and risks. *Interdisciplinary Toxicology*, *2*(2), 36–41. https://doi.org/10.2478/v10102-009-0006-2

Bosse, K. R., Sayers, M. J., Shuchman, R. A., Fahnenstiel, G. L., Ruberg, S. A., Fanslow, D. L., … Burtner, A. M. (2019). Spatial-temporal variability of in situ cyanobacteria vertical structure in Western Lake Erie: Implications for remote sensing observations. *Journal of Great Lakes Research*, *45*(3), 480–489. https://doi.org/10.1016/j.jglr.2019.02.003

Boyer, T., Danniels, B., & Melstrom, R. (2017). *Algal Blooms in Oklahoma: Economic Impacts - Oklahoma State University*. OSU. Retrieved from https://extension.okstate.edu/fact-sheets/algal-blooms-in-oklahoma-economic-impacts.html

Boyer, T., Sanders, L., Melstrom, R., Stoecker, A., & Ferrell, S. (2017, March 1). Water-based Recreation in Oklahoma: Water Rights, Valuation and Implications For Public Policy, Economic Development and Management - Oklahoma State University. Retrieved April 14, 2023, from OSU Extentsion website: https://extension.okstate.edu/fact-sheets/water-based-recreation-in-oklahoma.html

Breinlinger, S., Phillips, T. J., Haram, B. N., Mareš, J., Martínez Yerena, J. A., Hrouzek, P., … Wilde, S. B. (2021). Hunting the eagle killer: A cyanobacterial neurotoxin causes vacuolar myelinopathy. *Science*, *371*(6536), eaax9050. https://doi.org/10.1126/science.aax9050

Brezonik, P. L., Olmanson, L. G., Finlay, J. C., & Bauer, M. E. (2015). Factors affecting the measurement of CDOM by remote sensing of optically complex inland waters. *Remote Sensing of Environment*, *157*, 199–215. https://doi.org/10.1016/j.rse.2014.04.033

Briand, J.-F., Leboulanger, C., Humbert, J.-F., Bernard, C., & Dufour, P. (2004). Cylindrospermopsis Raciborskii (cyanobacteria) Invasion at Mid-Latitudes: Selection, Wide Physiological Tolerance, Orglobalwarming?1. *Journal of Phycology*, *40*(2), 231–238. https://doi.org/10.1111/j.1529-8817.2004.03118.x

Briones, A. (2021, June 30). Oklahoma City official warns people about blue-green algae in Lake Hefner. Retrieved March 6, 2023, from KOCO website: https://www.koco.com/article/oklahoma-city-official-warns-people-about-blue-green-algae-in-lake-hefner/36892851

Cannizzaro, J. P., & Carder, K. L. (2006). Estimating chlorophyll a concentrations from remote-sensing reflectance in optically shallow waters. *Remote Sensing of Environment*, *101*(1), 13–24. https://doi.org/10.1016/j.rse.2005.12.002

Carder, K. L., Cannizzaro, J. P., & Lee, Z. (2005). Ocean color algorithms in optically shallow waters: Limitations and improvements. *Remote Sensing of the Coastal Oceanic Environment*, *5885*, 57–67. SPIE. https://doi.org/10.1117/12.615039

Carmichael. (1992). *A Status Report on Planktonic Cyanobacteria (Blue-Green Algae) and their Toxins* (No. 600R92079). Retrieved from https://nepis.epa.gov/Exe/ZyNET.exe/91020WC1.TXT?ZyActionD=ZyDocument&Client=EPA&Index=1991+Thru+1994&Docs=&Query=&Time=&EndTime=&SearchMethod=1&TocRestrict=n&Toc=&TocEntry=&QField=&QFieldYear=&QFieldMonth=&QFieldDay=&IntQFieldOp=0&ExtQFieldOp=0&XmlQuery=&File=D%3A%5Czyfiles%5CIndex%20Data%5C91thru94%5CTxt%5C00000031%5C91020WC1.txt&User=ANONYMOUS&Password=anonymous&SortMethod=h%7C-&MaximumDocuments=1&FuzzyDegree=0&ImageQuality=r75g8/r75g8/x150y150g16/i425&Display=hpfr&DefSeekPage=x&SearchBack=ZyActionL&Back=ZyActionS&BackDesc=Results%20page&MaximumPages=1&ZyEntry=1&SeekPage=x&ZyPURL#

Carmichael, W. (2008). A world overview—One-hundred-twenty-seven years of research on toxic cyanobacteria—Where do we go from here? *Advances in Experimental Medicine and Biology*, *619*, 105–125. https://doi.org/10.1007/978-0-387-75865-7_4

Chang, M., Teurlincx, S., Janse, J., Paerl, H., Mooij, W., & Janssen, A. (2020). Exploring How Cyanobacterial Traits Affect Nutrient Loading Thresholds in Shallow Lakes: A Modelling Approach. *Water*, *12*, 2467. https://doi.org/10.3390/w12092467

Chavula, G., Brezonik, P., Thenkabail, P., Johnson, T., & Bauer, M. (2009). Estimating chlorophyll concentration in Lake Malawi from MODIS satellite imagery. *Physics and Chemistry of the Earth, Parts A/B/C*, *34*(13), 755–760. https://doi.org/10.1016/j.pce.2009.07.015

Chromophoric Dissolved Organic Matter. (2022). Retrieved March 14, 2023, from Environmental Measurement Systems website: https://www.fondriest.com/environmental-measurements/parameters/water-quality/chromophoric-dissolved-organic-matter/

Clark, J. M., Schaeffer, B. A., Darling, J. A., Urquhart, E. A., Johnston, J. M., Ignatius, A. R., … Stumpf, R. P. (2017). Satellite monitoring of cyanobacterial harmful algal bloom frequency in recreational waters and drinking water sources. *Ecological Indicators*, *80*, 84–95. https://doi.org/10.1016/j.ecolind.2017.04.046

Clark, J. S., Carpenter, S. R., Barber, M., Collins, S., Dobson, A., Foley, J. A., … Wear, D. (2001). Ecological Forecasts: An Emerging Imperative. *Science*, *293*(5530), 657–660. https://doi.org/10.1126/science.293.5530.657

Coffer, M. M., Schaeffer, B. A., Darling, J. A., Urquhart, E. A., & Salls, W. B. (2020). Quantifying national and regional cyanobacterial occurrence in US lakes using satellite remote sensing. *Ecological Indicators*, *111*, 105976. https://doi.org/10.1016/j.ecolind.2019.105976

Coffer, M. M., Schaeffer, B. A., Foreman, K., Porteous, A., Loftin, K. A., Stumpf, R. P., … Darling, J. A. (2021). Assessing cyanobacterial frequency and abundance at surface waters near drinking water intakes across the United States. *Water Research*, *201*, 117377. https://doi.org/10.1016/j.watres.2021.117377

Coffer, M. M., Schaeffer, B. A., Salls, W. B., Urquhart, E., Loftin, K. A., Stumpf, R. P., … Darling, J. A. (2021). Satellite remote sensing to assess cyanobacterial bloom frequency across the United States at multiple spatial scales. *Ecological Indicators*, *128*, 107822. https://doi.org/10.1016/j.ecolind.2021.107822

Cyanobacteria (Blue-Green Algae) Tracker. (2016, July 18). Retrieved February 27, 2023, from Vermont Department of Health website: https://www.healthvermont.gov/tracking/cyanobacteria-tracker

Davis, T. W., Stumpf, R., Bullerjahn, G. S., McKay, R. M. L., Chaffin, J. D., Bridgeman, T. B., & Winslow, C. (2019). Science meets policy: A framework for determining impairment designation criteria for large waterbodies affected by cyanobacterial harmful algal blooms. *Harmful Algae*, *81*, 59–64. https://doi.org/10.1016/j.hal.2018.11.016

DiBiase, D. (2018). 4. Spectral Response Patterns | The Nature of Geographic Information. Retrieved March 14, 2023, from The Nature of Geographic Information website: https://www.e-education.psu.edu/natureofgeoinfo/c8_p5.html

Doerffer, R., & Schiller, H. (2007). The MERIS Case 2 water algorithm. *International Journal of Remote Sensing*, *28*(3–4), 517–535. https://doi.org/10.1080/01431160600821127

Dog Days of Summer: Pet Deaths From Toxic Algae Blooms Already Mounting | Environmental Working Group. (2020, July 28). Retrieved March 2, 2023, from https://www.ewg.org/news-insights/news/dog-days-summer-pet-deaths-toxic-algae-blooms-already-mounting

Dörnhöfer, K., & Oppelt, N. (2016). Remote sensing for lake research and monitoring – Recent advances. *Ecological Indicators*, *64*, 105–122. https://doi.org/10.1016/j.ecolind.2015.12.009

Dvornikov, Y., Leibman, M., Heim, B., Bartsch, A., Herzschuh, U., Skorospekhova, T., … Rößler, S. (2018). Terrestrial CDOM in Lakes of Yamal Peninsula: Connection to Lake and Lake Catchment Properties. *Remote Sensing*, *10*(2), 167. https://doi.org/10.3390/rs10020167

Erickson, J. (2013, April 1). Record-breaking 2011 Lake Erie algae bloom may be sign of things to come. Retrieved March 17, 2023, from University of Michigan News website: https://news.umich.edu/record-breaking-2011-lake-erie-algae-bloom-may-be-sign-of-things-to-come/

European Space Agency. (2021). MERIS - Earth Online. Retrieved March 13, 2023, from https://earth.esa.int/eogateway/instruments/meris

European Space Agency. (2023a). Sentinel-3—Instrument Payload—OLCI - Sentinel Online—Sentinel Online. Retrieved February 21, 2023, from https://sentinels.copernicus.eu/web/sentinel/missions/sentinel-3/instrument-payload/olci

European Space Agency. (2023b). User Guides—Sentinel-3 OLCI - Sentinel Online—Sentinel Online. Retrieved March 13, 2023, from https://sentinels.copernicus.eu/web/sentinel/user-guides/sentinel-3-olci

Ferrão-Filho, A. da S., & Kozlowsky-Suzuki, B. (2011). Cyanotoxins: Bioaccumulation and Effects on Aquatic Animals. *Marine Drugs*, *9*(12), 2729–2772. https://doi.org/10.3390/md9122729

Fisheries, N. (2021, October 7). Hitting Us Where it Hurts: The Untold Story of Harmful Algal Blooms | NOAA Fisheries. Retrieved March 17, 2023, from NOAA website: https://www.fisheries.noaa.gov/west-coast/science-data/hitting-us-where-it-hurts-untold-story-harmful-algal-blooms

Fishman, J., Iraci, L. T., Al-Saadi, J., Chance, K., Chavez, F., Chin, M., … Wang, M. (2012). The United States' Next Generation of Atmospheric Composition and Coastal Ecosystem Measurements: NASA's Geostationary Coastal and Air Pollution Events (GEO-CAPE) Mission. *Bulletin of the American Meteorological Society*, *93*(10), 1547–1566. https://doi.org/10.1175/BAMS-D-11-00201.1

Fournie, J., Hilborn, E., Codd, G., Coveney, M., Dyble, J., Havens, K., … Litaker, W. (2008). Cyanobacterial Harmful Algal Blooms: Chapter 31: Ecosystem Effects Workgroup Report. *U.S. Environmental Protection Agency Papers*. Retrieved from https://digitalcommons.unl.edu/usepapapers/37

Gholizadeh, M. H., Melesse, A. M., & Reddi, L. (2016). A Comprehensive Review on Water Quality Parameters Estimation Using Remote Sensing Techniques. *Sensors*, *16*(8), 1298. https://doi.org/10.3390/s16081298

Giani, A., Taranu, Z. E., von Rückert, G., & Gregory-Eaves, I. (2020). Comparing key drivers of cyanobacteria biomass in temperate and tropical systems. *Harmful Algae*, *97*, 101859. https://doi.org/10.1016/j.hal.2020.101859

Giardino, C., Bresciani, M., Valentini, E., Gasperini, L., Bolpagni, R., & Brando, V. E. (2015). Airborne hyperspectral data to assess suspended particulate matter and aquatic vegetation in a shallow and turbid lake. *Remote Sensing of Environment*, *157*, 48–57. https://doi.org/10.1016/j.rse.2014.04.034

Gitelson, A. A., Dall'Olmo, G., Moses, W., Rundquist, D. C., Barrow, T., Fisher, T. R., … Holz, J. (2008). A simple semi-analytical model for remote estimation of chlorophyll-a in turbid waters: Validation. *Remote Sensing of Environment*, *112*(9), 3582–3593. https://doi.org/10.1016/j.rse.2008.04.015

Glen, S. (2015). Kruskal Wallis H Test: Definition, Examples, Assumptions, SPSS. Retrieved March 27, 2023, from Statistics How To website: https://www.statisticshowto.com/probability-and-statistics/statistics-definitions/kruskal-wallis/

González Vilas, L., Spyrakos, E., & Torres Palenzuela, J. M. (2011). Neural network estimation of chlorophyll a from MERIS full resolution data for the coastal waters of Galician rias (NW Spain). *Remote Sensing of Environment*, *115*(2), 524–535. https://doi.org/10.1016/j.rse.2010.09.021

Gordon, H. R. (1997). Atmospheric correction of ocean color imagery in the Earth Observing System era. *Journal of Geophysical Research: Atmospheres*, *102*(D14), 17081–17106. https://doi.org/10.1029/96JD02443

Gower, J., King, S., Borstad, G., & Brown, L. (2005). Detection of intense plankton blooms using the 709 nm band of the MERIS imaging spectrometer. *International Journal of Remote Sensing*, *26*(9), 2005–2012. https://doi.org/10.1080/01431160500075857

HABHRCA. (2017). Retrieved March 1, 2023, from NCCOS Coastal Science Website website: https://coastalscience.noaa.gov/science-areas/stressor-impacts-mitigation/habhrca/

Heim, B., Oberhaensli, H., Fietz, S., & Kaufmann, H. (2005). Variation in Lake Baikal's phytoplankton distribution and fluvial input assessed by SeaWiFS satellite data. *Global and Planetary Change*, *46*(1), 9–27. https://doi.org/10.1016/j.gloplacha.2004.11.011

Herman, J., Cede, A., Spinei, E., Mount, G., Tzortziou, M., & Abuhassan, N. (2009). NO2 column amounts from ground-based Pandora and MFDOAS spectrometers using the direct-sun DOAS technique: Intercomparisons and application to OMI validation. *Journal of Geophysical Research: Atmospheres*, *114*(D13). https://doi.org/10.1029/2009JD011848

Hirsch, R. M., & Slack, J. R. (1984). A Nonparametric Trend Test for Seasonal Data With Serial Dependence. *Water Resources Research*, *20*(6), 727–732. https://doi.org/10.1029/WR020i006p00727

Hoagland, P., Anderson, D., & Kaoru, Y. (2002). The economic effects of harmful algal blooms in the United States: Estimates, assessment issues, and information needs. *Estuaries*, *25*, 819–837.

Hoagland, P., & Scatasta, S. (2006). The Economic Effects of Harmful Algal Blooms. In E. Granéli & J. T. Turner (Eds.), *Ecology of Harmful Algae* (pp. 391–402). Berlin, Heidelberg: Springer. https://doi.org/10.1007/978-3-540-32210-8_30

Hu, C. (2009). A novel ocean color index to detect floating algae in the global oceans. *Remote Sensing of Environment*, *113*(10), 2118–2129. https://doi.org/10.1016/j.rse.2009.05.012

Hu, C., Lee, Z., Ma, R., Yu, K., Li, D., & Shang, S. (2010). Moderate Resolution Imaging Spectroradiometer (MODIS) observations of cyanobacteria blooms in Taihu Lake, China. *Journal of Geophysical Research: Oceans*, *115*(C4). https://doi.org/10.1029/2009JC005511

Hudnell, H. K. (2010). The state of U.S. freshwater harmful algal blooms assessments, policy and legislation. *Toxicon*, *55*(5), 1024–1034. https://doi.org/10.1016/j.toxicon.2009.07.021

Humpage, A. (2008). Toxin types, toxicokinetics and toxicodynamics. In H. K. Hudnell (Ed.), *Cyanobacterial Harmful Algal Blooms: State of the Science and Research Needs* (pp. 383–415). New York, NY: Springer. https://doi.org/10.1007/978-0-387-75865-7_16

IOCCG. (2023). Historical Ocean-Colour Sensors. Retrieved March 10, 2023, from International Ocean Color Coordinating Group website: https://ioccg.org/resources/missions-instruments/historical-ocean-colour-sensors/

Kakouei, K., Kraemer, B. M., Anneville, O., Carvalho, L., Feuchtmayr, H., Graham, J. L., … Adrian, R. (2021). Phytoplankton and cyanobacteria abundances in mid-21st century lakes depend strongly on future land use and climate projections. *Global Change Biology*, *27*(24), 6409–6422. https://doi.org/10.1111/gcb.15866

Khan, R. M., Salehi, B., Mahdianpari, M., Mohammadimanesh, F., Mountrakis, G., & Quackenbush, L. J. (2021). A Meta-Analysis on Harmful Algal Bloom (HAB) Detection and Monitoring: A Remote Sensing Perspective. *Remote Sensing*, *13*(21), 4347. https://doi.org/10.3390/rs13214347

Kim, S.-W., Heckel, A., Frost, G. J., Richter, A., Gleason, J., Burrows, J. P., … Trainer, M. (2009). NO2 columns in the western United States observed from space and simulated by a regional chemistry model and their implications for NOx emissions. *Journal of Geophysical Research: Atmospheres*, *114*(D11). https://doi.org/10.1029/2008JD011343

Kiselev, V., Bulgarelli, B., & Heege, T. (2015). Sensor independent adjacency correction algorithm for coastal and inland water systems. *Remote Sensing of Environment*, *157*, 85–95. https://doi.org/10.1016/j.rse.2014.07.025

Koponen, S., Attila, J., Pulliainen, J., Kallio, K., Pyhälahti, T., Lindfors, A., … Hallikainen, M. (2007). A case study of airborne and satellite remote sensing of a spring bloom event in the Gulf of Finland. *Continental Shelf Research*, *27*(2), 228–244. https://doi.org/10.1016/j.csr.2006.10.006

Korosov, A. A., Pozdnyakov, D. V., Pettersson, L. H., & Grassl, H. (2007). Satellite-data-based study of seasonal and spatial variations of water temperature and water quality parameters in Lake Ladoga. *Journal of Applied Remote Sensing*, *1*(1), 011508. https://doi.org/10.1117/1.2834770

Kouakou, C. R. C., & Poder, T. G. (2019). Economic impact of harmful algal blooms on human health: A systematic review. *Journal of Water and Health*, *17*(4), 499–516. https://doi.org/10.2166/wh.2019.064

Kudela, R. M., Palacios, S. L., Austerberry, D. C., Accorsi, E. K., Guild, L. S., & Torres-Perez, J. (2015). Application of hyperspectral remote sensing to cyanobacterial blooms in inland waters. *Remote Sensing of Environment*, *167*, 196–205. https://doi.org/10.1016/j.rse.2015.01.025

Kutser, T. (2004). Quantitative detection of chlorophyll in cyanobacterial blooms by satellite remote sensing. *Limnology and Oceanography*, *49*(6), 2179–2189. https://doi.org/10.4319/lo.2004.49.6.2179

Kutser, T. (2009). Passive optical remote sensing of cyanobacteria and other intense phytoplankton blooms in coastal and inland waters. *International Journal of Remote Sensing*, *30*(17), 4401–4425. https://doi.org/10.1080/01431160802562305

Landsberg, J. H., Hendrickson, J., Tabuchi, M., Kiryu, Y., Williams, B. J., & Tomlinson, M. C. (2020). A large-scale sustained fish kill in the St. Johns River, Florida: A complex consequence of cyanobacteria blooms. *Harmful Algae*, *92*, 101771. https://doi.org/10.1016/j.hal.2020.101771

Latysheva, N., Junker, V. L., Palmer, W. J., Codd, G. A., & Barker, D. (2012). The evolution of nitrogen fixation in cyanobacteria. *Bioinformatics*, *28*(5), 603–606. https://doi.org/10.1093/bioinformatics/bts008

Lee, C., Orne, T., & Schaeffer, B. (2014, May 28). *How Can Remote Sensing Be Used for Water Quality Monitoring?* Presented at the National Water Quality Monitoring Council, Cincinnati, OH. Cincinnati, OH. Retrieved from https://cfpub.epa.gov/si/si_public_record_report.cfm?Lab=NERL&dirEntryId=285441

Legleiter, C. J., King, T. V., Carpenter, K. D., Hall, N. C., Mumford, A. C., Slonecker, T., … Rosen, B. H. (2022). Spectral mixture analysis for surveillance of harmful algal blooms (SMASH): A field-, laboratory-, and satellite-based approach to identifying cyanobacteria genera from remotely sensed data. *Remote Sensing of Environment*, *279*, 113089. https://doi.org/10.1016/j.rse.2022.113089

Li, J., Hansson, L.-A., & Persson, K. M. (2018). Nutrient Control to Prevent the Occurrence of Cyanobacterial Blooms in a Eutrophic Lake in Southern Sweden, Used for Drinking Water Supply. *Water*, *10*(7), 919. https://doi.org/10.3390/w10070919

Li, L., Li, L., Shi, K., Li, Z., & Song, K. (2012). A semi-analytical algorithm for remote estimation of phycocyanin in inland waters. *Science of The Total Environment*, *435–436*, 141–150. https://doi.org/10.1016/j.scitotenv.2012.07.023

Li, Y., Zhou, Q., Zhang, Y., Li, J., & Shi, K. (2021). Research Trends in the Remote Sensing of Phytoplankton Blooms: Results from Bibliometrics. *Remote Sensing*, *13*(21), 4414. https://doi.org/10.3390/rs13214414

Liao, J., Zhao, L., Cao, X., Sun, J., Gao, Z., Wang, J., … Huang, Y. (2016). Cyanobacteria in lakes on Yungui Plateau, China are assembled via niche processes driven by water physicochemical property, lake morphology and watershed land-use. *Scientific Reports*, *6*(1), 36357. https://doi.org/10.1038/srep36357

Lin, S., Novitski, L. N., Qi, J., & Stevenson, R. J. (2018). Landsat TM/ETM+ and machine-learning algorithms for limnological studies and algal bloom management of inland lakes. *Journal of Applied Remote Sensing*, *12*(2), 026003. https://doi.org/10.1117/1.JRS.12.026003

Liu, S., Glamore, W., Tamburic, B., Morrow, A., & Johnson, F. (2022). Remote sensing to detect harmful algal blooms in inland waterbodies. *The Science of the Total Environment*, *851*(Pt 1), 158096. https://doi.org/10.1016/j.scitotenv.2022.158096

Lopez, C. B., Jewett, E. B., Dortch, Q., Walton, B. T., & Hudnell, H. K. (2008). Scientific assessment of freshwater harmful algal blooms. *Http://Aquaticcommons.Org/Id/Eprint/14921*. Retrieved from https://aquadocs.org/handle/1834/30787

Lunetta, R. S., Schaeffer, B. A., Stumpf, R. P., Keith, D., Jacobs, S. A., & Murphy, M. S. (2015). Evaluation of cyanobacteria cell count detection derived from MERIS imagery across the eastern USA. *Remote Sensing of Environment*, *157*, 24–34. https://doi.org/10.1016/j.rse.2014.06.008

Matarrese, R., Morea, A., Tijani, K., De Pasquale, V., Chiaradia, M. T., & Pasquariello, G. (2008). A Specialized Support Vector Machine for Coastal Water Chlorophyll Retrieval from Water Leaving Reflectances. *IGARSS 2008 - 2008 IEEE International Geoscience and Remote Sensing Symposium*, *4*, IV-910-IV–913. https://doi.org/10.1109/IGARSS.2008.4779871

Matthews, M. W., Bernard, S., & Robertson, L. (2012). An algorithm for detecting trophic status (chlorophyll-a), cyanobacterial-dominance, surface scums and floating vegetation in inland and coastal waters. *Remote Sensing of Environment*, *124*, 637–652. https://doi.org/10.1016/j.rse.2012.05.032

McLeod, A. I. (2022). *Kendall: Kendall Rank Correlation and Mann-Kendall Trend Test*. Retrieved from https://CRAN.R-project.org/package=Kendall

Merel, S., Walker, D., Chicana, R., Snyder, S., Baurès, E., & Thomas, O. (2013). State of knowledge and concerns on cyanobacterial blooms and cyanotoxins. *Environment International*, *59*, 303–327. https://doi.org/10.1016/j.envint.2013.06.013

Meyers, J. (2011, July 1). Sen. Jim Inhofe believes swimming in Grand Lake caused his illness. *The Oklahoman*. Retrieved from https://www.oklahoman.com/story/lifestyle/health-fitness/2011/07/01/sen-jim-inhofe-believes-swimming-in-grand-lake-caused-his-illness/61153071007/

Michalak, A. M., Anderson, E. J., Beletsky, D., Boland, S., Bosch, N. S., Bridgeman, T. B., … Zagorski, M. A. (2013). Record-setting algal bloom in Lake Erie caused by agricultural and meteorological trends consistent with expected future conditions. *Proceedings of the National Academy of Sciences of the United States of America*, *110*(16), 6448–6452.

Mishra, D. R., Narumalani, S., Rundquist, D., & Lawson, M. (2005). Characterizing the vertical diffuse attenuation coefficient for downwelling irradiance in coastal waters: Implications for water penetration by high resolution satellite data. *ISPRS Journal of Photogrammetry and Remote Sensing*, *60*(1), 48–64. https://doi.org/10.1016/j.isprsjprs.2005.09.003

Mishra, S., & Mishra, D. R. (2012). Normalized difference chlorophyll index: A novel model for remote estimation of chlorophyll-a concentration in turbid productive waters. *Remote Sensing of Environment*, *117*, 394–406. https://doi.org/10.1016/j.rse.2011.10.016

Mishra, S., Mishra, D. R., Lee, Z., & Tucker, C. S. (2013). Quantifying cyanobacterial phycocyanin concentration in turbid productive waters: A quasi-analytical approach. *Remote Sensing of Environment*, *133*, 141–151. https://doi.org/10.1016/j.rse.2013.02.004

Mishra, S., Stumpf, R. P., Schaeffer, B. A., Werdell, P. J., Loftin, K. A., & Meredith, A. (2019). Measurement of Cyanobacterial Bloom Magnitude using Satellite Remote Sensing. *Scientific Reports*, *9*(1), 18310. https://doi.org/10.1038/s41598-019-54453-y

Moradi, M. (2014). Comparison of the efficacy of MODIS and MERIS data for detecting cyanobacterial blooms in the southern Caspian Sea. *Marine Pollution Bulletin*, *87*(1), 311–322. https://doi.org/10.1016/j.marpolbul.2014.06.053

Morel, A., & Prieur, L. (1977). Analysis of variations in ocean color. *Limnology and Oceanography*, *22*(4), 709–722. https://doi.org/10.4319/lo.1977.22.4.0709

Morgan, K. L., Larkin, S. L., & Adams, C. M. (2010). Red tides and participation in marine-based activities: Estimating the response of Southwest Florida residents. *Harmful Algae*, *9*(3), 333–341. https://doi.org/10.1016/j.hal.2009.12.004

Mouw, C. B., Greb, S., Aurin, D., DiGiacomo, P. M., Lee, Z., Twardowski, M., … Craig, S. E. (2015). Aquatic color radiometry remote sensing of coastal and inland waters: Challenges and recommendations for future satellite missions. *Remote Sensing of Environment*, *160*, 15–30. https://doi.org/10.1016/j.rse.2015.02.001

NASA. (2016). Introduction to the Electromagnetic Spectrum | Science Mission Directorate. Retrieved March 14, 2023, from https://science.nasa.gov/ems/01_intro

NASA. (2020). SeaWiFS Project Information Page. Retrieved March 13, 2023, from https://oceancolor.gsfc.nasa.gov/SeaWiFS/BACKGROUND/

NASA. (2023a). MODIS Web. Retrieved March 13, 2023, from https://modis.gsfc.nasa.gov/

NASA. (2023b). NASA Ocean Color. Retrieved November 7, 2022, from https://oceancolor.gsfc.nasa.gov/projects/cyan/

NASA Ocean Biology Processing Group. (2020). *Sentinel-3A OLCI Earth-observation, Full Resolution (EFR) Ocean Color (OC) Data* [Data set]. NASA Ocean Biology DAAC. https://doi.org/10.5067/SENTINEL-3A/OLCI/L2/EFR/OC/2022

Nguy-Robertson, A., Li, L., Tedesco, L. P., Wilson, J. S., & Soyeux, E. (2013). Determination of absorption coefficients for chlorophyll a, phycocyanin, mineral matter and CDOM from three central Indiana reservoirs. *Journal of Great Lakes Research*, *39*, 151–160. https://doi.org/10.1016/j.jglr.2013.04.004

NOAA. (2016, April). What is a harmful algal bloom? Retrieved November 7, 2022, from National Oceanic and Atmospheric Administration website: https://www.noaa.gov/what-is-harmful-algal-bloom

Odermatt, D., Giardino, C., & Heege, T. (2010). Chlorophyll retrieval with MERIS Case-2-Regional in perialpine lakes. *Remote Sensing of Environment*, *114*(3), 607–617. https://doi.org/10.1016/j.rse.2009.10.016

Odriozola, E., Ballabene, N., & Salamanco, A. (1984). [Poisoning in cattle caused by blue-green algae]. *Revista Argentina De Microbiologia*, *16*(4), 219–224.

OK DEQ. (2023). Public Water Supply. Retrieved April 14, 2023, from Oklahoma Department of Environmental Quality website: https://www.deq.ok.gov/water-quality-division/public-water-supply/

Oliver, R. L., & Walsby, A. E. (1988). [55] Buoyancy and suspension of planktonic cyanobacteria. In *Cyanobacteria*: *Vol. 167*. *Methods in Enzymology* (pp. 521–527). Academic Press. https://doi.org/10.1016/0076-6879(88)67058-3

Olmanson, L. G., Brezonik, P. L., & Bauer, M. E. (2011). Evaluation of medium to low resolution satellite imagery for regional lake water quality assessments. *Water Resources Research*, *47*(9). https://doi.org/10.1029/2011WR011005

O'Neil, J. M., Davis, T. W., Burford, M. A., & Gobler, C. J. (2012). The rise of harmful cyanobacteria blooms: The potential roles of eutrophication and climate change. *Harmful Algae*, *14*, 313–334. https://doi.org/10.1016/j.hal.2011.10.027

OWRB. (2018). *2017 Oklahoma Lakes Report: Beneficial Use Monitoring Program*. Oklahoma Water Resource Board.

Paerl, H. W., & Fulton, R. S. (2006). Ecology of Harmful Cyanobacteria. In E. Granéli & J. T. Turner (Eds.), *Ecology of Harmful Algae* (pp. 95–109). Berlin, Heidelberg: Springer. https://doi.org/10.1007/978-3-540-32210-8_8

Paerl, H. W., Fulton, R. S., Moisander, P. H., & Dyble, J. (2001). Harmful freshwater algal blooms, with an emphasis on cyanobacteria. *TheScientificWorldJournal*, *1*, 76–113. https://doi.org/10.1100/tsw.2001.16

Paerl, Hans W., Hall, N. S., & Calandrino, E. S. (2011). Controlling harmful cyanobacterial blooms in a world experiencing anthropogenic and climatic-induced change. *Science of The Total Environment*, *409*(10), 1739–1745. https://doi.org/10.1016/j.scitotenv.2011.02.001

Paerl, Hans W., & Huisman, J. (2008). Climate. Blooms like it hot. *Science (New York, N.Y.)*, *320*(5872), 57–58. https://doi.org/10.1126/science.1155398

Paerl, Hans W., & Paul, V. J. (2012). Climate change: Links to global expansion of harmful cyanobacteria. *Water Research*, *46*(5), 1349–1363. https://doi.org/10.1016/j.watres.2011.08.002

Pahlevan, N., Smith, B., Schalles, J., Binding, C., Cao, Z., Ma, R., … Stumpf, R. (2020). Seamless retrievals of chlorophyll-a from Sentinel-2 (MSI) and Sentinel-3 (OLCI) in inland and coastal waters: A machine-learning approach. *Remote Sensing of Environment*, *240*, 111604. https://doi.org/10.1016/j.rse.2019.111604

Palmer, S. C. J., Odermatt, D., Hunter, P. D., Brockmann, C., Présing, M., Balzter, H., & Tóth, V. R. (2015). Satellite remote sensing of phytoplankton phenology in Lake Balaton using 10years of MERIS observations. *Remote Sensing of Environment*, *158*, 441–452. https://doi.org/10.1016/j.rse.2014.11.021

Palmer, Stephanie C. J., Kutser, T., & Hunter, P. D. (2015). Remote sensing of inland waters: Challenges, progress and future directions. *Remote Sensing of Environment*, *157*, 1–8. https://doi.org/10.1016/j.rse.2014.09.021

Paulino, R. S., Martins, V. S., Novo, E. M. L. M., Barbosa, C. C. F., de Carvalho, L. A. S., & Begliomini, F. N. (2022). Assessment of Adjacency Correction over Inland Waters Using Sentinel-2 MSI Images. *Remote Sensing*, *14*(8), 1829. https://doi.org/10.3390/rs14081829

Pegram, R. A., Nichols, T., Etheridge, S., Humpage, A., LeBlanc, S., Love, A., … Thacker, R. (2008). Cyanotoxins Workgroup Report. In H. K. Hudnell (Ed.), *Cyanobacterial Harmful Algal Blooms: State of the Science and Research Needs* (pp. 317–381). New York, NY: Springer. https://doi.org/10.1007/978-0-387-75865-7_15

Philpot, W. D. (1991). The derivative ratio algorithm: Avoiding atmospheric effects in remote sensing. *IEEE Transactions on Geoscience and Remote Sensing*, *29*(3), 350–357. https://doi.org/10.1109/36.79425

Pohlert, T. (2020). *trend: Non-Parametric Trend Tests and Change-Point Detection*. Retrieved from https://CRAN.R-project.org/package=trend

Pozdnyakov, D., Korosov, A., Grassl, H., & Pettersson, L. (2005). An advanced algorithm for operational retrieval of water quality from satellite data in the visible. *International Journal of Remote Sensing*, *26*(12), 2669–2687. https://doi.org/10.1080/01431160500044697

Pozdnyakov, D. V., Korosov, A. A., Petrova, N. A., & Grassl, H. (2013). Multi-year satellite observations of Lake Ladoga's biogeochemical dynamics in relation to the lake's trophic status. *Journal of Great Lakes Research*, *39*, 34–45. https://doi.org/10.1016/j.jglr.2013.05.002

Prepas, E. E., Kotak, B. G., Campbell, L. M., & Evans, J. C. (1997). Accumulation and elimination of cyanobacterial hepatotoxins by the freshwater clam Anodonta grandis simpsoniana. *Canadian Journal of Fisheries and Aquatic Sciences*, *54*(1), 41–46. https://doi.org/10.1139/f96-261

Psilovikos, A., Margoni, S., & Psilovikos, A. (2006). Simulation and Trend Analysis of the Water Quality Monitoring Daily Data in Nestos River Delta. Contribution to the Sustainable Management and Results for the Years 2000–2002. *Environmental Monitoring and Assessment*, *116*(1), 543–562. https://doi.org/10.1007/s10661-006-7671-9

Qin, B., Li, W., Zhu, G., Zhang, Y., Wu, T., & Gao, G. (2015). Cyanobacterial bloom management through integrated monitoring and forecasting in large shallow eutrophic Lake Taihu (China). *Journal of Hazardous Materials*, *287*, 356–363. https://doi.org/10.1016/j.jhazmat.2015.01.047

R: The R Project for Statistical Computing. (2023). Retrieved March 6, 2023, from https://www.r-project.org/

Randolph, K., Wilson, J., Tedesco, L., Li, L., Pascual, D. L., & Soyeux, E. (2008). Hyperspectral remote sensing of cyanobacteria in turbid productive water using optically active pigments, chlorophyll a and phycocyanin. *Remote Sensing of Environment*, *112*(11), 4009–4019. https://doi.org/10.1016/j.rse.2008.06.002

Rao, Y. R., Howell, T., Watson, S. B., & Abernethy, S. (2014). On hypoxia and fish kills along the north shore of Lake Erie. *Journal of Great Lakes Research*, *40*(1), 187–191. https://doi.org/10.1016/j.jglr.2013.11.007

Reinart, A., & Kutser, T. (2006). Comparison of different satellite sensors in detecting cyanobacterial bloom events in the Baltic Sea. *Remote Sensing of Environment*, *102*(1), 74–85. https://doi.org/10.1016/j.rse.2006.02.013

Reinl, K. L., Brookes, J. D., Carey, C. C., Harris, T. D., Ibelings, B. W., Morales-Williams, A. M., … Zhan, Q. (2021). Cyanobacterial blooms in oligotrophic lakes: Shifting the high-nutrient paradigm. *Freshwater Biology*. https://doi.org/10.1111/fwb.13791

Richardson, J., Miller, C., Maberly, S. C., Taylor, P., Globevnik, L., Hunter, P., … Carvalho, L. (2018). Effects of multiple stressors on cyanobacteria abundance vary with lake type. *Global Change Biology*, *24*(11), 5044–5055. https://doi.org/10.1111/gcb.14396

Richter, R., Bachmann, M., Dorigo, W., & Muller, A. (2006). Influence of the Adjacency Effect on Ground Reflectance Measurements. *IEEE Geoscience and Remote Sensing Letters*, *3*(4), 565–569. https://doi.org/10.1109/LGRS.2006.882146

Ritchie, J., Zimba, P., & Everitt, J. (2003). Remote Sensing Techniques to Assess Water Quality. *Photogrammetric Engineering & Remote Sensing*, *69*. https://doi.org/10.14358/PERS.69.6.695

Rodger, H. D., Turnbull, T., Edwards, C., & Codd, G. A. (1994). Cyanobacterial (blue-green algal) bloom associated pathology in brown trout, Salmo trutta L., in Loch Leven, Scotland. *Journal of Fish Diseases*, *17*(2), 177–181. https://doi.org/10.1111/j.1365-2761.1994.tb00211.x

Ruiz-Verdú, A., Simis, S. G. H., de Hoyos, C., Gons, H. J., & Peña-Martínez, R. (2008). An evaluation of algorithms for the remote sensing of cyanobacterial biomass. *Remote Sensing of Environment*, *112*(11), 3996–4008. https://doi.org/10.1016/j.rse.2007.11.019

Sawaya, K. E., Olmanson, L. G., Heinert, N. J., Brezonik, P. L., & Bauer, M. E. (2003). Extending satellite remote sensing to local scales: Land and water resource monitoring using high-resolution imagery. *Remote Sensing of Environment*, *88*(1), 144–156. https://doi.org/10.1016/j.rse.2003.04.006

Schaeffer, B. A., Bailey, S. W., Conmy, R. N., Galvin, M., Ignatius, A. R., Johnston, J. M., … Wolfe, K. (2018). Mobile device application for monitoring cyanobacteria harmful algal blooms using Sentinel-3 satellite Ocean and Land Colour Instruments. *Environmental Modelling & Software : With Environment Data News*, *109*, 93–103. https://doi.org/10.1016/j.envsoft.2018.08.015

Schaeffer, B. A., Urquhart, E., Coffer, M., Salls, W., Stumpf, R. P., Loftin, K. A., & Jeremy Werdell, P. (2022a). Satellites quantify the spatial extent of cyanobacterial blooms across the United States at multiple scales. *Ecological Indicators*, *140*, 108990. https://doi.org/10.1016/j.ecolind.2022.108990

Schaeffer, B. A., Urquhart, E., Coffer, M., Salls, W., Stumpf, R. P., Loftin, K. A., & Jeremy Werdell, P. (2022b). Satellites quantify the spatial extent of cyanobacterial blooms across the United States at multiple scales. *Ecological Indicators*, *140*, 108990. https://doi.org/10.1016/j.ecolind.2022.108990

Sebastiá-Frasquet, M.-T., Aguilar-Maldonado, J.-A., Herrero-Durá, I., Santamaría-del-Ángel, E., Morell-Monzó, S., & Estornell, J. (2020). Advances in the Monitoring of Algal Blooms by Remote Sensing: A Bibliometric Analysis. *Applied Sciences*, *10*(21), 7877. https://doi.org/10.3390/app10217877

Seegers, B. N., Werdell, P. J., Vandermeulen, R. A., Salls, W., Stumpf, R. P., Schaeffer, B. A., … Loftin, K. A. (2021). Satellites for long-term monitoring of inland U.S. lakes: The MERIS time series and application for chlorophyll-a. *Remote Sensing of Environment*, *266*, 112685. https://doi.org/10.1016/j.rse.2021.112685

Seppälä, J., Ylöstalo, P., Kaitala, S., Hällfors, S., Raateoja, M., & Maunula, P. (2007). Ship-of-opportunity based phycocyanin fluorescence monitoring of the filamentous cyanobacteria bloom dynamics in the Baltic Sea. *Estuarine, Coastal and Shelf Science*, *73*(3), 489–500. https://doi.org/10.1016/j.ecss.2007.02.015

Shen, L., Xu, H., & Guo, X. (2012). Satellite Remote Sensing of Harmful Algal Blooms (HABs) and a Potential Synthesized Framework. *Sensors (Basel, Switzerland)*, *12*(6), 7778–7803. https://doi.org/10.3390/s120607778

Shen, M., Duan, H., Cao, Z., Xue, K., Loiselle, S., & Yesou, H. (2017). Determination of the Downwelling Diffuse Attenuation Coefficient of Lake Water with the Sentinel-3A OLCI. *Remote Sensing*, *9*(12), 1246. https://doi.org/10.3390/rs9121246

Shi, K., Zhang, Y., Qin, B., & Zhou, B. (2019). Remote sensing of cyanobacterial blooms in inland waters: Present knowledge and future challenges. *Science Bulletin*, *64*(20), 1540–1556. https://doi.org/10.1016/j.scib.2019.07.002

Simis, S. G. H., Peters, S. W. M., & Gons, H. J. (2005). Remote sensing of the cyanobacterial pigment phycocyanin in turbid inland water. *Limnology and Oceanography*, *50*(1), 237–245. https://doi.org/10.4319/lo.2005.50.1.0237

Smithee, D., Cauthron, J., Wright, C., Armstrong, G., & Gillilans, T. (2012). *Protocols for Harmful Algae Bloom Monitoring in Oklahoma Lakes*. Oklahoma Office of the Secretary of Environment.

Southard, G. M., Fries, L. T., & Barkoh, A. (2010). Prymnesium parvum: The Texas Experience1. *JAWRA Journal of the American Water Resources Association*, *46*(1), 14–23. https://doi.org/10.1111/j.1752-1688.2009.00387.x

Stal, L. J. (2011). Cyanobacteria, Diversity and Evolution of. In M. Gargaud, R. Amils, J. C. Quintanilla, H. J. (Jim) Cleaves, W. M. Irvine, D. L. Pinti, & M. Viso (Eds.), *Encyclopedia of Astrobiology* (pp. 397–401). Berlin, Heidelberg: Springer. https://doi.org/10.1007/978-3-642-11274-4_379

Stal, L. J. (2015). Nitrogen Fixation in Cyanobacteria. In *ELS* (pp. 1–9). John Wiley & Sons, Ltd. https://doi.org/10.1002/9780470015902.a0021159.pub2

Steffensen, D. A. (2008). Economic cost of cyanobacterial blooms. In H. K. Hudnell (Ed.), *Cyanobacterial Harmful Algal Blooms: State of the Science and Research Needs* (pp. 855–865). New York, NY: Springer. https://doi.org/10.1007/978-0-387-75865-7_37

Sterckx, S., Knaeps, S., Kratzer, S., & Ruddick, K. (2015). SIMilarity Environment Correction (SIMEC) applied to MERIS data over inland and coastal waters. *Remote Sensing of Environment*, *157*, 96–110. https://doi.org/10.1016/j.rse.2014.06.017

Stewart, I., Seawright, A. A., & Shaw, G. R. (2008). Cyanobacterial poisoning in livestock, wild mammals and birds – an overview. In H. K. Hudnell (Ed.), *Cyanobacterial Harmful Algal Blooms: State of the Science and Research Needs* (pp. 613–637). New York, NY: Springer. https://doi.org/10.1007/978-0-387-75865-7_28

Stumpf, R. P., Davis, T. W., Wynne, T. T., Graham, J. L., Loftin, K. A., Johengen, T. H., … Burtner, A. (2016a). Challenges for mapping cyanotoxin patterns from remote sensing of cyanobacteria. *Harmful Algae*, *54*, 160–173. https://doi.org/10.1016/j.hal.2016.01.005

Stumpf, R. P., Davis, T. W., Wynne, T. T., Graham, J. L., Loftin, K. A., Johengen, T. H., … Burtner, A. (2016b). Challenges for mapping cyanotoxin patterns from remote sensing of cyanobacteria. *Harmful Algae*, *54*, 160–173. https://doi.org/10.1016/j.hal.2016.01.005

Stumpf, R. P., Wynne, T. T., Baker, D. B., & Fahnenstiel, G. L. (2012). Interannual Variability of Cyanobacterial Blooms in Lake Erie. *PLOS ONE*, *7*(8), e42444. https://doi.org/10.1371/journal.pone.0042444

Sturm, M., & Denchak, M. (2019, August). Freshwater Harmful Algal Blooms 101. Retrieved March 1, 2023, from NRDC website: https://www.nrdc.org/stories/freshwater-harmful-algal-blooms-101

Taheri Shahraiyni, H., Bagheri Shouraki, S., Fell, F., Schaale, M., Fischer, J., Tavakoli, A., … Khodaparast, H. (2009). Application of the active learning method to the retrieval of pigment from spectral remote sensing reflectance data. *International Journal of Remote Sensing*, *30*(4), 1045–1065. https://doi.org/10.1080/01431160802448927

Tao, B., Mao, Z., Pan, D., Shen, Y., Zhu, Q., & Chen, J. (2013). Influence of bio-optical parameter variability on the reflectance peak position in the red band of algal bloom waters. *Ecological Informatics*, *16*, 17–24. https://doi.org/10.1016/j.ecoinf.2013.04.005

Tencalla, F. G., Dietrich, D. R., & Schlatter, C. (1994). *Toxicity of Microcystis aeruginosa peptide toxin to yearling rainbow trout (Oncorhynchus mykiss)*. Retrieved from http://kops.uni-konstanz.de/handle/123456789/6605

Topp, S. N., Pavelsky, T. M., Jensen, D., Simard, M., & Ross, M. R. V. (2020). Research Trends in the Use of Remote Sensing for Inland Water Quality Science: Moving Towards Multidisciplinary Applications. *Water*, *12*(1), 169. https://doi.org/10.3390/w12010169

Tucker, C. S. (2000). Off-Flavor Problems in Aquaculture. *Reviews in Fisheries Science*, *8*(1), 45–88. https://doi.org/10.1080/10641260091129170

Tyler, A. N., Hunter, P. D., Spyrakos, E., Groom, S., Constantinescu, A. M., & Kitchen, J. (2016). Developments in Earth observation for the assessment and monitoring of inland, transitional, coastal and shelf-sea waters. *Science of The Total Environment*, *572*, 1307–1321. https://doi.org/10.1016/j.scitotenv.2016.01.020

Urquhart, E. A., Schaeffer, B. A., Stumpf, R. P., Loftin, K. A., & Werdell, P. J. (2017). A method for examining temporal changes in cyanobacterial harmful algal bloom spatial extent using satellite remote sensing. *Harmful Algae*, *67*, 144–152. https://doi.org/10.1016/j.hal.2017.06.001

US EPA. (2018a, June 6). Causes of CyanoHABs [Overviews and Factsheets]. Retrieved November 7, 2022, from United States Environmental Protection Agengy website: https://www.epa.gov/cyanohabs/causes-cyanohabs

US EPA. (2018b, June 6). Learn about Cyanobacteria and Cyanotoxins [Overviews and Factsheets]. Retrieved November 7, 2022, from United States Environmental Protection Agengy website: https://www.epa.gov/cyanohabs/learn-about-cyanobacteria-and-cyanotoxins

US EPA. (2021). *Response to September 29, 2021 Inspector General Final Report "EPA Needs an Agencywide Strategic Action Plan to Address Harmful Algal Blooms"* [Memorandum].

US EPA. (2022, December 15). Cyanobacteria Assessment Network (CyAN). Retrieved February 27, 2023, from https://www.epa.gov/water-research/cyanobacteria-assessment-network-cyan

US EPA OIG. (2021). *EPA Needs an Agencywide Strategic Action Plan to Address Harmful Algal Blooms* (No. #21-E-0264). EPA Office of Inspector General.

US EPA, ORD. (2014a, June 18). Cyanobacteria Assessment Network (CyAN) [Overviews and Factsheets]. Retrieved November 7, 2022, from https://www.epa.gov/water-research/cyanobacteria-assessment-network-cyan

US EPA, ORD. (2014b, June 18). Cyanobacteria Assessment Network (CyAN) [Overviews and Factsheets]. Retrieved November 30, 2022, from https://www.epa.gov/water-research/cyanobacteria-assessment-network-cyan

US EPA, ORD. (2015, November 16). Ecoregions [Data and Tools]. Retrieved March 6, 2023, from https://www.epa.gov/eco-research/ecoregions

US EPA, ORD. (2016, March 9). Ecoregion Download Files by State—Region 6 [Data and Tools]. Retrieved March 6, 2023, from https://www.epa.gov/eco-research/ecoregion-download-files-state-region-6

US EPA, ORD. (2019, March 18). Cyanobacteria Assessment Network Application (CyAN app) [Data and Tools]. Retrieved March 20, 2023, from https://www.epa.gov/water-research/cyanobacteria-assessment-network-application-cyan-app

US EPA, OW. (2013, December 4). Indicators: Algal Toxins (microcystin) [Overviews and Factsheets]. Retrieved March 1, 2023, from https://www.epa.gov/national-aquatic-resource-surveys/indicators-algal-toxins-microcystin

US EPA, OW. (2015, November 27). Fourth Unregulated Contaminant Monitoring Rule [Data and Tools]. Retrieved March 1, 2023, from https://www.epa.gov/dwucmr/fourth-unregulated-contaminant-monitoring-rule

US EPA, OW. (2016, October 27). Additional Information about Cyanotoxins in Drinking Water [Data and Tools]. Retrieved March 1, 2023, from https://www.epa.gov/ground-water-and-drinking-water/additional-information-about-cyanotoxins-drinking-water

US EPA, OW. (2021, March 22). The Harmful Algal Bloom and Hypoxia Research and Control Amendments Act (HABHRCA) [Overviews and Factsheets]. Retrieved March 1, 2023, from https://www.epa.gov/cyanohabs/harmful-algal-bloom-and-hypoxia-research-and-control-amendments-act-habhrca

USGS. (2015). What is remote sensing and what is it used for? | U.S. Geological Survey. Retrieved March 14, 2023, from https://www.usgs.gov/faqs/what-remote-sensing-and-what-it-used

Vincent, W. F., & Quesada, A. (2012). Cyanobacteria in High Latitude Lakes, Rivers and Seas. In B. A. Whitton (Ed.), *Ecology of Cyanobacteria II: Their Diversity in Space and Time* (pp. 371–385). Dordrecht: Springer Netherlands. https://doi.org/10.1007/978-94-007-3855-3_13

Weber, S. J., Mishra, D. R., Wilde, S. B., & Kramer, E. (2020). Risks for cyanobacterial harmful algal blooms due to land management and climate interactions. *Science of The Total Environment*, *703*, 134608. https://doi.org/10.1016/j.scitotenv.2019.134608

Werdell, B. A. S., K. Loftin, R. P. Stumpf, P. J. (2015). *Agencies Collaborate, Develop a Cyanobacteria Assessment Network*. EOS. Retrieved from http://eos.org/science-updates/agencies-collaborate-develop-a-cyanobacteria-assessment-network

What is a spectral signature in remote sensing? – Geospatial Technology. (2023). Retrieved March 14, 2023, from https://mapasyst.extension.org/what-is-a-spectral-signature-in-remote-sensing/

Wheeler, G. (2022, July 12). Oklahoma officials urge caution near toxic blue-green algal bloom in Grand Lake. *KGOU*. Retrieved from https://www.kgou.org/science-technology-and-environment/2022-07-12/oklahoma-officials-urge-caution-near-toxic-blue-green-algal-bloom-in-grand-lake

Wiegand, C., & Pflugmacher, S. (2005). Ecotoxicological effects of selected cyanobacterial secondary metabolites a short review. *Toxicology and Applied Pharmacology*, *203*(3), 201–218. https://doi.org/10.1016/j.taap.2004.11.002

Wolf, D., Georgic, W., & Klaiber, H. A. (2017). Reeling in the damages: Harmful algal blooms' impact on Lake Erie's recreational fishing industry. *Journal of Environmental Management*, *199*, 148–157. https://doi.org/10.1016/j.jenvman.2017.05.031

World Health Organization. (2003). *Guidelines for safe recreational water environments. Volume 1, Coastal and fresh waters*. World Health Organization. Retrieved from World Health Organization website: https://apps.who.int/iris/handle/10665/42591

Wynne, T., Andrew, M., Briggs, T., Litaker, W., & Stumpf, R. P. (2020). *Harmful Algal Bloom Forecasting Branch Ocean Color Satellite Imagery Processing Guidelines, 2020 Update*. https://doi.org/10.25923/606T-M243

Wynne, T., Stumpf, R. P., Tomlinson, M. C., Fahnenstiel, G. L., Dyble, J., Schwab, D. J., & Joshi, S. J. (2013). Evolution of a cyanobacterial bloom forecast system in western Lake Erie: Development and initial evaluation. *Journal of Great Lakes Research*, *39*, 90–99. https://doi.org/10.1016/j.jglr.2012.10.003

Wynne, T., Stumpf, R., Tomlinson, M., & Dyble, J. (2010). Characterizing a cyanobacterial bloom in Western Lake Erie using satellite imagery and meteorological data. *Limnology and Oceanography - LIMNOL OCEANOGR*, *55*. https://doi.org/10.4319/lo.2010.55.5.2025

Wynne, T. T., Stumpf, R. P., Tomlinson, M. C., Warner, R. A., Tester, P. A., Dyble, J., & Fahnenstiel, G. L. (2008). Relating spectral shape to cyanobacterial blooms in the Laurentian Great Lakes. *International Journal of Remote Sensing*, *29*(12), 3665–3672. https://doi.org/10.1080/01431160802007640

Wynne, Timothy T., & Stumpf, R. P. (2015). Spatial and Temporal Patterns in the Seasonal Distribution of Toxic Cyanobacteria in Western Lake Erie from 2002–2014. *Toxins*, *7*(5), 1649–1663. https://doi.org/10.3390/toxins7051649

Yang, H., Kong, J., Hu, H., Du, Y., Gao, M., & Chen, F. (2022). A Review of Remote Sensing for Water Quality Retrieval: Progress and Challenges. *Remote Sensing*, *14*(8), 1770. https://doi.org/10.3390/rs14081770

Zach. (2020, September 29). Dunn's Test for Multiple Comparisons. Retrieved March 27, 2023, from Statology website: https://www.statology.org/dunns-test/

Zhang, M., Duan, H., Shi, X., Yu, Y., & Kong, F. (2012). Contributions of meteorology to the phenology of cyanobacterial blooms: Implications for future climate change. *Water Research*, *46*(2), 442–452. https://doi.org/10.1016/j.watres.2011.11.013

Zhang, Y., Ma, R., Zhang, M., Duan, H., Loiselle, S., & Xu, J. (2015). Fourteen-Year Record (2000–2013) of the Spatial and Temporal Dynamics of Floating Algae Blooms in Lake Chaohu, Observed from Time Series of MODIS Images. *Remote Sensing*, *7*(8), 10523–10542. https://doi.org/10.3390/rs70810523

Zhu, W., Yu, Q., Tian, Y. Q., Becker, B. L., Zheng, T., & Carrick, H. J. (2014). An assessment of remote sensing algorithms for colored dissolved organic matter in complex freshwater environments. *Remote Sensing of Environment*, *140*, 766–778. https://doi.org/10.1016/j.rse.2013.10.015

Zimba, P. V., Khoo, L., Gaunt, P. S., Brittain, S., & Carmichael, W. W. (2001). Confirmation of catfish, Ictalurus punctatus (Rafinesque), mortality from Microcystis toxins. *Journal of Fish Diseases*, *24*(1), 41–47. https://doi.org/10.1046/j.1365-2761.2001.00273.x

APPENDICES

APPENDIX A: Kruskal Wallis tests

Table A1: Kruskal Wallis for difference between waterbodies bloom frequency

Kruskal-Wallis Test	P value	Effect Size	Magnitude
High Frequency	3.29E-38	0.787	Large
Medium Frequency	7.14E-36	0.748	Large
Low Frequency	2.57E-32	0.689	Large
No Bloom Frequency	2.59E-36	0.756	Large
Total Bloom Frequency	4.71E-38	0.784	Large

Table A2: Kruskal Wallis test for difference in high bloom frequency by waterbody trophic state

Kruskal-Wallis Test	P value	Effect Size	Magnitude
High Bloom Frequency	7.60E-08	0.804	Moderate
Medium Bloom Frequency	0.325	0.00113	Small
Low Bloom Frequency	0.00341	0.026	Small
No Bloom Frequency	0.013	0.0189	Small
Total Bloom Frequency	7.82E-05	0.0454	Small

Table A3: Kruskal Wallis test of weekly bloom frequency differences between waterbodies

Kruskal-Wallis Test	P value	Effect Size	Magnitude
Weekly High Risk Bloom	8.32E-38	0.789	Large
Weekly Medium Risk Bloom	4.95E-21	0.499	Large
Weekly Low Risk Bloom	1.04E-05	0.178	Large
Weekly No Bloom	1.40E-37	0.785	Large
Weekly Total Bloom	1.40E-37	0.785	Large

Table A4: Kruskal Wallis test for difference in weekly bloom frequency between trophic states

Kruskal-Wallis Test	P value	Effect Size	Magnitude
High Bloom Week Trop	**0.0406**	**0.0129**	**small**
Medium Bloom Week Trop	**0.000597**	**0.035**	**small**
Low Bloom Week Trop	0.953	-0.0065	small
No Bloom Week Trop	0.0941	0.00827	small
Total Bloom Week Trop	0.0941	0.00827	small

Table A5: KW for difference in max bloom intensity between trophic states

Kruskal-Wallis Test	P value	Effect Size	Magnitude
Max Bloom Intensity	1.07E-31	0.686	Large

Table A6: Kruskal-Wallis test for difference in monthly bloom percent coverage between trophic waterbodies

Kruskal-Wallis Test	P value	Effect Size	Magnitude
High Risk Percent Coverage	2.40E-27	0.0251	small
Medium Risk Percent Coverage	7.40E-15	0.0133	small
Low Risk Percent Coverage	2.14E-25	0.0232	small
Total Bloom Percent Coverage	5.67E-23	0.0209	small

APPENDIX B: Dunn's pairwise comparisons

Table B1: Dunn's Pairwise Comparison of high-risk bloom frequency between trophic states

Pairs	Adjusted p value	Adjusted p significance
Hypereutrophic ~ Mesotrophic	**7.73E-07**	****
Eutrophic ~ Mesotrophic	**5.03E-05**	****
Hypereutrophic ~ Oligotrophic	**0.01270558**	*
Eutrophic ~ Oligotrophic	**0.03572199**	*
Eutrophic ~ Hypereutrophic	1	ns
Mesotrophic ~ Oligotrophic	1	ns

Table B2: Dunn's PWC for low bloom frequency between trophic states

Pairs	Adjusted p value	Adjusted p significance
Eutrophic ~ Hypereutrophic	1	ns
Eutrophic ~ Mesotrophic	1	ns
Eutrophic ~ Oligotrophic	**0.00267497**	**
Hypereutrophic ~ Mesotrophic	1	ns
Hypereutrophic ~ Oligotrophic	**0.00199132**	**
Mesotrophic ~ Oligotrophic	**0.00145594**	**

Table B3: Dunn's PWC difference in no bloom frequency between trophic states

Pairs	Adjusted p value	Adjusted p significance
Eutrophic ~ Hypereutrophic	**0.04953342**	*
Eutrophic ~ Mesotrophic	1	ns
Eutrophic ~ Oligotrophic	0.68100618	ns
Hypereutrophic ~ Mesotrophic	0.70238058	ns
Hypereutrophic ~ Oligotrophic	0.13815667	ns
Mesotrophic ~ Oligotrophic	0.53672934	ns

Table B4: Dunn's PWC for total bloom frequency between trophic states

Pairs	Adjusted p value	Adjusted p significance
Eutrophic ~ Hypereutrophic	1	ns
Eutrophic ~ Mesotrophic	**0.00351971**	**
Eutrophic ~ Oligotrophic	0.21845274	ns
Hypereutrophic ~ Mesotrophic	**0.00022711**	***
Hypereutrophic ~ Oligotrophic	0.1104455	ns
Mesotrophic ~ Oligotrophic	1	ns

Table B5: Dunn's PWC for high-risk weekly frequency

Pairs	Adjusted p value	Adjusted p significance
Eutrophic ~ Hypereutrophic	0.02941067	*
Eutrophic ~ Mesotrophic	1	ns
Eutrophic ~ Oligotrophic	1	ns
Hypereutrophic ~ Mesotrophic	1	ns
Hypereutrophic ~ Oligotrophic	1	ns
Mesotrophic ~ Oligotrophic	1	ns

Table B6: Dunn's PWC for medium bloom week frequency

Pairs	Adjusted p value	Adjusted p significance
Eutrophic ~ Hypereutrophic	0.10374597	ns
Eutrophic ~ Mesotrophic	0.46857768	ns
Eutrophic ~ Oligotrophic	0.00204727	**
Hypereutrophic ~ Mesotrophic	1	ns
Hypereutrophic ~ Oligotrophic	0.01962937	*
Mesotrophic ~ Oligotrophic	0.02094405	*

Table B7: Dunn's PWC between Max bloom intensity trophic states

Pairs	Adjusted p value	Adjusted p significance
Eutrophic ~ Hypereutrophic	0.90383755	ns
Eutrophic ~ Mesotrophic	0.00125451	**
Eutrophic ~ Oligotrophic	0.05384488	ns
Hypereutrophic ~ Mesotrophic	1.64E-05	****
Hypereutrophic ~ Oligotrophic	0.01717431	*
Mesotrophic ~ Oligotrophic	1	ns

Table B8: Dunn's PWC for high-risk bloom percent coverage by trophic state

Pairs	Adjusted p value	Adjusted p significance
Eutrophic ~ Hypereutrophic	4.30E-06	****
Eutrophic ~ Mesotrophic	2.57E-06	****
Eutrophic ~ Oligotrophic	6.52E-11	****
Hypereutrophic ~ Mesotrophic	2.23E-17	****
Hypereutrophic ~ Oligotrophic	4.02E-15	****
Mesotrophic ~ Oligotrophic	3.81E-06	****

Table B9: Dunn's PWC for medium-risk bloom percent coverage by trophic state

Pairs	Adjusted p value	Adjusted p significance
Eutrophic ~ Hypereutrophic	4.50E-08	****
Eutrophic ~ Mesotrophic	1	ns
Eutrophic ~ Oligotrophic	2.02E-07	****
Hypereutrophic ~ Mesotrophic	6.87E-07	****
Hypereutrophic ~ Oligotrophic	0.00041824	***
Mesotrophic ~ Oligotrophic	7.81E-08	****

Table B10: Dunn's PWC for no bloom percent coverage by trophic state

Pairs	Adjusted p value	Adjusted p significance
Eutrophic ~ Hypereutrophic	1.76E-10	****
Eutrophic ~ Mesotrophic	2.32E-07	****
Eutrophic ~ Oligotrophic	0.18497301	ns
Hypereutrophic ~ Mesotrophic	1.32E-24	****
Hypereutrophic ~ Oligotrophic	1	ns
Mesotrophic ~ Oligotrophic	0.0005694	***

Table B11: Dunn's PWC for total bloom monthly percent coverage by trophic status

Pairs	Adjusted p value	Adjusted p significance
Eutrophic ~ Hypereutrophic	0.00019831	***
Eutrophic ~ Mesotrophic	1.08E-05	****
Eutrophic ~ Oligotrophic	4.04E-10	****
Hypereutrophic ~ Mesotrophic	3.70E-14	****
Hypereutrophic ~ Oligotrophic	1.83E-13	****
Mesotrophic ~ Oligotrophic	9.01E-06	****

APPENDIX C: Trend Analysis

Table C1: Mann Kendall and Sen's Slope to assess for trends in lake high-risk bloom frequency. Waterbodies with significant results are bolded.

Waterbody	tau	MK P value	Sen's Slope	Sen's p.value
Robert.S.Kerr.Reservoir.1	**0.86667**	**0.02417**	**0.00090**	**0.02417**
Sooner.Lake	**0.86667**	**0.02417**	**0.00305**	**0.02417**
Tom.Steed.Reservoir	**0.86667**	**0.02417**	**0.08548**	**0.02417**
Carl.Blackwell.Lake	0.73333	0.06029	0.02774	0.06029
Copan.Lake	0.73333	0.06029	0.01618	0.06029
Eufaula.Lake.2	0.73333	0.06029	0.00263	0.06029
Eufaula.Lake.5	0.73333	0.06029	0.01371	0.06029
Keystone.Lake.2	0.73333	0.06029	0.00413	0.06029
Keystone.Lake.3	0.73333	0.06029	0.00340	0.06029
Lake.Hudson.1	0.73333	0.06029	0.00544	0.06029
Lake.of.the.Arbuckles	0.73333	0.06029	0.01209	0.06029
Lugert.Altus.Reservoir	0.73333	0.06029	0.06106	0.06029
Birch.Reservoir	0.60000	0.13285	0.00323	0.13285
Eufaula.Lake	0.60000	0.13285	0.00464	0.13285
Eufaula.Lake.4	0.60000	0.13285	0.00632	0.13285
Keystone.Lake	0.60000	0.13285	0.00545	0.13285
Lake.Fuqua	0.60000	0.13285	0.02248	0.13285
Lake.Texoma.1	0.60000	0.13285	0.01421	0.13285
Lake.Texoma.3	0.60000	0.13285	0.01019	0.13285
Lake.Thunderbird	0.60000	0.13285	0.02025	0.13285
Oologah.Lake	0.60000	0.13285	0.00387	0.13285
Skiatook.Lake	0.60000	0.13285	0.00538	0.13285
Hugo.Lake	-0.60000	0.13285	-0.00558	0.13285
Lake.Hudson	0.55205	0.18060	0.00111	0.18060
Canton.Lake	0.46667	0.25966	0.04294	0.25966
Eufaula.Lake.1	0.46667	0.25966	0.00809	0.25966
Eufaula.Lake.3	0.46667	0.25966	0.00670	0.25966
Fort.Gibson.Lake.1	0.46667	0.25966	0.00908	0.25966
Fort.Supply.Reservoir	0.46667	0.25966	0.01232	0.25966
Grand.Lake.O..the.Cherokees.1	0.46667	0.25966	0.00171	0.25966

Keystone.Lake.1	0.46667	0.25966	0.00210	0.25966
Lake.Texoma.2	0.46667	0.25966	0.00296	0.25966
Lake.Texoma.4	0.46667	0.25966	0.02332	0.25966
Sardis.Lake	0.46667	0.25966	0.00611	0.25966
Waurika.Lake	0.46667	0.25966	0.02672	0.25966
Webbers.Falls.Reservoir	0.46667	0.25966	0.00160	0.25966
Stanley.Draper.Lake	0.41404	0.33889	0.00107	0.33889
Atoka.Reservoir	0.33333	0.45237	0.01169	0.45237
Broken.Bow.Lake	0.33333	0.45237	0.00058	0.45237
Fort.Cobb.Reservoir	0.33333	0.45237	0.04352	0.45237
Fort.Gibson.Lake	0.33333	0.45237	0.00428	0.45237
Hulah.Lake	0.33333	0.45237	0.00247	0.45237
Lake.Chickasha	0.33333	0.45237	0.05115	0.45237
Lake.Ellsworth	0.33333	0.45237	0.03520	0.45237
Lake.Texoma	0.33333	0.45237	0.01218	0.45237
McGee.Creek.Reservoir	0.33333	0.45237	0.00035	0.45237
Pine.Creek.Lake	0.33333	0.45237	0.01036	0.45237
Wes.Watkins.Reservoir	0.33333	0.45237	0.01386	0.45237
Spavinaw.Lake	-0.27603	0.56609	-0.00009	0.56609
Grand.Lake.O..the.Cherokees	0.20000	0.70711	0.00283	0.70711
Grand.Lake.O..the.Cherokees.2	0.20000	0.70711	0.00028	0.70711
Great.Salt.Plains.Reservoir	0.20000	0.70711	0.00223	0.70711
Kaw.Lake	0.20000	0.70711	0.00048	0.70711
Lake.Lawtonka	-0.20000	0.70711	-0.02613	0.70711
Lake.McAlester	0.20000	0.70711	0.00796	0.70711
Lake.McMurtry	0.20000	0.70711	0.00231	0.70711
Shawnee.Twin.Lakes..1	0.20000	0.70711	0.00148	0.70711
Wister.Lake	0.20000	0.70711	0.01823	0.70711
Lake.Eucha	-0.13801	0.84831	-0.00004	0.84831
Lake.Murray	0.13801	0.84831	0.00007	0.84831
Foss.Reservoir	0.06667	1.00000	0.00155	1.00000
Kaw.Lake.1	-0.06667	1.00000	-0.00020	1.00000
Lake.Arcadia	0.06667	1.00000	0.00617	1.00000
Lake.Hefner	0.06667	1.00000	0.00095	1.00000
Lake.Konawa	-0.06667	1.00000	-0.00504	1.00000
Lake.Overholser	-0.06667	1.00000	-0.02397	1.00000
Robert.S..Kerr.Reservoir	0.06667	1.00000	0.00006	1.00000
Tenkiller.Lake	-0.06667	1.00000	-0.00011	1.00000
Tenkiller.Lake.1	-0.06667	1.00000	-0.00001	1.00000

Table C2: Mann Kendall and Sen's Slope for average medium-risk bloom frequency by waterbody trends over 2017-2022

Waterbody	tau	MK P value	Sen's Slope	Sen's p.value
Grand.Lake.O..the.Cherokees.1	**0.86667**	**0.02417**	**0.00220**	**0.02417**
Sooner.Lake	**0.86667**	**0.02417**	**0.00728**	**0.02417**
Lake.Thunderbird	**-0.86667**	**0.02417**	**-0.00804**	**0.02417**
Eufaula.Lake.4	0.73333	0.06029	0.00478	0.06029
Keystone.Lake	0.73333	0.06029	0.00097	0.06029
Keystone.Lake.1	0.73333	0.06029	0.00393	0.06029
Keystone.Lake.3	0.73333	0.06029	0.00068	0.06029
Lake.Hudson	0.73333	0.06029	0.00338	0.06029
Lake.Hudson.1	0.73333	0.06029	0.00601	0.06029
Webbers.Falls.Reservoir	0.69007	0.08517	0.00077	0.08517
Atoka.Reservoir	0.60000	0.13285	0.00672	0.13285
Birch.Reservoir	0.60000	0.13285	0.00327	0.13285
Eufaula.Lake.1	0.60000	0.13285	0.00310	0.13285
Eufaula.Lake.2	0.60000	0.13285	0.00259	0.13285
Fort.Gibson.Lake.1	0.60000	0.13285	0.00241	0.13285
Grand.Lake.O..the.Cherokees	0.60000	0.13285	0.00302	0.13285
Lake.Texoma.1	0.60000	0.13285	0.01581	0.13285
Lake.Texoma.3	0.60000	0.13285	0.01731	0.13285
Robert.S..Kerr.Reservoir.1	0.60000	0.13285	0.00098	0.13285
Skiatook.Lake	0.60000	0.13285	0.00315	0.13285
Stanley.Draper.Lake	0.60000	0.13285	0.00552	0.13285
Lake.Arcadia	-0.60000	0.13285	-0.00327	0.13285
Kaw.Lake	0.55205	0.18060	0.00092	0.18060
Pine.Creek.Lake	0.55205	0.18060	0.00116	0.18060
Broken.Bow.Lake	0.46667	0.25966	0.00096	0.25966
Eufaula.Lake.5	0.46667	0.25966	0.01494	0.25966
Fort.Gibson.Lake	0.46667	0.25966	0.00241	0.25966
Keystone.Lake.2	0.46667	0.25966	0.00152	0.25966
Lake.of.the.Arbuckles	0.46667	0.25966	0.00668	0.25966
Lake.Texoma.2	0.46667	0.25966	0.01110	0.25966
Lake.Texoma.4	0.46667	0.25966	0.00083	0.25966
McGee.Creek.Reservoir	0.46667	0.25966	0.00047	0.25966
Oologah.Lake	0.46667	0.25966	0.00358	0.25966

Waurika.Lake	0.46667	0.25966	0.00915	0.25966
Great.Salt.Plains.Reservoir	-0.33333	0.45237	-0.00047	0.45237
Hulah.Lake	-0.33333	0.45237	-0.00104	0.45237
Lake.Overholser	-0.33333	0.45237	-0.00451	0.45237
Wister.Lake	-0.33333	0.45237	-0.00878	0.45237
Canton.Lake	0.33333	0.45237	0.01731	0.45237
Copan.Lake	0.33333	0.45237	0.01041	0.45237
Fort.Cobb.Reservoir	0.33333	0.45237	0.00446	0.45237
Grand.Lake.O..the.Cherokees.2	0.33333	0.45237	0.00072	0.45237
Kaw.Lake.1	0.33333	0.45237	0.00043	0.45237
Lake.McMurtry	0.33333	0.45237	0.00662	0.45237
Shawnee.Twin.Lakes..1	0.33333	0.45237	0.00203	0.45237
Lake.Murray	0.27603	0.56609	0.00007	0.56609
Eufaula.Lake	0.20000	0.70711	0.00137	0.70711
Hugo.Lake	-0.20000	0.70711	-0.00697	0.70711
Lake.Chickasha	0.20000	0.70711	0.00326	0.70711
Lake.Ellsworth	0.20000	0.70711	0.00559	0.70711
Lake.Lawtonka	0.20000	0.70711	0.01662	0.70711
Sardis.Lake	0.20000	0.70711	0.01132	0.70711
Spavinaw.Lake	-0.20000	0.70711	-0.00110	0.70711
Tom.Steed.Reservoir	0.20000	0.70711	0.00272	0.70711
Carl.Blackwell.Lake	-0.06667	1.00000	-0.00137	1.00000
Eufaula.Lake.3	-0.06667	1.00000	-0.00130	1.00000
Fort.Supply.Reservoir	-0.06667	1.00000	-0.00359	1.00000
Foss.Reservoir	-0.06667	1.00000	-0.00507	1.00000
Lake.Eucha	0.00000	1.00000	0.00000	1.00000
Lake.Fuqua	0.06667	1.00000	0.00116	1.00000
Lake.Hefner	0.06667	1.00000	0.00026	1.00000
Lake.Konawa	0.06667	1.00000	0.00047	1.00000
Lake.McAlester	-0.06667	1.00000	-0.00022	1.00000
Lake.Texoma	-0.06667	1.00000	-0.00035	1.00000
Lugert.Altus.Reservoir	-0.06667	1.00000	-0.00008	1.00000
Robert.S..Kerr.Reservoir	0.06667	1.00000	0.00241	1.00000
Tenkiller.Lake	0.06667	1.00000	0.00039	1.00000
Tenkiller.Lake.1	-0.06667	1.00000	-0.00016	1.00000
Wes.Watkins.Reservoir	-0.06667	1.00000	-0.00026	1.00000

Table C3: Mann Kendall and Sen's slope trend detection for average annual low-risk bloom frequency per waterbody

Waterbody	Tau	MK p value	Sen's Slope	Sen's p value
Eufaula.Lake	**0.86666662**	**0.02417052**	**0.00064665**	**0.02417055**
Lake.Konawa	**0.86666662**	**0.02417052**	**0.00070442**	**0.02417055**
Lake.Texoma.1	**0.86666662**	**0.02417052**	**0.00025536**	**0.02417055**
Lake.Texoma.2	**0.86666662**	**0.02417052**	**0.00041328**	**0.02417055**
Sooner.Lake	**0.89442718**	**0.02677274**	**0.00053419**	**0.02677277**
McGee.Creek.Reservoir	**0.82807863**	**0.03537822**	**0.00149935**	**0.03537817**
Copan.Lake	0.73333329	0.06028914	0.00048598	0.06028917
Grand.Lake.O..the.Cherokees.1	0.73333329	0.06028914	0.00286777	0.06028917
Great.Salt.Plains.Reservoir	0.73333329	0.06028914	0.00187405	0.06028917
Sardis.Lake	0.73333329	0.06028914	0.00022462	0.06028917
Wister.Lake	0.6900655	0.08516788	0.00020102	0.08516791
Hugo.Lake	0.64450341	0.11900401	6.18E-05	0.11900407
Atoka.Reservoir	0.59999996	0.13285494	0.00113333	0.13285496
Foss.Reservoir	0.59999996	0.13285494	0.00048774	0.13285496
Kaw.Lake	0.59999996	0.13285494	9.79E-05	0.13285496
Keystone.Lake.1	0.59999996	0.13285494	0.00026344	0.13285496
Lake.Arcadia	0.59999996	0.13285494	0.00050884	0.13285496
Lake.Ellsworth	0.59999996	0.13285494	0.0006725	0.13285496
Lake.Fuqua	0.59999996	0.13285494	0.00088897	0.13285496
Spavinaw.Lake	0.59999996	0.13285494	0.00036284	0.13285496
Webbers.Falls.Reservoir	0.59999996	0.13285494	0.0003663	0.13285496
Keystone.Lake.3	-0.5520524	0.1805996	-0.0002426	0.18059962
Eufaula.Lake.2	-0.4666666	0.25965631	-0.0016209	0.25965636
Eufaula.Lake.4	0.46666664	0.25965631	0.00032778	0.25965636
Grand.Lake.O..the.Cherokees	-0.4666666	0.25965631	-0.0001519	0.25965636
Keystone.Lake	0.46666664	0.25965631	0.0002034	0.25965636
Lake.Lawtonka	-0.4666666	0.25965631	-0.0006277	0.25965636
Lake.McAlester	-0.4666666	0.25965631	-0.0003685	0.25965636
Lake.Overholser	0.46666664	0.25965631	0.00404858	0.25965636
Oologah.Lake	0.46666664	0.25965631	0.00217978	0.25965636
Keystone.Lake.2	0.41403931	0.33888781	3.62E-05	0.33888783
Lugert.Altus.Reservoir	0.35805744	0.43569469	0.00022624	0.4356948
Lake.Hudson.1	-0.3333333	0.45237035	-0.0002634	0.45237036
Birch.Reservoir	0.33333331	0.45237041	0.00027844	0.45237036
Fort.Gibson.Lake.1	0.33333331	0.45237041	0.00067793	0.45237036
Grand.Lake.O..the.Cherokees.2	0.33333331	0.45237041	0.00223132	0.45237036
Hulah.Lake	0.33333331	0.45237041	0.00041587	0.45237036
Lake.Chickasha	0.33333331	0.45237041	0.00010204	0.45237036
Lake.of.the.Arbuckles	0.33333331	0.45237041	0.00031469	0.45237036
Robert.S..Kerr.Reservoir	0.33333331	0.45237041	0.00056034	0.45237036
Robert.S..Kerr.Reservoir.1	0.33333331	0.45237041	2.82E-05	0.45237036
Shawnee.Twin.Lakes..1	0.33333331	0.45237041	0.00015675	0.45237036
Wes.Watkins.Reservoir	0.33333331	0.45237041	0.00025345	0.45237036

Fort.Gibson.Lake	0.27602619	0.56609023	0.00012488	0.56609026
Skiatook.Lake	0.27602619	0.56609023	4.86E-05	0.56609026
Eufaula.Lake.5	0.21483447	0.6967274	2.38E-05	0.69672742
Fort.Cobb.Reservoir	-0.2	0.70711422	-0.0001716	0.70711423
Lake.Hudson	0.19999999	0.70711422	0.00034464	0.70711423
Lake.Texoma	-0.2	0.70711422	-0.0020489	0.70711423
Lake.Texoma.3	0.19999999	0.70711422	6.70E-05	0.70711423
Lake.Texoma.4	0.19999999	0.70711422	0.00106309	0.70711423
Lake.Thunderbird	0.19999999	0.70711422	0.00047134	0.70711423
Pine.Creek.Lake	0.19999999	0.70711422	0.00011246	0.70711423
Waurika.Lake	0.19999999	0.70711422	0.00051338	0.70711423
Broken.Bow.Lake	-0.1490712	0.8404274	0	0.8404274
Lake.McMurtry	-0.1490712	0.8404274	0	0.8404274
Fort.Supply.Reservoir	0.13801309	0.84831166	0.00021017	0.8483117
Lake.Hefner	0.13801309	0.84831166	0.00017417	0.8483117
Tom.Steed.Reservoir	0.13801309	0.84831166	0.00042816	0.8483117
Canton.Lake	-0.0666667	1	-0.000221	1
Carl.Blackwell.Lake	0.06666666	1	0.00017325	1
Eufaula.Lake.1	-0.0666667	1	-0.0003928	1
Eufaula.Lake.3	0.06666666	1	0.00037341	1
Kaw.Lake.1	0.07161149	1	0	1
Lake.Eucha	-0.0666667	1	-1.40E-05	1
Lake.Murray	-0.0666667	1	-9.91E-05	1
Stanley.Draper.Lake	0.0860663	1	0	1
Tenkiller.Lake	0	1	0	1
Tenkiller.Lake.1	-0.0666667	1	-5.09E-05	1

Table C4: Mann Kendall and Sen's slope trend detection for average annual no bloom frequency per waterbody

Waterbody	Tau	MK p value	Sen's Slope	Sen's p value
Lugert.Altus.Reservoir	**-0.8666666**	**0.02417055**	**-0.103736**	**0.02417055**
Tom.Steed.Reservoir	**-0.8666666**	**0.02417055**	**-0.0804433**	**0.02417055**
Hugo.Lake	0.59999996	0.13285494	0.03892267	0.13285496
Lake.Eucha	0.59999996	0.13285494	0.02202234	0.13285496
Tenkiller.Lake.1	0.59999996	0.13285494	0.02186054	0.13285496
Canton.Lake	-0.4666666	0.25965631	-0.0379852	0.25965636
Copan.Lake	-0.4666666	0.25965631	-0.0248305	0.25965636
Eufaula.Lake	0.46666664	0.25965631	0.01399791	0.25965636
Grand.Lake.O..the.Cherokees	0.46666664	0.25965631	0.01194329	0.25965636
Keystone.Lake.3	-0.4666666	0.25965631	-0.0142342	0.25965636
Lake.Chickasha	-0.4666666	0.25965631	-0.0404215	0.25965636
Lake.Konawa	0.46666664	0.25965631	0.01019336	0.25965636
Lake.Texoma.1	-0.4666666	0.25965631	-0.0144355	0.25965636
Lake.Texoma.4	-0.4666666	0.25965631	-0.0268405	0.25965636
Lake.Thunderbird	0.46666664	0.25965631	0.0117556	0.25965636
McGee.Creek.Reservoir	0.46666664	0.25965631	0.02601463	0.25965636
Robert.S..Kerr.Reservoir.1	0.46666664	0.25965631	0.02811086	0.25965636
Stanley.Draper.Lake	0.46666664	0.25965631	0.01021273	0.25965636
Tenkiller.Lake	0.46666664	0.25965631	0.02687998	0.25965636
Eufaula.Lake.5	-0.3333333	0.45237035	-0.018838	0.45237036
Kaw.Lake	-0.3333333	0.45237035	-0.0053258	0.45237036
Keystone.Lake	-0.3333333	0.45237035	-0.0117786	0.45237036
Lake.Texoma.3	-0.3333333	0.45237035	-0.0151642	0.45237036
Waurika.Lake	-0.3333333	0.45237035	-0.0233562	0.45237036
Broken.Bow.Lake	0.33333331	0.45237041	0.01711675	0.45237036
Eufaula.Lake.3	0.33333331	0.45237041	0.01572687	0.45237036
Foss.Reservoir	0.33333331	0.45237041	0.01711028	0.45237036
Grand.Lake.O..the.Cherokees.1	0.33333331	0.45237041	0.01652533	0.45237036
Grand.Lake.O..the.Cherokees.2	0.33333331	0.45237041	0.02178952	0.45237036
Great.Salt.Plains.Reservoir	0.33333331	0.45237041	0.00288719	0.45237036
Lake.Hudson	0.33333331	0.45237041	0.01464661	0.45237036
Lake.Murray	0.33333331	0.45237041	0.01301115	0.45237036
Pine.Creek.Lake	0.33333331	0.45237041	0.01965342	0.45237036
Robert.S..Kerr.Reservoir	0.33333331	0.45237041	0.01091248	0.45237036
Spavinaw.Lake	0.33333331	0.45237041	0.01983715	0.45237036
Atoka.Reservoir	0.19999999	0.70711422	0.00589783	0.70711423
Carl.Blackwell.Lake	-0.2	0.70711422	-0.0148826	0.70711423
Eufaula.Lake.2	0.19999999	0.70711422	0.00537516	0.70711423
Fort.Cobb.Reservoir	-0.2	0.70711422	-0.0351721	0.70711423
Fort.Gibson.Lake.1	0.19999999	0.70711422	0.00241222	0.70711423
Kaw.Lake.1	0.19999999	0.70711422	0.0061144	0.70711423
Lake.Arcadia	0.19999999	0.70711422	0.00636863	0.70711423
Lake.Ellsworth	-0.2	0.70711422	-0.0245883	0.70711423
Lake.Hefner	0.19999999	0.70711422	0.0115383	0.70711423

Lake.Hudson.1	0.19999999	0.70711422	0.00396551	0.70711423
Lake.McMurtry	-0.2	0.70711422	-0.0346154	0.70711423
Lake.Texoma	-0.2	0.70711422	-0.0135286	0.70711423
Shawnee.Twin.Lakes..1	0.19999999	0.70711422	0.00684171	0.70711423
Skiatook.Lake	0.19999999	0.70711422	0.00723811	0.70711423
Birch.Reservoir	0.06666666	1	0.01107692	1
Eufaula.Lake.1	0.06666666	1	0.00199704	1
Eufaula.Lake.4	-0.0666667	1	-0.0012492	1
Fort.Gibson.Lake	0.06666666	1	0.00428085	1
Fort.Supply.Reservoir	0.06666666	1	0.00342548	1
Hulah.Lake	0.06666666	1	0.00194137	1

Table C5: Mann Kendall and Sen's Slope to assess for trends in lake total bloom frequency. Waterbodies with significant results are bolded.

Waterbody	tau	MK P value	Sen's Slope	Sen's p.value
Kaw.Lake	**0.86667**	**0.02417**	**0.00244**	**0.02417**
Keystone.Lake.1	**0.86667**	**0.02417**	**0.00656**	**0.02417**
Lugert.Altus.Reservoir	**0.86667**	**0.02417**	**0.05877**	**0.02417**
Sooner.Lake	**0.86667**	**0.02417**	**0.01218**	**0.02417**
Birch.Reservoir	0.73333	0.06029	0.00577	0.06029
Carl.Blackwell.Lake	0.73333	0.06029	0.02622	0.06029
Eufaula.Lake.2	0.73333	0.06029	0.00775	0.06029
Eufaula.Lake.4	0.73333	0.06029	0.01950	0.06029
Eufaula.Lake.5	0.73333	0.06029	0.03168	0.06029
Fort.Gibson.Lake.1	0.73333	0.06029	0.01223	0.06029
Grand.Lake.O..the.Cherokees.1	0.73333	0.06029	0.00413	0.06029
Keystone.Lake	0.73333	0.06029	0.00647	0.06029
Keystone.Lake.2	0.73333	0.06029	0.00771	0.06029
Keystone.Lake.3	0.73333	0.06029	0.00333	0.06029
Lake.Hudson.1	0.73333	0.06029	0.01199	0.06029
Lake.of.the.Arbuckles	0.73333	0.06029	0.01676	0.06029
Robert.S..Kerr.Reservoir.1	0.73333	0.06029	0.00211	0.06029
Tom.Steed.Reservoir	0.73333	0.06029	0.08855	0.06029
Webbers.Falls.Reservoir	0.73333	0.06029	0.00216	0.06029
Canton.Lake	0.60000	0.13285	0.05921	0.13285
Copan.Lake	0.60000	0.13285	0.03239	0.13285
Lake.Fuqua	0.60000	0.13285	0.02158	0.13285
Lake.Hudson	0.60000	0.13285	0.00464	0.13285
Lake.Texoma.1	0.60000	0.13285	0.03301	0.13285
Lake.Texoma.3	0.60000	0.13285	0.02938	0.13285
McGee.Creek.Reservoir	0.60000	0.13285	0.00076	0.13285
Skiatook.Lake	0.60000	0.13285	0.00549	0.13285
Atoka.Reservoir	0.46667	0.25966	0.02038	0.25966
Eufaula.Lake.1	0.46667	0.25966	0.00861	0.25966
Fort.Gibson.Lake	0.46667	0.25966	0.00752	0.25966
Grand.Lake.O..the.Cherokees.2	0.46667	0.25966	0.00080	0.25966
Lake.Texoma.2	0.46667	0.25966	0.01659	0.25966
Lake.Texoma.4	0.46667	0.25966	0.02434	0.25966
Lake.Thunderbird	0.46667	0.25966	0.01441	0.25966
Oologah.Lake	0.46667	0.25966	0.00800	0.25966
Pine.Creek.Lake	0.46667	0.25966	0.01102	0.25966

Waurika.Lake	0.46667	0.25966	0.03661	0.25966
Hugo.Lake	-0.33333	0.45237	-0.01671	0.45237
Broken.Bow.Lake	0.33333	0.45237	0.00195	0.45237
Eufaula.Lake.3	0.33333	0.45237	0.00480	0.45237
Fort.Cobb.Reservoir	0.33333	0.45237	0.05308	0.45237
Grand.Lake.O..the.Cherokees	0.33333	0.45237	0.00414	0.45237
Lake.Ellsworth	0.33333	0.45237	0.03553	0.45237
Lake.Texoma	0.33333	0.45237	0.01420	0.45237
Stanley.Draper.Lake	0.33333	0.45237	0.00863	0.45237
Wes.Watkins.Reservoir	0.33333	0.45237	0.01342	0.45237
Eufaula.Lake	0.20000	0.70711	0.00640	0.70711
Lake.Chickasha	0.20000	0.70711	0.05170	0.70711
Lake.Eucha	-0.20000	0.70711	-0.00019	0.70711
Lake.McAlester	0.20000	0.70711	0.00847	0.70711
Lake.McMurtry	0.20000	0.70711	0.00500	0.70711
Lake.Murray	0.20000	0.70711	0.00043	0.70711
Robert.S..Kerr.Reservoir	-0.20000	0.70711	-0.00088	0.70711
Sardis.Lake	0.20000	0.70711	0.01948	0.70711
Shawnee.Twin.Lakes..1	0.20000	0.70711	0.00730	0.70711
Spavinaw.Lake	-0.20000	0.70711	-0.00119	0.70711
Wister.Lake	0.20000	0.70711	0.01718	0.70711
Fort.Supply.Reservoir	0.06667	1.00000	0.00589	1.00000
Foss.Reservoir	-0.06667	1.00000	-0.00437	1.00000
Great.Salt.Plains.Reservoir	0.06667	1.00000	0.00043	1.00000
Hulah.Lake	-0.06667	1.00000	-0.00237	1.00000
Kaw.Lake.1	0.06667	1.00000	0.00031	1.00000
Lake.Arcadia	0.06667	1.00000	0.00164	1.00000
Lake.Hefner	0.06667	1.00000	0.00139	1.00000
Lake.Konawa	-0.06667	1.00000	-0.01734	1.00000
Lake.Lawtonka	-0.06667	1.00000	-0.00631	1.00000
Lake.Overholser	-0.06667	1.00000	-0.03390	1.00000
Tenkiller.Lake	-0.06667	1.00000	-0.00027	1.00000
Tenkiller.Lake.1	-0.06667	1.00000	-0.00030	1.00000

Table C6: Mann Kendall and Sen's Slope to assess for trends in weekly lake high-risk bloom frequency. Waterbodies with significant results are bolded.

Waterbody	tau	MK P value	Sen's Slope	Sen's p.value
Eufaula.Lake	**0.86667**	**0.02417**	**0.05769**	**0.02417**
Great.Salt.Plains.Reservoir	**0.86667**	**0.02417**	**0.06923**	**0.02417**
Lake.Chickasha	**0.86667**	**0.02417**	**0.04311**	**0.02417**
Lake.Ellsworth	**0.86667**	**0.02417**	**0.07231**	**0.02417**
McGee.Creek.Reservoir	**0.86667**	**0.02417**	**0.04082**	**0.02417**
Hulah.Lake	**0.82808**	**0.03538**	**0.03846**	**0.03538**
Lake.Arcadia	**0.82808**	**0.03538**	**0.05897**	**0.03538**
Lake.Texoma.3	**0.82808**	**0.03538**	**0.02525**	**0.03538**
Copan.Lake	0.73333	0.06029	0.05128	0.06029
Grand.Lake.O..the.Cherokees.2	0.73333	0.06029	0.06471	0.06029
Lake.Texoma.2	0.73333	0.06029	0.06410	0.06029
Sooner.Lake	0.73333	0.06029	0.04487	0.06029
Spavinaw.Lake	0.73333	0.06029	0.03971	0.06029
Lake.Texoma.4	0.69007	0.08517	0.05529	0.08517
Fort.Cobb.Reservoir	0.60000	0.13285	0.07692	0.13285
Fort.Gibson.Lake.1	0.60000	0.13285	0.03877	0.13285
Foss.Reservoir	0.60000	0.13285	0.04173	0.13285
Hugo.Lake	0.60000	0.13285	0.07654	0.13285
Lake.Konawa	0.60000	0.13285	0.05045	0.13285
Pine.Creek.Lake	0.60000	0.13285	0.05769	0.13285
Sardis.Lake	0.60000	0.13285	0.03130	0.13285
Skiatook.Lake	0.60000	0.13285	0.07184	0.13285
Webbers.Falls.Reservoir	0.60000	0.13285	0.05553	0.13285
Lake.Hudson	0.55205	0.18060	0.06667	0.18060
Lugert.Altus.Reservoir	0.55205	0.18060	0.02570	0.18060
Eufaula.Lake.2	-0.55205	0.18060	-0.01397	0.18060
Canton.Lake	0.46667	0.25966	0.01212	0.25966
Carl.Blackwell.Lake	0.46667	0.25966	0.02000	0.25966
Lake.Hefner	0.46667	0.25966	0.02092	0.25966
Lake.Lawtonka	-0.46667	0.25966	-0.01538	0.25966
Lake.Overholser	0.46667	0.25966	0.05430	0.25966
Lake.Texoma.1	0.46667	0.25966	0.04902	0.25966
Stanley.Draper.Lake	0.46667	0.25966	0.04846	0.25966
Waurika.Lake	0.46667	0.25966	0.03345	0.25966
Wister.Lake	0.46667	0.25966	0.05053	0.25966
Atoka.Reservoir	0.41404	0.33889	0.02083	0.33889

Keystone.Lake.2	-0.41404	0.33889	-0.00118	0.33889
Shawnee.Twin.Lakes..1	0.41404	0.33889	0.03190	0.33889
Wes.Watkins.Reservoir	0.41404	0.33889	0.02308	0.33889
Birch.Reservoir	0.33333	0.45237	0.03846	0.45237
Eufaula.Lake.4	0.33333	0.45237	0.02450	0.45237
Grand.Lake.O..the.Cherokees.1	0.33333	0.45237	0.03846	0.45237
Kaw.Lake.1	0.33333	0.45237	0.01879	0.45237
Keystone.Lake.1	0.33333	0.45237	0.03450	0.45237
Lake.Fuqua	0.33333	0.45237	0.01943	0.45237
Lake.of.the.Arbuckles	0.33333	0.45237	0.01289	0.45237
Eufaula.Lake.5	0.27603	0.56609	0.00613	0.56609
Grand.Lake.O..the.Cherokees	0.27603	0.56609	0.02885	0.56609
Lake.McMurtry	-0.21483	0.69673	-0.00521	0.69673
Eufaula.Lake.1	0.20000	0.70711	0.03149	0.70711
Fort.Supply.Reservoir	0.20000	0.70711	0.01294	0.70711
Kaw.Lake	0.20000	0.70711	0.00622	0.70711
Lake.Murray	0.20000	0.70711	0.00962	0.70711
Oologah.Lake	0.20000	0.70711	0.05229	0.70711
Robert.S..Kerr.Reservoir.1	-0.20000	0.70711	-0.00405	0.70711
Broken.Bow.Lake	0.13801	0.84831	0.00078	0.84831
Eufaula.Lake.3	0.13801	0.84831	0.02583	0.84831
Fort.Gibson.Lake	0.13801	0.84831	0.00651	0.84831
Lake.Thunderbird	0.13801	0.84831	0.00462	0.84831
Keystone.Lake	0.06667	1.00000	0.01538	1.00000
Keystone.Lake.3	0.06667	1.00000	0.00196	1.00000
Lake.Eucha	0.06667	1.00000	0.02090	1.00000
Lake.Hudson.1	-0.06667	1.00000	-0.02594	1.00000
Lake.McAlester	0.06667	1.00000	0.03318	1.00000
Lake.Texoma	-0.06667	1.00000	-0.00980	1.00000
Robert.S..Kerr.Reservoir	0.06667	1.00000	0.00363	1.00000
Tenkiller.Lake	-0.06667	1.00000	-0.01615	1.00000
Tenkiller.Lake.1	0.06667	1.00000	0.01885	1.00000
Tom.Steed.Reservoir	0.06667	1.00000	0.01094	1.00000

Table C7: Mann Kendall and Sen's Slope to assess for trends in weekly lake medium-risk bloom frequency. Waterbodies with significant results are bolded.

Waterbody	Tau	MK p value	Sen's Slope	Sen's p value
Lake.Texoma.4	**-0.8280786**	**0.03537817**	**-0.0249608**	**0.03537817**
Eufaula.Lake	**0.82807863**	**0.03537822**	**0.02564103**	**0.03537817**
Spavinaw.Lake	0.73333329	0.06028914	0.0275264	0.06028917
Atoka.Reservoir	0.6900655	0.08516788	0.03076923	0.08516791
Shawnee.Twin.Lakes..1	0.59999996	0.13285494	0.029209	0.13285496
Great.Salt.Plains.Reservoir	-0.6	0.13285497	-0.0096154	0.13285496
Waurika.Lake	-0.6	0.13285497	-0.018128	0.13285496
McGee.Creek.Reservoir	0.59628481	0.15870869	0.00641026	0.15870873
Lake.Arcadia	-0.6024641	0.17606752	-0.0076923	0.1760675
Grand.Lake.O..the.Cherokees.2	0.55205238	0.18059957	0.01470588	0.18059962
Sooner.Lake	0.55205238	0.18059957	0.00961538	0.18059962
Fort.Cobb.Reservoir	-0.5520524	0.1805996	-0.0096154	0.18059962
Lake.Texoma.2	-0.5520524	0.1805996	-0.0192308	0.18059962
Kaw.Lake.1	-0.5012804	0.24231267	-0.0008741	0.24231273
Lake.Hudson	-0.5012804	0.24231267	-0.0094118	0.24231273
Copan.Lake	0.46666664	0.25965631	0.01461538	0.25965636
Eufaula.Lake.1	0.46666664	0.25965631	0.01538462	0.25965636
Lake.Konawa	-0.4666666	0.25965631	-0.0147392	0.25965636
Lake.Texoma.1	-0.4666666	0.25965631	-0.011103	0.25965636
Grand.Lake.O..the.Cherokees	-0.4472136	0.31406254	-0.0005887	0.31406258
Skiatook.Lake	0.44721359	0.3140626	0.00406386	0.31406258
Canton.Lake	0.41403931	0.33888781	0.0041806	0.33888783
Carl.Blackwell.Lake	-0.4140393	0.33888781	-0.0007692	0.33888783
Eufaula.Lake.3	-0.4140393	0.33888781	-0.0192308	0.33888783
Keystone.Lake.1	0.41403931	0.33888781	0.00653595	0.33888783
Keystone.Lake.2	0.41403931	0.33888781	0.005	0.33888783
Oologah.Lake	-0.4140393	0.33888781	-0.010181	0.33888783
Robert.S..Kerr.Reservoir	0.41403931	0.33888781	0.00960784	0.33888783
Webbers.Falls.Reservoir	-0.4140393	0.33888781	-0.02	0.33888783
Wes.Watkins.Reservoir	0.41403931	0.33888781	0.02307692	0.33888783
Lake.Ellsworth	-0.4303315	0.36707002	0	0.36707002
Keystone.Lake	-0.3333333	0.45237035	-0.0064103	0.45237036
Keystone.Lake.3	-0.3333333	0.45237035	-0.0270588	0.45237036
Foss.Reservoir	0.33333331	0.45237041	0.01513912	0.45237036
Lake.Fuqua	0.33333331	0.45237041	0.00511509	0.45237036
Tenkiller.Lake.1	0.33333331	0.45237041	0.0073718	0.45237036
Fort.Gibson.Lake	0.2981424	0.54581666	0.00038462	0.54581675
Lake.Texoma.3	0.2981424	0.54581666	0.01085819	0.54581675
Tenkiller.Lake	0.2981424	0.54581666	0.00641026	0.54581675
Lake.Thunderbird	-0.2981424	0.54581672	-0.0012821	0.54581675
Hugo.Lake	0.34641016	0.55818462	0	0.55818465
Stanley.Draper.Lake	0.34641016	0.55818462	0	0.55818465
Birch.Reservoir	0.27602619	0.56609023	0.00641026	0.56609026
Hulah.Lake	-0.2760262	0.56609023	-0.0320513	0.56609026
Lake.Hefner	0.27602619	0.56609023	0.00117647	0.56609026

Lake.McAlester	-0.2760262	0.56609023	-0.0001538	0.56609026
Lake.McMurtry	0.27602619	0.56609023	0.00320513	0.56609026
Lake.Texoma	-0.2760262	0.56609023	-0.0015083	0.56609026
Lugert.Altus.Reservoir	-0.2760262	0.56609023	-0.0007692	0.56609026
Eufaula.Lake.5	-0.2	0.70711422	-0.0016026	0.70711423
Lake.Murray	-0.2	0.70711422	-0.0059851	0.70711423
Lake.of.the.Arbuckles	0.19999999	0.70711422	0.01897939	0.70711423
Lake.Overholser	-0.2	0.70711422	-0.0126797	0.70711423
Kaw.Lake	0.1490712	0.8404274	0	0.8404274
Grand.Lake.O..the.Cherokees.1	0.13801309	0.84831166	0.00961538	0.8483117
Lake.Chickasha	0.13801309	0.84831166	0.00769231	0.8483117
Lake.Eucha	-0.1380131	0.84831166	-0.0002721	0.8483117
Lake.Lawtonka	0.13801309	0.84831166	0.00546757	0.8483117
Sardis.Lake	0.13801309	0.84831166	0.00043541	0.8483117
Tom.Steed.Reservoir	-0.1380131	0.84831166	-0.0037015	0.8483117
Broken.Bow.Lake	-0.0860663	1	0	1
Eufaula.Lake.2	-0.0666667	1	-0.0015385	1
Eufaula.Lake.4	-0.0666667	1	-0.0006285	1
Fort.Gibson.Lake.1	0.07161149	1	0	1
Fort.Supply.Reservoir	0.0860663	1	0	1
Lake.Hudson.1	-0.0860663	1	0	1
Pine.Creek.Lake	0.0860663	1	0	1
Robert.S..Kerr.Reservoir.1	1	1	0	NaN
Wister.Lake	0.06666666	1	0.00226244	1

Table C8: Mann Kendall and Sen's Slope to assess for trends in weekly lake low-risk bloom frequency. Waterbodies with significant results are bolded.

Waterbody	Tau	MK p value	Sen's Slope	Sen's p value
Lake.Thunderbird	**-0.8944272**	**0.0288538**	**-0.004**	**0.02885379**
Atoka.Reservoir	0.70064902	0.10008264	0.00961538	0.10008268
Eufaula.Lake.4	0.60246408	0.17606747	0.00384615	0.1760675
Tenkiller.Lake.1	0.60246408	0.17606747	0.00641026	0.1760675
Pine.Creek.Lake	-0.5773503	0.2415666	0	0.24156659
Robert.S..Kerr.Reservoir	-0.5773503	0.2415666	0	0.24156659
Lake.Murray	0.57735026	0.24156666	0	0.24156659
Tom.Steed.Reservoir	0.57735026	0.24156666	0	0.24156659
Lake.Arcadia	0.50128043	0.24231267	0.00641026	0.24231273
Sardis.Lake	-0.5012804	0.24231267	-0.0067974	0.24231273
Shawnee.Twin.Lakes..1	0.46666664	0.25965631	0.00113208	0.25965636
Eufaula.Lake.3	-0.4303315	0.36707002	0	0.36707002
Lake.Ellsworth	-0.3892495	0.41094798	-0.0002564	0.41094803
Wes.Watkins.Reservoir	0.36514837	0.48745322	0	0.48745329
Fort.Gibson.Lake.1	0.2981424	0.54581666	0.00369231	0.54581675
Keystone.Lake.3	0.34641016	0.55818462	0	0.55818465
Lake.Lawtonka	0.34641016	0.55818462	0	0.55818465
Lugert.Altus.Reservoir	0.34641016	0.55818462	0	0.55818465
Robert.S..Kerr.Reservoir.1	0.34641016	0.55818462	0	0.55818465
Sooner.Lake	0.34641016	0.55818462	0	0.55818465
Grand.Lake.O..the.Cherokees	-0.3464102	0.55818468	0	0.55818465
Keystone.Lake.1	-0.3464102	0.55818468	0	0.55818465
Lake.Hudson	-0.3464102	0.55818468	0	0.55818465
Stanley.Draper.Lake	-0.3464102	0.55818468	0	0.55818465
Wister.Lake	-0.3464102	0.55818468	0	0.55818465
Eufaula.Lake	-0.2581989	0.65199846	0	0.65199847
Fort.Cobb.Reservoir	0.25819889	0.65199852	0	0.65199847
Lake.of.the.Arbuckles	0.25819889	0.65199852	0	0.65199847
Lake.Texoma	0.25819889	0.65199852	0	0.65199847
Eufaula.Lake.2	-0.2335497	0.6809895	0	0.68098951
Lake.Chickasha	-0.2335497	0.6809895	0	0.68098951
Lake.Texoma.3	0.23354967	0.6809895	0	0.68098951
Lake.Overholser	0.1490712	0.8404274	0	0.8404274
Copan.Lake	-0.1380131	0.84831166	-0.0004085	0.8483117
Lake.Texoma.2	-0.1380131	0.84831166	-0.0037736	0.8483117
Birch.Reservoir	-0.0716115	1	0	1
Broken.Bow.Lake	1	1	0	NaN
Canton.Lake	1	1	0	NaN
Carl.Blackwell.Lake	1	1	0	NaN
Eufaula.Lake.1	0.0860663	1	0	1
Eufaula.Lake.5	1	1	0	NaN
Fort.Gibson.Lake	1	1	0	NaN
Fort.Supply.Reservoir	1	1	0	NaN
Foss.Reservoir	-0.0666667	1	-0.0005563	1
Grand.Lake.O..the.Cherokees .1	1	1	0	NaN

Grand.Lake.O..the.Cherokees.2	1	1	0	NaN
Great.Salt.Plains.Reservoir	1	1	0	NaN
Hugo.Lake	1	1	0	NaN
Hulah.Lake	-0.0778499	1	0	1
Kaw.Lake	1	1	0	NaN
Kaw.Lake.1	1	1	0	NaN
Keystone.Lake	1	1	0	NaN
Keystone.Lake.2	1	1	0	NaN
Lake.Eucha	1	1	0	NaN
Lake.Fuqua	1	1	0	NaN
Lake.Hefner	0.0860663	1	0	1
Lake.Hudson.1	1	1	0	NaN
Lake.Konawa	0	1	0	1
Lake.McAlester	1	1	0	NaN
Lake.McMurtry	1	1	0	NaN
Lake.Texoma.1	0.11547004	1	0	1
Lake.Texoma.4	1	1	0	NaN
McGee.Creek.Reservoir	1	1	0	NaN
Oologah.Lake	-0.0778499	1	0	1
Skiatook.Lake	0.07784989	1	0	1
Spavinaw.Lake	-0.0860663	1	0	1
Tenkiller.Lake	1	1	0	NaN
Waurika.Lake	0	1	0	1
Webbers.Falls.Reservoir	-0.11547	1	0	1

Table C9: Mann Kendall and Sen's Slope to assess for trends in weekly lake no bloom frequency. Waterbodies with significant results are bolded.

Waterbody	Tau	MK p value	Sen's Slope	Sen's p value
Grand.Lake.O..the.Cherokees.2	**-0.9999999**	**0.00853492**	**-0.0804739**	**0.00853492**
Lake.Ellsworth	**-0.9999999**	**0.00853492**	**-0.0576923**	**0.00853492**
Lake.Texoma.3	**-0.9999999**	**0.00853492**	**-0.0343407**	**0.00853492**
Great.Salt.Plains.Reservoir	**-0.8666666**	**0.02417055**	**-0.056184**	**0.02417055**
Lake.Chickasha	**-0.8666666**	**0.02417055**	**-0.0607089**	**0.02417055**
Shawnee.Twin.Lakes..1	**-0.8666666**	**0.02417055**	**-0.071267**	**0.02417055**
Lake.Texoma.2	**-0.8944272**	**0.02677276**	**-0.0431267**	**0.02677277**
Eufaula.Lake	**-0.8280786**	**0.03537817**	**-0.0833846**	**0.03537817**
McGee.Creek.Reservoir	**-0.8280786**	**0.03537817**	**-0.0440869**	**0.03537817**
Eufaula.Lake.4	-0.7333333	0.06028918	-0.0143478	0.06028917
Lake.Arcadia	-0.7333333	0.06028918	-0.0576923	0.06028917
Sooner.Lake	-0.7333333	0.06028918	-0.0538462	0.06028917
Spavinaw.Lake	-0.7333333	0.06028918	-0.0641026	0.06028917
Lugert.Altus.Reservoir	-0.6900655	0.08516791	-0.0320513	0.08516791
Sardis.Lake	-0.6900655	0.08516791	-0.0244557	0.08516791
Atoka.Reservoir	-0.6	0.13285497	-0.0615385	0.13285496
Canton.Lake	-0.6	0.13285497	-0.0235862	0.13285496
Copan.Lake	-0.6	0.13285497	-0.0742308	0.13285496
Fort.Cobb.Reservoir	-0.6	0.13285497	-0.0673077	0.13285496
Foss.Reservoir	-0.6	0.13285497	-0.0368249	0.13285496
Hugo.Lake	-0.6	0.13285497	-0.0765385	0.13285496
Lake.Fuqua	-0.6	0.13285497	-0.0115283	0.13285496
Lake.Hefner	-0.6	0.13285497	-0.04	0.13285496
Lake.of.the.Arbuckles	-0.6	0.13285497	-0.030178	0.13285496
Lake.Texoma.1	-0.6	0.13285497	-0.0321154	0.13285496
Pine.Creek.Lake	-0.6	0.13285497	-0.0528846	0.13285496
Skiatook.Lake	-0.6	0.13285497	-0.0627828	0.13285496
Stanley.Draper.Lake	-0.6	0.13285497	-0.055	0.13285496
Wes.Watkins.Reservoir	-0.6	0.13285497	-0.0296311	0.13285496
Grand.Lake.O..the.Cherokees.1	-0.5520524	0.1805996	-0.025641	0.18059962
Lake.Texoma.4	-0.5520524	0.1805996	-0.0247253	0.18059962
Carl.Blackwell.Lake	-0.4666666	0.25965631	-0.0192308	0.25965636
Eufaula.Lake.2	0.46666664	0.25965631	0.01009434	0.25965636
Fort.Gibson.Lake.1	-0.4666666	0.25965631	-0.0477941	0.25965636
Keystone.Lake.1	-0.4666666	0.25965631	-0.0192308	0.25965636
Lake.Hudson	-0.4666666	0.25965631	-0.06	0.25965636
Lake.Konawa	-0.4666666	0.25965631	-0.0357143	0.25965636
Waurika.Lake	-0.4140393	0.33888781	-0.0110305	0.33888783
Birch.Reservoir	-0.3333333	0.45237035	-0.0384615	0.45237036
Hulah.Lake	-0.3333333	0.45237035	-0.0128205	0.45237036
Lake.Overholser	-0.3333333	0.45237035	-0.0673077	0.45237036
Wister.Lake	-0.3333333	0.45237035	-0.0441523	0.45237036
Keystone.Lake.3	0.33333331	0.45237041	0.01856209	0.45237036
Eufaula.Lake.1	-0.2760262	0.56609023	-0.0209276	0.56609026

Keystone.Lake.2	-0.2760262	0.56609023	-0.0047959	0.56609026
Broken.Bow.Lake	0.19999999	0.70711422	0.00080032	0.70711423
Fort.Supply.Reservoir	-0.2	0.70711422	-0.0229412	0.70711423
Grand.Lake.O..the.Cherokees	-0.2	0.70711422	-0.0192308	0.70711423
Kaw.Lake	-0.2	0.70711422	-0.0065359	0.70711423
Kaw.Lake.1	-0.2	0.70711422	-0.0134238	0.70711423
Lake.Eucha	-0.2	0.70711422	-0.0192308	0.70711423
Lake.Lawtonka	0.19999999	0.70711422	0.00593891	0.70711423
Robert.S..Kerr.Reservoir	0.19999999	0.70711422	0.00410256	0.70711423
Webbers.Falls.Reservoir	-0.2	0.70711422	-0.0248922	0.70711423
Eufaula.Lake.3	-0.0666667	1	-0.0071644	1
Eufaula.Lake.5	0	1	0	1
Fort.Gibson.Lake	-0.0666667	1	-0.0115094	1
Keystone.Lake	-0.0666667	1	-0.0076923	1
Lake.Hudson.1	0.06666666	1	0.02593537	1
Lake.McAlester	-0.0666667	1	-0.0480769	1
Lake.McMurtry	0	1	0	1
Lake.Murray	0	1	0	1
Lake.Texoma	0.06666666	1	0.00490196	1
Lake.Thunderbird	0	1	0	1
Oologah.Lake	-0.0666667	1	-0.0192308	1
Robert.S..Kerr.Reservoir.1	-0.0666667	1	-0.0026144	1
Tenkiller.Lake	-0.0666667	1	-0.02	1
Tenkiller.Lake.1	0.06666666	1	0.00038462	1
Tom.Steed.Reservoir	-0.0666667	1	-0.0065611	1

Table C10: Mann Kendall and Sen's Slope to assess for trends in weekly lake total bloom frequency. Waterbodies with significant results are bolded.

Waterbody	tau	MK P value	Sen's Slope	Sen's p.value
Grand.Lake.O..the.Cherokees.2	**1.00000**	**0.00853**	**0.08047**	**0.00853**
Lake.Ellsworth	**1.00000**	**0.00853**	**0.05769**	**0.00853**
Lake.Texoma.3	**1.00000**	**0.00853**	**0.03434**	**0.00853**
Great.Salt.Plains.Reservoir	**0.86667**	**0.02417**	**0.05618**	**0.02417**
Lake.Chickasha	**0.86667**	**0.02417**	**0.06071**	**0.02417**
Shawnee.Twin.Lakes..1	**0.86667**	**0.02417**	**0.07127**	**0.02417**
Lake.Texoma.2	**0.89443**	**0.02677**	**0.04313**	**0.02677**
Eufaula.Lake	**0.82808**	**0.03538**	**0.08338**	**0.03538**
McGee.Creek.Reservoir	**0.82808**	**0.03538**	**0.04409**	**0.03538**
Eufaula.Lake.4	0.73333	0.06029	0.01435	0.06029
Lake.Arcadia	0.73333	0.06029	0.05769	0.06029
Sooner.Lake	0.73333	0.06029	0.05385	0.06029
Spavinaw.Lake	0.73333	0.06029	0.06410	0.06029
Lugert.Altus.Reservoir	0.69007	0.08517	0.03205	0.08517
Sardis.Lake	0.69007	0.08517	0.02446	0.08517
Atoka.Reservoir	0.60000	0.13285	0.06154	0.13285
Canton.Lake	0.60000	0.13285	0.02359	0.13285
Copan.Lake	0.60000	0.13285	0.07423	0.13285
Fort.Cobb.Reservoir	0.60000	0.13285	0.06731	0.13285
Foss.Reservoir	0.60000	0.13285	0.03682	0.13285
Hugo.Lake	0.60000	0.13285	0.07654	0.13285
Lake.Fuqua	0.60000	0.13285	0.01153	0.13285
Lake.Hefner	0.60000	0.13285	0.04000	0.13285
Lake.of.the.Arbuckles	0.60000	0.13285	0.03018	0.13285
Lake.Texoma.1	0.60000	0.13285	0.03212	0.13285
Pine.Creek.Lake	0.60000	0.13285	0.05288	0.13285
Skiatook.Lake	0.60000	0.13285	0.06278	0.13285
Stanley.Draper.Lake	0.60000	0.13285	0.05500	0.13285
Wes.Watkins.Reservoir	0.60000	0.13285	0.02963	0.13285
Grand.Lake.O..the.Cherokees.1	0.55205	0.18060	0.02564	0.18060
Lake.Texoma.4	0.55205	0.18060	0.02473	0.18060
Carl.Blackwell.Lake	0.46667	0.25966	0.01923	0.25966
Eufaula.Lake.2	-0.46667	0.25966	-0.01009	0.25966
Fort.Gibson.Lake.1	0.46667	0.25966	0.04779	0.25966
Keystone.Lake.1	0.46667	0.25966	0.01923	0.25966
Lake.Hudson	0.46667	0.25966	0.06000	0.25966

Lake.Konawa	0.46667	0.25966	0.03571	0.25966
Waurika.Lake	0.41404	0.33889	0.01103	0.33889
Keystone.Lake.3	-0.33333	0.45237	-0.01856	0.45237
Birch.Reservoir	0.33333	0.45237	0.03846	0.45237
Hulah.Lake	0.33333	0.45237	0.01282	0.45237
Lake.Overholser	0.33333	0.45237	0.06731	0.45237
Wister.Lake	0.33333	0.45237	0.04415	0.45237
Eufaula.Lake.1	0.27603	0.56609	0.02093	0.56609
Keystone.Lake.2	0.27603	0.56609	0.00480	0.56609
Broken.Bow.Lake	-0.20000	0.70711	-0.00080	0.70711
Fort.Supply.Reservoir	0.20000	0.70711	0.02294	0.70711
Grand.Lake.O..the.Cherokees	0.20000	0.70711	0.01923	0.70711
Kaw.Lake	0.20000	0.70711	0.00654	0.70711
Kaw.Lake.1	0.20000	0.70711	0.01342	0.70711
Lake.Eucha	0.20000	0.70711	0.01923	0.70711
Lake.Lawtonka	-0.20000	0.70711	-0.00594	0.70711
Robert.S..Kerr.Reservoir	-0.20000	0.70711	-0.00410	0.70711
Webbers.Falls.Reservoir	0.20000	0.70711	0.02489	0.70711
Eufaula.Lake.3	0.06667	1.00000	0.00716	1.00000
Eufaula.Lake.5	0.00000	1.00000	0.00000	1.00000
Fort.Gibson.Lake	0.06667	1.00000	0.01151	1.00000
Keystone.Lake	0.06667	1.00000	0.00769	1.00000
Lake.Hudson.1	-0.06667	1.00000	-0.02594	1.00000
Lake.McAlester	0.06667	1.00000	0.04808	1.00000
Lake.McMurtry	0.00000	1.00000	0.00000	1.00000
Lake.Murray	0.00000	1.00000	0.00000	1.00000
Lake.Texoma	-0.06667	1.00000	-0.00490	1.00000
Lake.Thunderbird	0.00000	1.00000	0.00000	1.00000
Oologah.Lake	0.06667	1.00000	0.01923	1.00000
Robert.S..Kerr.Reservoir.1	0.06667	1.00000	0.00261	1.00000
Tenkiller.Lake	0.06667	1.00000	0.02000	1.00000
Tenkiller.Lake.1	-0.06667	1.00000	-0.00038	1.00000
Tom.Steed.Reservoir	-0.14827	1.03202	-0.00207	1.03202

Table C11: MK and Sen's slope for annual trends in max bloom severity.

Waterbody	tau	MK P value	Sen's Slope (cells/mL/year)	Sen's p.value
Grand.Lake.O..the.Cherokees.1	**0.82808**	**0.03538**	**45237**	**0.03538**
Tom.Steed.Reservoir	0.69007	0.08517	83803	0.08517
Lake.Chickasha	0.60000	0.13285	38683	0.13285
Lake.Ellsworth	0.60000	0.13285	196038	0.13285
Wister.Lake	0.60000	0.13285	103848	0.13285
Canton.Lake	0.60000	0.13285	91254	0.13285
Keystone.Lake.1	0.60000	0.13285	132162	0.13285
Grand.Lake.O..the.Cherokees.2	0.60000	0.13285	80516	0.13285
Eufaula.Lake.3	0.55205	0.18060	47714	0.18060
Lake.of.the.Arbuckles	0.55205	0.18060	122821	0.18060
Eufaula.Lake.5	-0.55205	0.18060	-76470	0.18060
Keystone.Lake.3	0.46667	0.25966	414418	0.25966
Atoka.Reservoir	0.46667	0.25966	124946	0.25966
Eufaula.Lake	0.46667	0.25966	122141	0.25966
Lake.Texoma.3	0.46667	0.25966	68468	0.25966
Fort.Gibson.Lake.1	0.46667	0.25966	91550	0.25966
Stanley.Draper.Lake	0.46667	0.25966	90132	0.25966
Birch.Reservoir	0.46667	0.25966	45439	0.25966
Lake.Texoma.4	0.41404	0.33889	124223	0.33889
Lake.Overholser	-0.41404	0.33889	-41459	0.33889
Lake.Lawtonka	-0.41404	0.33889	-35287	0.33889
Lake.Texoma.2	0.41404	0.33889	59929	0.33889
Robert.S..Kerr.Reservoir.1	0.41404	0.33889	73798	0.33889
Copan.Lake	0.35806	0.43569	109519	0.43569
Keystone.Lake	0.33333	0.45237	270711	0.45237
Fort.Gibson.Lake	0.33333	0.45237	77568	0.45237
Lake.Fuqua	0.33333	0.45237	34627	0.45237
Wes.Watkins.Reservoir	0.33333	0.45237	105952	0.45237
Webbers.Falls.Reservoir	0.33333	0.45237	67943	0.45237
Lake.Hefner	0.33333	0.45237	121569	0.45237
Skiatook.Lake	0.33333	0.45237	40503	0.45237
Lake.Hudson.1	0.33333	0.45237	45237	0.45237
Keystone.Lake.2	0.33333	0.45237	107011	0.45237
Foss.Reservoir	0.33333	0.45237	36907	0.45237
Sooner.Lake	0.33333	0.45237	164814	0.45237
Lake.Hudson	0.33333	0.45237	48947	0.45237
Lake.Arcadia	-0.27603	0.56609	-13624	0.56609

Eufaula.Lake.1	0.20000	0.70711	187925	0.70711
Grand.Lake.O..the.Cherokees	-0.20000	0.70711	-90141	0.70711
Hulah.Lake	0.20000	0.70711	40245	0.70711
Carl.Blackwell.Lake	0.20000	0.70711	24474	0.70711
Robert.S..Kerr.Reservoir	0.20000	0.70711	76370	0.70711
Eufaula.Lake.4	-0.20000	0.70711	-33237	0.70711
Lake.McAlester	0.20000	0.70711	74213	0.70711
Tenkiller.Lake	-0.20000	0.70711	-25269	0.70711
Broken.Bow.Lake	0.20000	0.70711	112172	0.70711
Lake.Konawa	-0.20000	0.70711	-101913	0.70711
Lake.Eucha	-0.20000	0.70711	-29511	0.70711
Great.Salt.Plains.Reservoir	-0.13801	0.84831	-50287	0.84831
Hugo.Lake	0.13801	0.84831	26876	0.84831
Sardis.Lake	0.13801	0.84831	8756	0.84831
Lake.Murray	0.13801	0.84831	11195	0.84831
Lake.Texoma	0.00000	1.00000	0	1.00000
Waurika.Lake	0.06667	1.00000	207882	1.00000
Fort.Cobb.Reservoir	0.06667	1.00000	11412	1.00000
Lake.Texoma.1	0.06667	1.00000	32611	1.00000
Eufaula.Lake.2	0.06667	1.00000	10504	1.00000
Lake.Thunderbird	0.00000	1.00000	0	1.00000
Fort.Supply.Reservoir	0.00000	1.00000	0	1.00000
Kaw.Lake	0.06667	1.00000	85241	1.00000
Lugert.Altus.Reservoir	-0.06667	1.00000	-62876	1.00000
Oologah.Lake	0.00000	1.00000	0	1.00000
Pine.Creek.Lake	0.06667	1.00000	10504	1.00000
Lake.McMurtry	-0.06667	1.00000	-25966	1.00000
McGee.Creek.Reservoir	0.06667	1.00000	13544	1.00000
Kaw.Lake.1	-0.06667	1.00000	-53635	1.00000
Shawnee.Twin.Lakes..1	0.06667	1.00000	8237	1.00000
Tenkiller.Lake.1	0.06667	1.00000	8463	1.00000
Spavinaw.Lake	0.06667	1.00000	84723	1.00000

Table C12: Seasonal Mann Kendal and Sen's slope for monthly high-risk bloom percent coverage

Waterbody	tau	MK P value	Sen's Slope(% coverage)	Sen's p.value
Tom.Steed.Reservoir	**0.55446**	**0.00000**	**0.00703**	**0.00004**
Lake.Texoma.3	**0.51219**	**0.00000**	**0.00037**	**0.00006**
Skiatook.Lake	**0.47173**	**0.00001**	**0.00059**	**0.00442**
Lugert.Altus.Reservoir	**0.43829**	**0.00002**	**0.00758**	**0.00001**
Waurika.Lake	**0.40645**	**0.00015**	**0.00140**	**0.00034**
Canton.Lake	**0.37997**	**0.00028**	**0.00189**	**0.00126**
Lake.Texoma.4	**0.37585**	**0.00030**	**0.00165**	**0.00288**
Keystone.Lake.3	**0.37542**	**0.00050**	**0.00018**	**0.00782**
Lake.Hudson.1	**0.37256**	**0.00093**	**0.00000**	**0.00714**
Eufaula.Lake.4	**0.36218**	**0.00094**	**0.00012**	**0.02656**
Lake.Texoma.2	**0.40236**	**0.00107**	**0.00000**	**0.00068**
Webbers.Falls.Reservoir	**0.33144**	**0.00176**	**0.00013**	**0.01135**
Lake.of.the.Arbuckles	**0.33055**	**0.00230**	**0.00000**	**0.01660**
Pine.Creek.Lake	**0.31193**	**0.00253**	**0.00116**	**0.03799**
Eufaula.Lake.5	**0.30714**	**0.00298**	**0.00151**	**0.02830**
Keystone.Lake	**0.31066**	**0.00311**	**0.00020**	**0.02916**
Lake.Texoma.1	**0.30171**	**0.00331**	**0.00116**	**0.00788**
Lake.Hudson	**0.33126**	**0.00351**	**0.00000**	**0.00553**
Robert.S..Kerr.Reservoir.1	**0.34756**	**0.00395**	**0.00000**	**0.00228**
Fort.Gibson.Lake.1	**0.31894**	**0.00491**	**0.00000**	**0.02577**
Keystone.Lake.1	**0.35932**	**0.00531**	**0.00000**	**0.00954**
Keystone.Lake.2	**0.32696**	**0.00609**	**0.00000**	**0.00903**
Broken.Bow.Lake	**0.42410**	**0.00669**	**0.00000**	**0.15414**
Grand.Lake.O..the.Cherokees.1	**0.28394**	**0.00699**	**0.00014**	**0.01167**
Sardis.Lake	**0.26185**	**0.01069**	**0.00197**	**0.01026**
Sooner.Lake	**0.40188**	**0.01785**	**0.00000**	**0.02923**
Eufaula.Lake.1	**0.23333**	**0.02274**	**0.00141**	**0.04725**
Eufaula.Lake.2	**0.24958**	**0.02315**	**0.00001**	**0.13336**
McGee.Creek.Reservoir	**0.25400**	**0.02389**	**0.00000**	**0.05618**
Kaw.Lake	**0.25145**	**0.02464**	**0.00000**	**0.04315**
Copan.Lake	**0.23112**	**0.02494**	**0.00330**	**0.02342**
Lake.Ellsworth	**0.24721**	**0.02716**	**0.00000**	**0.11762**
Carl.Blackwell.Lake	**0.25870**	**0.03329**	**0.00000**	**0.12301**
Eufaula.Lake	**0.21859**	**0.03346**	**0.00027**	**0.13168**
Birch.Reservoir	**0.26405**	**0.04700**	**0.00000**	**0.04095**
Stanley.Draper.Lake	0.27846	0.05693	0.00000	0.03616

Eufaula.Lake.3	0.19500	0.05731	0.00112	0.14326
Atoka.Reservoir	0.19241	0.06765	0.00042	0.10942
Lake.Fuqua	0.21575	0.09781	0.00000	0.14631
Lake.Chickasha	0.18247	0.10140	0.00034	0.04574
Wister.Lake	0.16761	0.10272	0.00121	0.19743
Oologah.Lake	0.16667	0.10374	0.00032	0.08351
Lake.Texoma	0.16763	0.10697	0.00037	0.28331
Grand.Lake.O..the.Cherokees.2	0.23312	0.10974	0.00000	0.19579
Lake.Hefner	0.17631	0.11144	0.00000	0.29732
Fort.Cobb.Reservoir	0.15918	0.12819	0.00160	0.06247
Kaw.Lake.1	0.19197	0.14780	0.00000	0.10969
Grand.Lake.O..the.Cherokees	0.14702	0.15940	0.00032	0.07865
Fort.Gibson.Lake	0.13890	0.18736	0.00000	0.43348
Fort.Supply.Reservoir	0.14874	0.19106	0.00000	0.11548
Lake.McMurtry	0.12719	0.23476	0.00000	0.23914
Hugo.Lake	-0.10118	0.32563	-0.00012	0.72240
Spavinaw.Lake	-0.13267	0.33528	0.00000	0.53670
Lake.Thunderbird	0.09904	0.34119	0.00028	0.26826
Lake.McAlester	0.09187	0.44232	0.00000	0.26269
Foss.Reservoir	-0.07371	0.54672	0.00000	0.51780
Lake.Murray	0.10638	0.58851	0.00000	0.49271
Tenkiller.Lake	0.05942	0.65169	0.00000	0.64934
Wes.Watkins.Reservoir	0.05405	0.66770	0.00000	0.36015
Lake.Eucha	-0.07166	0.69489	0.00000	0.56293
Lake.Konawa	-0.03164	0.77837	0.00000	0.85079
Shawnee.Twin.Lakes..1	0.03961	0.79476	0.00000	0.44094
Lake.Lawtonka	-0.02429	0.81835	0.00000	0.71164
Hulah.Lake	-0.01701	0.86929	0.00000	0.76963
Lake.Overholser	0.01497	0.89840	0.00000	0.32360
Great.Salt.Plains.Reservoir	-0.00633	0.95265	0.00000	0.75660
Robert.S..Kerr.Reservoir	0.00557	0.95669	0.00006	0.74097
Lake.Arcadia	0.00000	1.00000	0.00000	0.55490
Tenkiller.Lake.1	0.00000	1.00000	0.00000	0.98203

Table C13: Seasonal Mann Kendal and Sen's slope for monthly medium-risk bloom percent coverage

Waterbody	tau	MK P value	Sen's Slope(% coverage)	Sen's p.value
Lake.Texoma.1	**0.4401325**	**0.0000178**	**0.0010229**	**0.0003328**
Lake.Hudson.1	**0.4712209**	**0.0000194**	**0.0008723**	**0.0000266**
Grand.Lake.O..the.Cherokees	**0.4286301**	**0.0000366**	**0.0006698**	**0.0000983**
Lake.Texoma.3	**0.4175435**	**0.0000644**	**0.0003679**	**0.0002860**
Keystone.Lake	**0.4185955**	**0.0001383**	**0.0001927**	**0.0004175**
Keystone.Lake.1	**0.4249001**	**0.0002463**	**0.0000000**	**0.0001610**
Lake.Texoma.2	**0.4079502**	**0.0003206**	**0.0000000**	**0.0009697**
Kaw.Lake.1	**0.3990964**	**0.0006291**	**0.0000000**	**0.0004836**
Grand.Lake.O..the.Cherokees.1	**0.3464021**	**0.0007453**	**0.0006811**	**0.0001543**
Lake.Hudson	**0.3496116**	**0.0008643**	**0.0004885**	**0.0011963**
Eufaula.Lake.2	**0.3471271**	**0.0013029**	**0.0004170**	**0.0229796**
Sooner.Lake	**0.5194519**	**0.0020756**	**0.0000000**	**0.0014563**
Grand.Lake.O..the.Cherokees.2	**0.2735401**	**0.0120792**	**0.0000000**	**0.0056689**
Broken.Bow.Lake	**0.3033191**	**0.0158132**	**0.0000000**	**0.0569864**
Skiatook.Lake	**0.2406508**	**0.0201368**	**0.0005775**	**0.0020360**
Waurika.Lake	**0.2399474**	**0.0244737**	**0.0001764**	**0.0183981**
Webbers.Falls.Reservoir	**0.2329344**	**0.0275421**	**0.0001146**	**0.0211813**
Fort.Gibson.Lake.1	**0.2317037**	**0.0284158**	**0.0001980**	**0.0157535**
Fort.Gibson.Lake	**0.2248356**	**0.0289368**	**0.0004001**	**0.0048590**
Tenkiller.Lake	**0.2425134**	**0.0344997**	**0.0000000**	**0.0784327**
Stanley.Draper.Lake	**0.2677463**	**0.0392110**	**0.0000000**	**0.0528407**
Atoka.Reservoir	0.1971103	0.0583861	0.0006588	0.0307803
Lake.McMurtry	0.2015903	0.0587582	0.0000000	0.0702946
Canton.Lake	-0.1919432	0.0654926	0.0000000	0.3450544
Lake.Lawtonka	0.1936134	0.0691785	0.0000000	0.0478460
Eufaula.Lake.5	0.1849007	0.0722365	0.0013615	0.0371880
Lake.Chickasha	-0.2026640	0.0734423	0.0000000	0.0322325
Keystone.Lake.2	0.1874497	0.0758888	0.0000324	0.0249554
Robert.S..Kerr.Reservoir.1	0.2031694	0.0768812	0.0000000	0.0207789
Eufaula.Lake	0.1777778	0.0826623	0.0003315	0.0379123
Keystone.Lake.3	0.2282774	0.0883600	0.0000000	0.0410805
Birch.Reservoir	0.1994631	0.0887367	0.0000000	0.0200691
Robert.S..Kerr.Reservoir	0.1666667	0.1037417	0.0002771	0.2959453
Kaw.Lake	0.1674944	0.1106121	0.0001422	0.0231943
Lake.Texoma.4	0.1718308	0.1150501	0.0000000	0.1724502

Eufaula.Lake.4	0.1703368	0.1167738	0.0001746	0.0517065
Sardis.Lake	0.1444444	0.1585255	0.0014007	0.0861583
Fort.Supply.Reservoir	-0.1641972	0.1633723	0.0000000	0.1412827
Spavinaw.Lake	-0.1786251	0.1830105	0.0000000	0.4621559
McGee.Creek.Reservoir	0.1527607	0.1867487	0.0000000	0.1450810
Copan.Lake	-0.1236195	0.2300623	-0.0001989	0.6686802
Lake.Texoma	-0.1238484	0.2362271	-0.0000784	0.1057296
Lake.Thunderbird	-0.1169973	0.2540516	-0.0001845	0.2488855
Wister.Lake	-0.1169973	0.2540516	-0.0002901	0.3710387
Lake.Konawa	0.1243294	0.2664898	0.0000000	0.1892572
Oologah.Lake	0.1111111	0.2780757	0.0005964	0.0835188
Shawnee.Twin.Lakes..1	0.1432070	0.3449651	0.0000000	0.3361710
Eufaula.Lake.1	0.0952519	0.3544205	0.0007350	0.0932639
Lake.Murray	0.1312863	0.4013266	0.0000000	0.4526680
Great.Salt.Plains.Reservoir	-0.0899927	0.4106554	0.0000000	0.5063468
Hulah.Lake	-0.0840458	0.4138701	-0.0003351	0.4302071
Lake.Ellsworth	0.0603179	0.5679724	0.0000000	0.7443820
Carl.Blackwell.Lake	-0.0493666	0.6594539	0.0000000	0.8337295
Lake.Eucha	0.0830100	0.6612572	0.0000000	0.2845065
Eufaula.Lake.3	-0.0444444	0.6643894	0.0003407	0.5273254
Wes.Watkins.Reservoir	-0.0553731	0.6722361	0.0000000	0.7835056
Lake.Arcadia	-0.0478238	0.7160847	0.0000000	0.7987593
Lake.Fuqua	0.0429795	0.7212119	0.0000000	0.1932248
Fort.Cobb.Reservoir	0.0374034	0.7257959	0.0000000	0.8691928
Lugert.Altus.Reservoir	-0.0335228	0.7441543	-0.0002967	0.3579439
Lake.Overholser	-0.0295574	0.8185458	0.0000000	0.3103350
Tom.Steed.Reservoir	-0.0227436	0.8260664	0.0000000	0.5217036
Hugo.Lake	-0.0222222	0.8282625	-0.0005347	0.5466279
Lake.Hefner	0.0218275	0.8433025	0.0000000	0.4508574
Foss.Reservoir	-0.0220922	0.8486154	0.0000000	0.4234864
Lake.McAlester	0.0158208	0.8914223	0.0000000	0.3897630
Pine.Creek.Lake	0.0111743	0.9133725	0.0001862	0.5725179
Tenkiller.Lake.1	-0.0095906	0.9378220	0.0000000	0.8238891
Lake.of.the.Arbuckles	0.0000000	1.0000000	0.0000181	0.1967425

Table C14: Seasonal Mann Kendal and Sen's slope for monthly low-risk bloom percent coverage

Waterbody	tau	MK P value	Sen's Slope(% coverage)	Sen's p.value
Lake.Texoma.1	**0.44444**	**0.00002**	**0.00015**	**0.00001**
Lake.Texoma.2	**0.41958**	**0.00045**	**0.00000**	**0.00319**
Kaw.Lake.1	**0.37679**	**0.00064**	**0.00000**	**0.00017**
Sooner.Lake	**0.56188**	**0.00099**	**0.00000**	**0.00088**
Eufaula.Lake.2	**0.35769**	**0.00115**	**0.00008**	**0.00426**
Grand.Lake.O..the.Cherokees	**0.35073**	**0.00155**	**0.00006**	**0.00229**
Lake.Texoma.3	**0.35877**	**0.00206**	**0.00000**	**0.00358**
Keystone.Lake.1	**0.43583**	**0.00334**	**0.00000**	**0.00232**
Keystone.Lake.2	**0.32617**	**0.00515**	**0.00000**	**0.00427**
Lake.Chickasha	**-0.46590**	**0.00779**	**0.00000**	**0.01830**
Pine.Creek.Lake	**0.27498**	**0.01126**	**0.00000**	**0.01978**
Robert.S..Kerr.Reservoir	**0.25222**	**0.01414**	**0.00010**	**0.01333**
Robert.S..Kerr.Reservoir.1	**0.42101**	**0.01552**	**0.00000**	**0.00441**
Grand.Lake.O..the.Cherokees.1	**0.24855**	**0.01684**	**0.00007**	**0.00649**
Broken.Bow.Lake	**0.28813**	**0.03042**	**0.00000**	**0.05913**
Lake.Hudson.1	**0.23483**	**0.03700**	**0.00000**	**0.00315**
Lake.of.the.Arbuckles	**0.24766**	**0.04114**	**0.00000**	**0.05438**
Hulah.Lake	**-0.22692**	**0.04382**	**0.00000**	**0.21537**
Fort.Gibson.Lake.1	0.22263	0.05562	0.00000	0.04105
McGee.Creek.Reservoir	0.23947	0.05975	0.00000	0.03869
Stanley.Draper.Lake	0.23876	0.06469	0.00000	0.03156
Shawnee.Twin.Lakes..1	0.35414	0.06823	0.00000	0.04961
Fort.Cobb.Reservoir	-0.31060	0.07604	0.00000	0.06304
Waurika.Lake	0.19159	0.07933	0.00000	0.01621
Lake.Texoma.4	0.30476	0.08189	0.00000	0.13646
Eufaula.Lake	0.18009	0.08455	0.00005	0.02008
Grand.Lake.O..the.Cherokees.2	0.18396	0.09465	0.00000	0.02577
Keystone.Lake	0.20370	0.10967	0.00000	0.07029
Wes.Watkins.Reservoir	0.34641	0.12819	0.00000	0.11454
Kaw.Lake	0.16417	0.14065	0.00000	0.10555
Foss.Reservoir	0.18180	0.16621	0.00000	0.07903
Copan.Lake	-0.14359	0.17377	0.00000	0.14629
Lake.Hudson	0.14065	0.19365	0.00000	0.04975
Webbers.Falls.Reservoir	0.14843	0.21419	0.00000	0.32922
Tom.Steed.Reservoir	-0.12357	0.24663	0.00000	0.13627
Oologah.Lake	0.10585	0.30210	0.00009	0.19930

Lake.McMurtry	0.12355	0.30405	0.00000	0.35212
Tenkiller.Lake	0.12670	0.33280	0.00000	0.23247
Wister.Lake	-0.09978	0.34965	0.00000	0.38922
Canton.Lake	-0.11532	0.39085	0.00000	0.33961
Fort.Supply.Reservoir	-0.13791	0.40936	0.00000	0.15144
Fort.Gibson.Lake	0.08697	0.41315	0.00000	0.09496
Sardis.Lake	0.08357	0.41525	0.00013	0.36066
Skiatook.Lake	0.08615	0.41685	0.00000	0.12579
Lake.Ellsworth	-0.08793	0.42812	0.00000	0.65724
Eufaula.Lake.4	0.08469	0.44073	0.00002	0.09454
Atoka.Reservoir	0.07661	0.47486	0.00000	0.16004
Lake.Texoma	-0.07845	0.50352	0.00000	0.49335
Eufaula.Lake.5	0.06236	0.54624	0.00007	0.26618
Lake.Thunderbird	0.06087	0.57551	0.00000	0.56349
Lake.Murray	0.10638	0.58851	0.00000	0.52104
Lake.McAlester	0.06846	0.61708	0.00000	0.35129
Hugo.Lake	0.05014	0.62497	0.00007	0.28675
Lake.Lawtonka	0.06585	0.65472	0.00000	0.54068
Tenkiller.Lake.1	0.06911	0.66623	0.00000	0.61052
Keystone.Lake.3	0.11547	0.67885	0.00000	0.58357
Eufaula.Lake.1	0.04169	0.69110	0.00012	0.04766
Eufaula.Lake.3	-0.04040	0.69810	0.00000	0.64684
Lake.Fuqua	0.05435	0.71192	0.00000	0.25274
Spavinaw.Lake	-0.05379	0.75488	0.00000	0.69112
Great.Salt.Plains.Reservoir	0.04317	0.77041	0.00000	0.78277
Lake.Overholser	-0.05319	0.78677	0.00000	0.68224
Lugert.Altus.Reservoir	0.02990	0.79816	0.00000	0.55621
Lake.Hefner	-0.03059	0.83714	0.00000	0.98646
Carl.Blackwell.Lake	0.02331	0.86481	0.00000	0.63564
Lake.Arcadia	0.02032	0.90766	0.00000	0.88687
Birch.Reservoir	-0.00960	0.93986	0.00000	0.39985
Lake.Eucha	0.00000	1.00000	0.00000	0.84214
Lake.Konawa	0.00000	1.00000	0.00000	0.68521

Table C15: Seasonal Mann Kendal and Sen's slope for monthly total bloom percent coverage

Waterbody	tau	MK P value	Sen's Slope(% coverage)	Sen's p.value
Skiatook.Lake	**0.49042**	**0.00000**	**0.00219**	**0.00021**
Lake.Texoma.3	**0.47635**	**0.00001**	**0.00103**	**0.00012**
Waurika.Lake	**0.44843**	**0.00002**	**0.00335**	**0.00025**
Tom.Steed.Reservoir	**0.43213**	**0.00003**	**0.00937**	**0.00003**
Lake.Texoma.1	**0.40670**	**0.00007**	**0.00272**	**0.00095**
Canton.Lake	**0.40134**	**0.00012**	**0.00178**	**0.00010**
Lake.Texoma.4	**0.38915**	**0.00017**	**0.00206**	**0.00221**
Lake.Texoma.2	**0.40109**	**0.00038**	**0.00010**	**0.00060**
Grand.Lake.O..the.Cherokees.1	**0.36213**	**0.00042**	**0.00114**	**0.00058**
Lugert.Altus.Reservoir	**0.35758**	**0.00050**	**0.00532**	**0.00030**
Keystone.Lake.1	**0.40095**	**0.00050**	**0.00000**	**0.00041**
Lake.Hudson	**0.36169**	**0.00053**	**0.00080**	**0.00139**
Grand.Lake.O..the.Cherokees	**0.35912**	**0.00054**	**0.00138**	**0.00884**
Lake.Hudson.1	**0.37774**	**0.00058**	**0.00138**	**0.00045**
Keystone.Lake.3	**0.35812**	**0.00082**	**0.00040**	**0.00677**
Lake.Ellsworth	**0.34565**	**0.00093**	**0.00113**	**0.01735**
Kaw.Lake.1	**0.35387**	**0.00098**	**0.00016**	**0.00038**
Eufaula.Lake.2	**0.34483**	**0.00137**	**0.00065**	**0.05827**
Eufaula.Lake.4	**0.33730**	**0.00182**	**0.00063**	**0.02519**
Eufaula.Lake.5	**0.31937**	**0.00190**	**0.00371**	**0.01437**
Keystone.Lake	**0.31952**	**0.00212**	**0.00079**	**0.00963**
Fort.Gibson.Lake.1	**0.31001**	**0.00332**	**0.00057**	**0.00594**
Pine.Creek.Lake	**0.30000**	**0.00341**	**0.00252**	**0.05237**
Robert.S..Kerr.Reservoir.1	**0.31844**	**0.00503**	**0.00000**	**0.00236**
Eufaula.Lake	**0.27778**	**0.00670**	**0.00072**	**0.07441**
Broken.Bow.Lake	**0.31557**	**0.00821**	**0.00000**	**0.04419**
Webbers.Falls.Reservoir	**0.27177**	**0.00928**	**0.00062**	**0.00404**
Sooner.Lake	**0.37501**	**0.00955**	**0.00000**	**0.00343**
Atoka.Reservoir	**0.26668**	**0.01044**	**0.00169**	**0.03403**
Keystone.Lake.2	**0.25822**	**0.01361**	**0.00035**	**0.00721**
Grand.Lake.O..the.Cherokees.2	**0.26523**	**0.01376**	**0.00000**	**0.00314**
Stanley.Draper.Lake	**0.29677**	**0.02064**	**0.00000**	**0.01654**
Sardis.Lake	**0.22222**	**0.03006**	**0.00408**	**0.04022**
Lake.of.the.Arbuckles	**0.22614**	**0.03127**	**0.00152**	**0.03386**
Copan.Lake	**0.21852**	**0.03363**	**0.00379**	**0.02696**
Birch.Reservoir	**0.24549**	**0.03618**	**0.00000**	**0.01623**

Lake.Chickasha	**0.24838**	**0.04589**	**0.00000**	**0.03009**
Fort.Cobb.Reservoir	0.19985	0.05579	0.00114	0.08044
Lake.Hefner	0.19782	0.07148	0.00000	0.30140
Kaw.Lake	0.18370	0.07909	0.00036	0.03233
Eufaula.Lake.1	0.17778	0.08266	0.00244	0.10130
Carl.Blackwell.Lake	0.18906	0.09045	0.00000	0.12733
Fort.Gibson.Lake	0.16863	0.10137	0.00086	0.03478
Lake.McMurtry	0.16852	0.10945	0.00000	0.23807
Foss.Reservoir	-0.18018	0.11745	0.00000	0.74062
McGee.Creek.Reservoir	0.17266	0.11758	0.00000	0.14424
Oologah.Lake	0.15556	0.12889	0.00126	0.07520
Lake.Texoma	0.14178	0.16983	0.00043	0.48343
Wister.Lake	0.13928	0.17452	0.00103	0.37104
Spavinaw.Lake	-0.16094	0.20470	0.00000	0.65340
Tenkiller.Lake	0.13085	0.25138	0.00000	0.50534
Lake.Fuqua	0.13141	0.27257	0.00000	0.10740
Lake.McAlester	0.09412	0.38465	0.00000	0.21617
Hugo.Lake	-0.08889	0.38555	-0.00052	0.77424
Lake.Murray	0.13129	0.40133	0.00000	0.44365
Fort.Supply.Reservoir	0.09377	0.41422	0.00000	0.08664
Shawnee.Twin.Lakes..1	0.10484	0.49058	0.00000	0.30950
Eufaula.Lake.3	0.06667	0.51518	0.00143	0.25317
Robert.S..Kerr.Reservoir	0.06667	0.51518	0.00042	0.61658
Hulah.Lake	-0.05043	0.62395	-0.00037	0.72617
Lake.Thunderbird	-0.05014	0.62497	0.00050	0.38943
Lake.Overholser	0.05648	0.63671	0.00000	0.54101
Tenkiller.Lake.1	0.02798	0.81924	0.00000	0.75838
Lake.Arcadia	-0.02701	0.83377	0.00000	0.49135
Lake.Konawa	0.02322	0.83535	0.00000	0.65034
Lake.Lawtonka	0.02020	0.85250	0.00000	0.92068
Great.Salt.Plains.Reservoir	-0.01884	0.85960	0.00000	0.67909
Lake.Eucha	-0.01551	0.92592	0.00000	0.59703
Wes.Watkins.Reservoir	0.00000	1.00000	0.00000	0.53686

APPENDIX D : Monthly spatial extent for high-risk blooms (km^2)

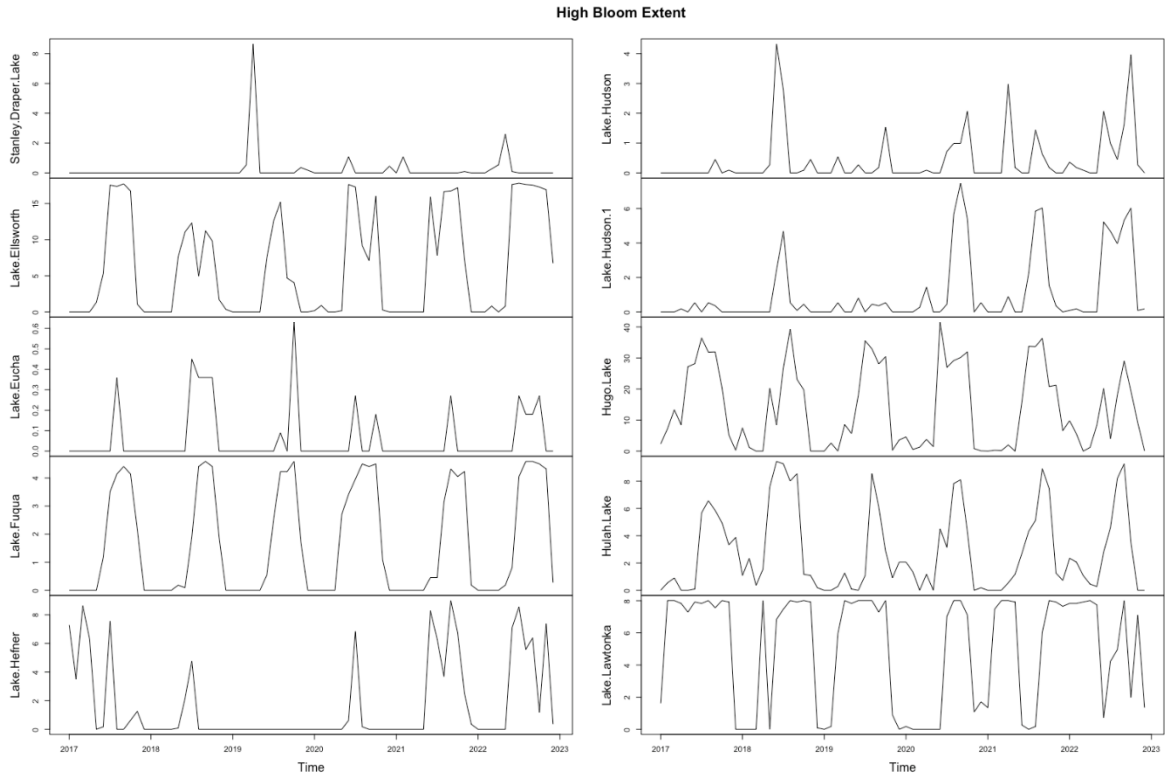

Figure D1: Waterbody monthly high risk spatial extent

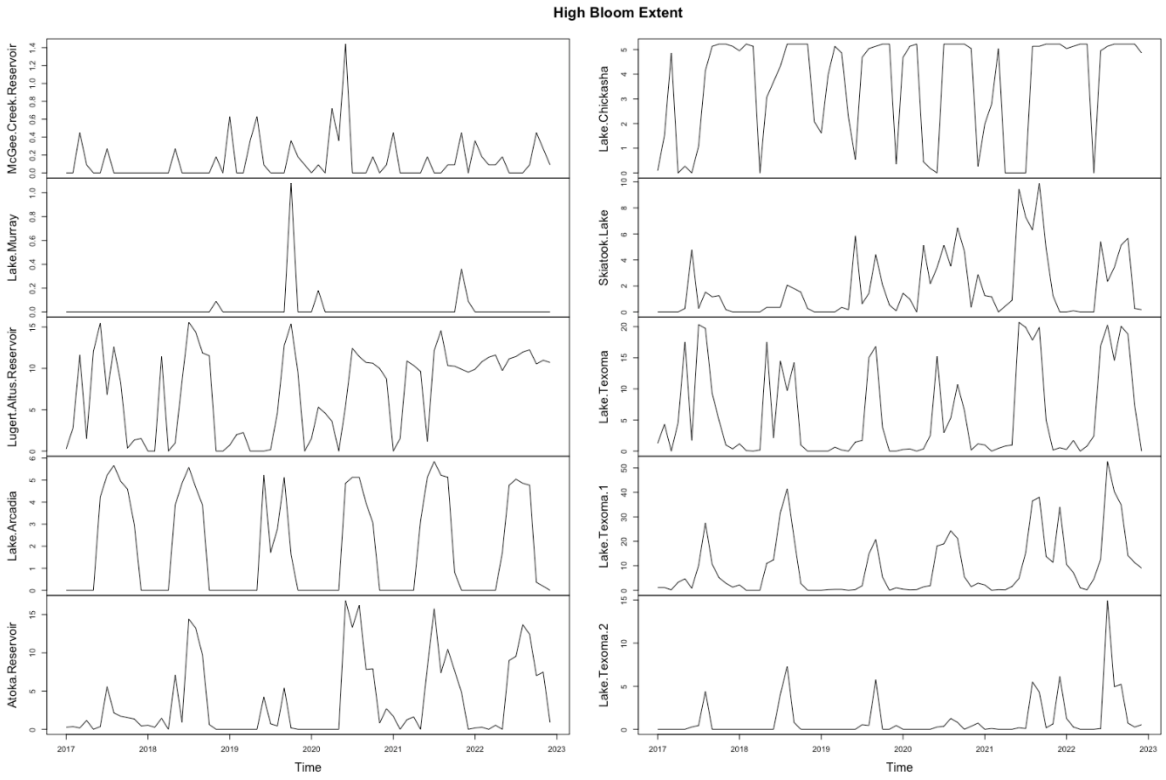
High Bloom Extent
McGee.Creek.Reservoir
Lake.Murray
Lugert.Altus.Reservoir
Lake.Arcadia
Atoka.Reservoir
Lake.Chickasha
Skiatook.Lake
Lake.Texoma
Lake.Texoma.1
Lake.Texoma.2
2017
2018
2019
2020
2021
2022
2023
Time

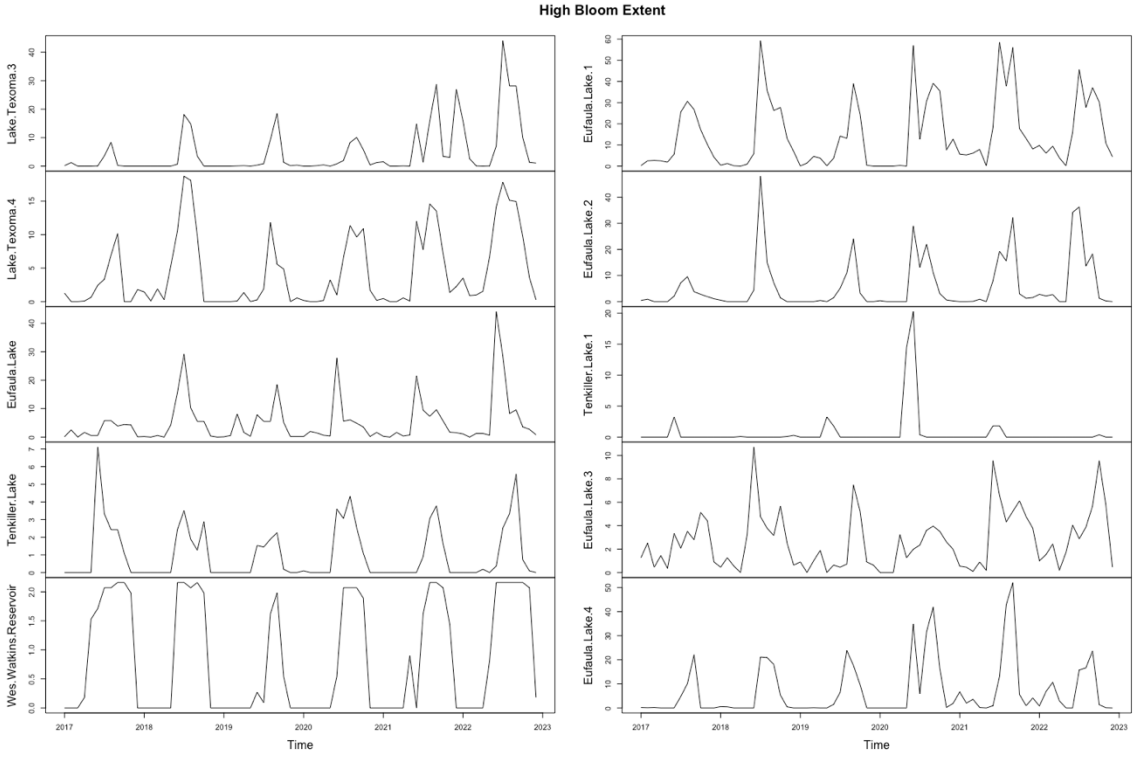
High Bloom Extent
Lake.Texoma.3
Lake.Texoma.4
Eufaula.Lake
Tenkiller.Lake
Wes.Watkins.Reservoir
Eufaula.Lake.1
Eufaula.Lake.2
Tenkiller.Lake.1
Eufaula.Lake.3
Eufaula.Lake.4
2017
2018
2019
2020
2021
2022
2023
Time

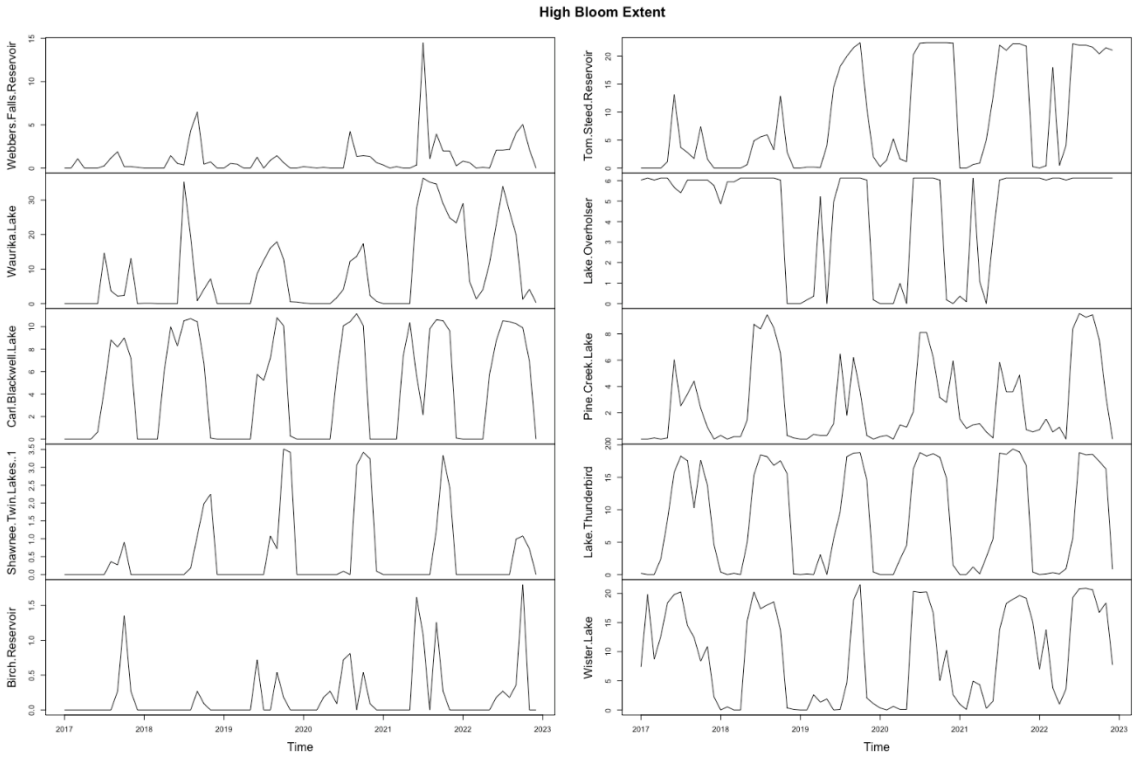
High Bloom Extent
Webbers.Falls.Reservoir
Waurika.Lake
Carl.Blackwell.Lake
Shawnee.Twin.Lakes..1
Birch.Reservoir
Tom.Steed.Reservoir
Lake.Overholser
Pine.Creek.Lake
Lake.Thunderbird
Wister.Lake
2017
2018
2019
2020
2021
2022
2023
Time

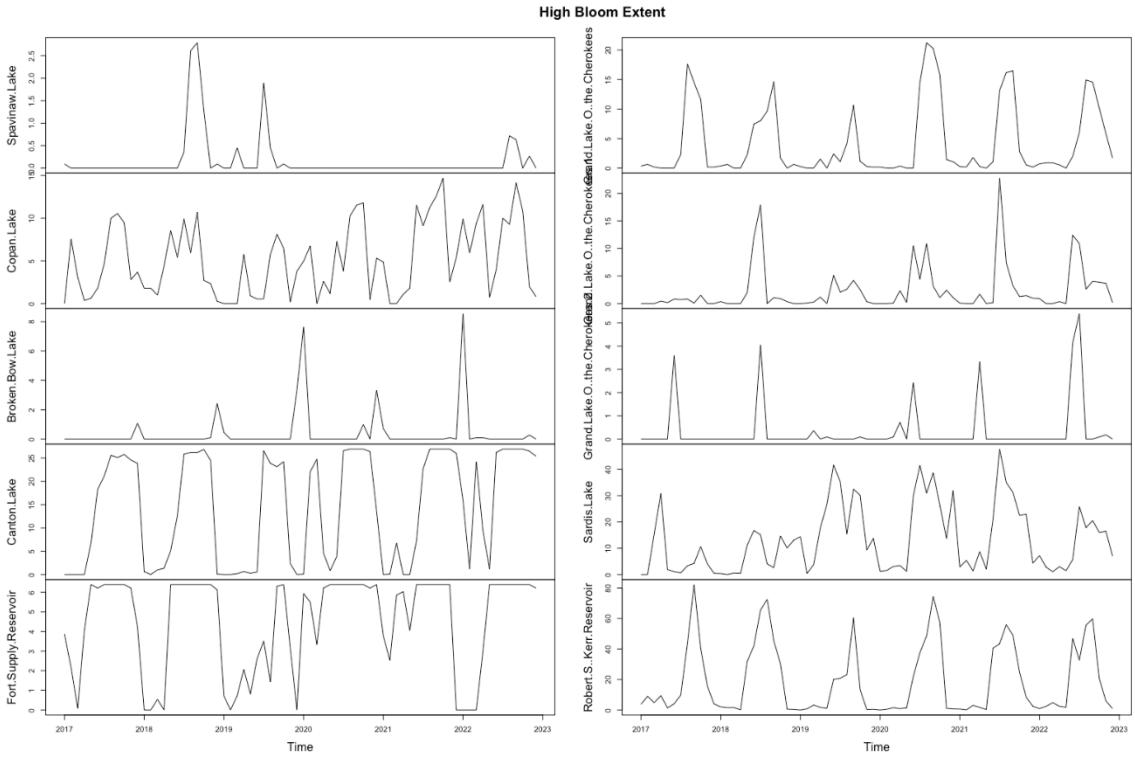
High Bloom Extent
Spavinaw.Lake
Copan.Lake
Broken.Bow.Lake
Canton.Lake
Fort.Supply.Reservoir
Grand.Lake.O..the.Cherokees
Grand.Lake.O..the.Cherokees.1
Grand.Lake.O..the.Cherokees.2
Sardis.Lake
Robert.S..Kerr.Reservoir
2017
2018
2019
2020
2021
2022
2023
Time

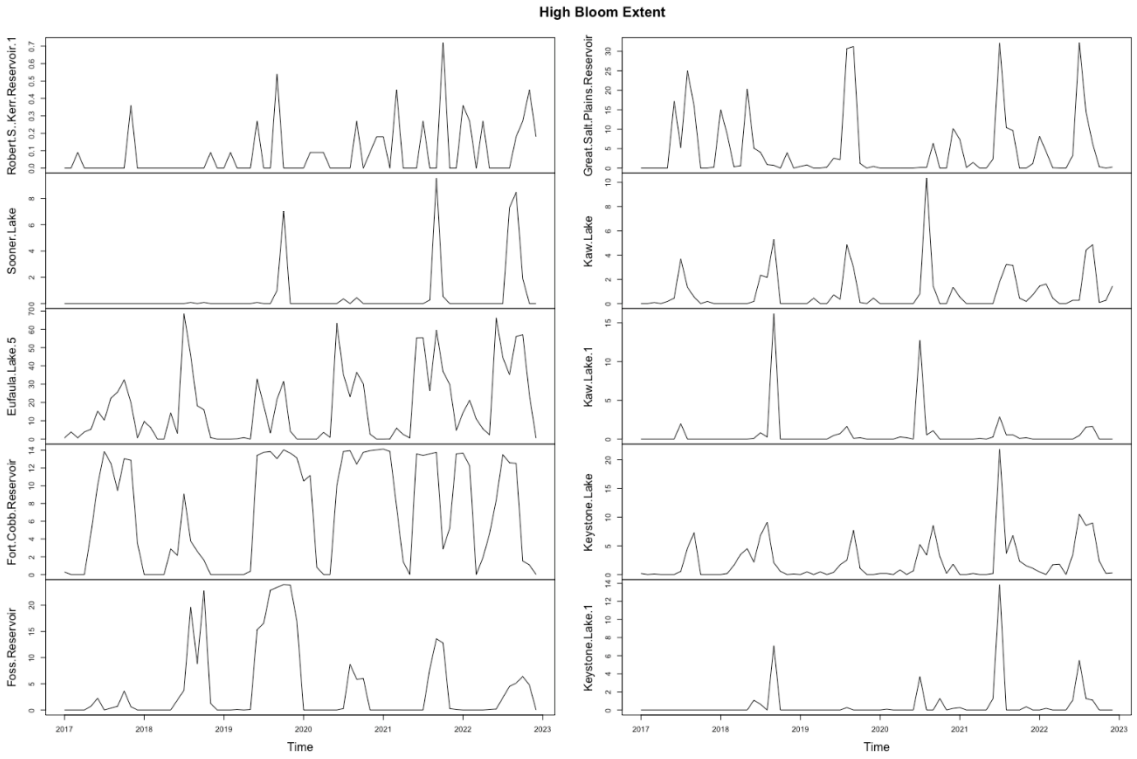
High Bloom Extent
Robert.S..Kerr.Reservoir.1
Great.Salt.Plains.Reservoir
Sooner.Lake
Kaw.Lake
Eufaula.Lake.5
Kaw.Lake.1
Fort.Cobb.Reservoir
Keystone.Lake
Foss.Reservoir
Keystone.Lake.1
2017
2018
2019
2020
2021
2022
2023
Time

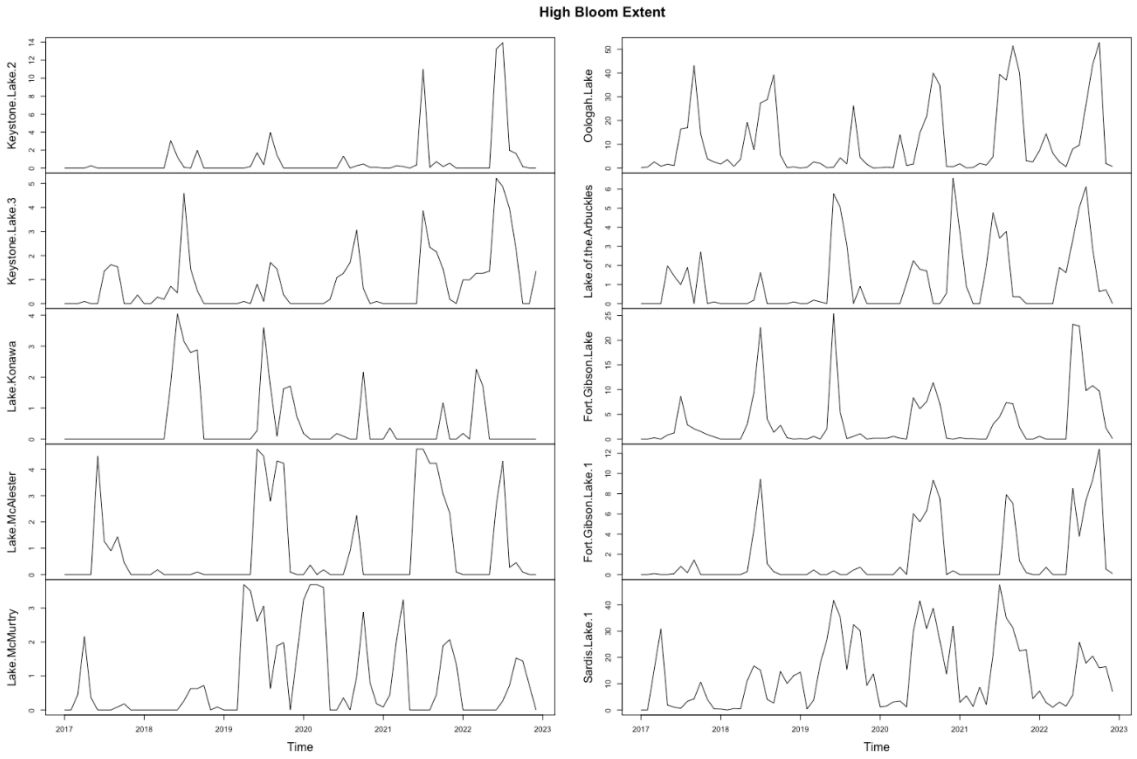
High Bloom Extent
Keystone.Lake.2
Oologah.Lake
Keystone.Lake.3
Lake.of.the.Arbuckles
Lake.Konawa
Fort.Gibson.Lake
Lake.McAlester
Fort.Gibson.Lake.1
Lake.McMurtry
Sardis.Lake.1
2017
2018
2019
2020
2021
2022
2023
Time

APPENDIX E: Trophic State Graphs

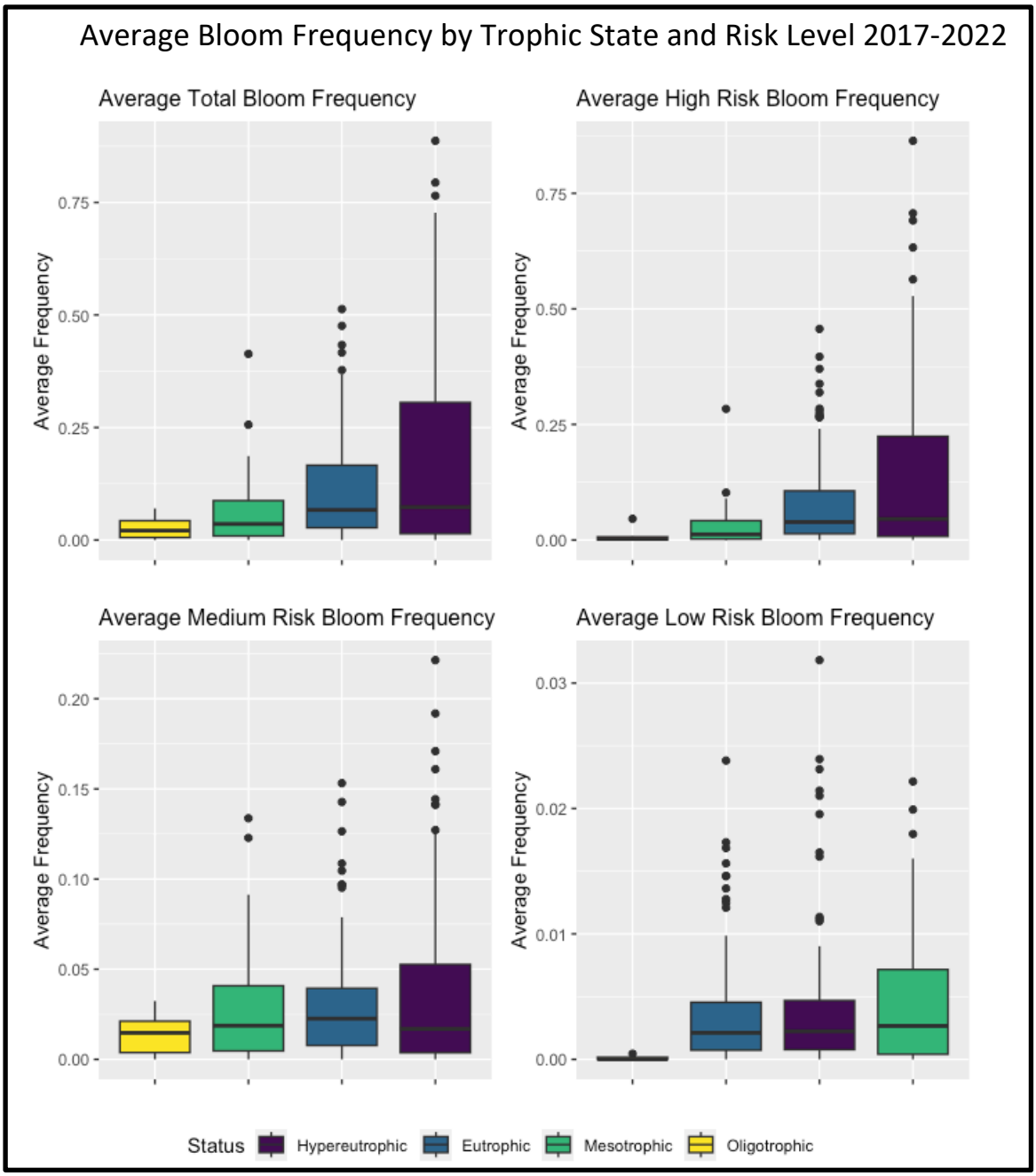

Figure E1: Average annual cyanoHAB bloom frequency by trophic state and risk level of bloom.

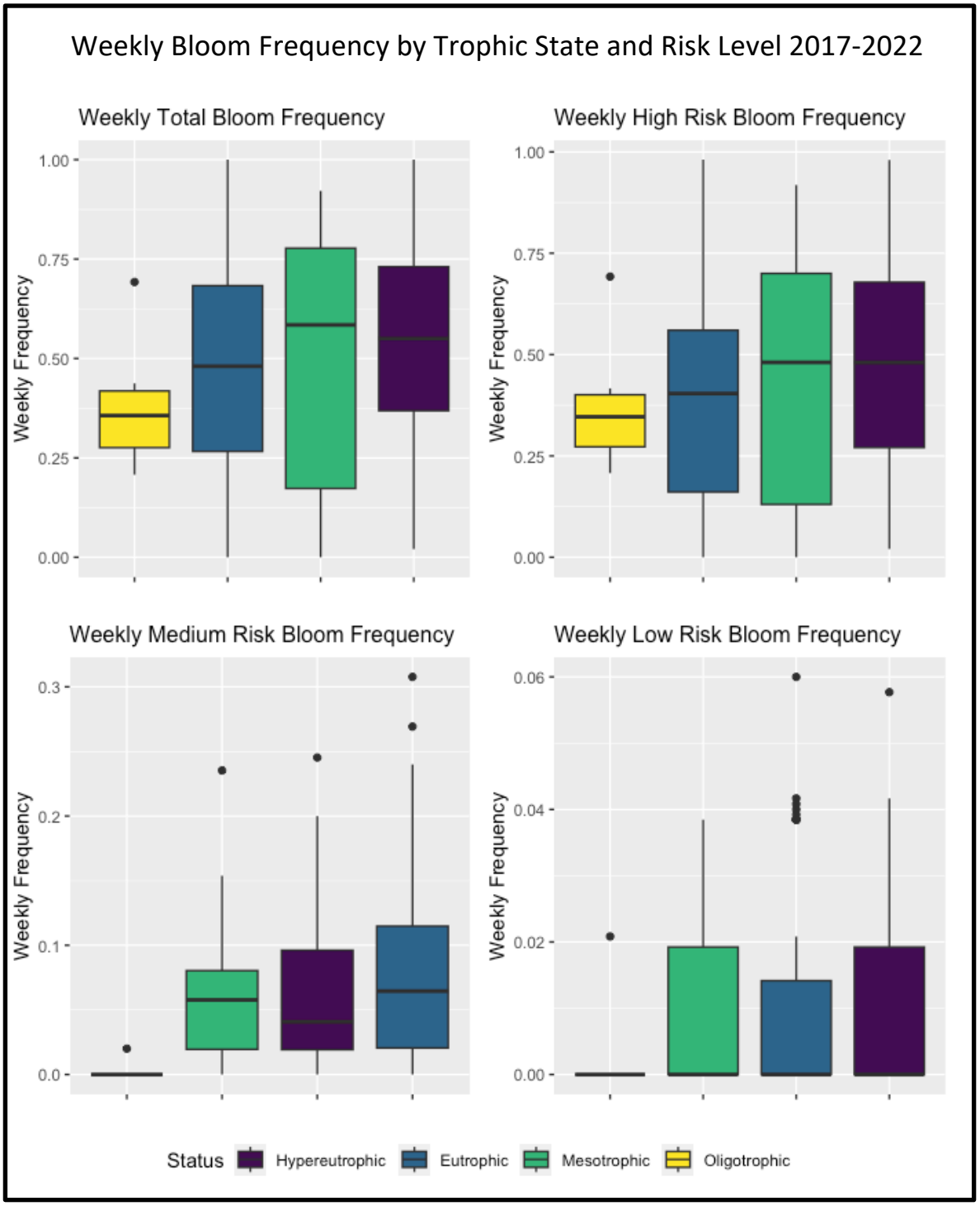

Figure E2: Weekly cyanoHAB bloom frequency by trophic state and risk level of bloom.

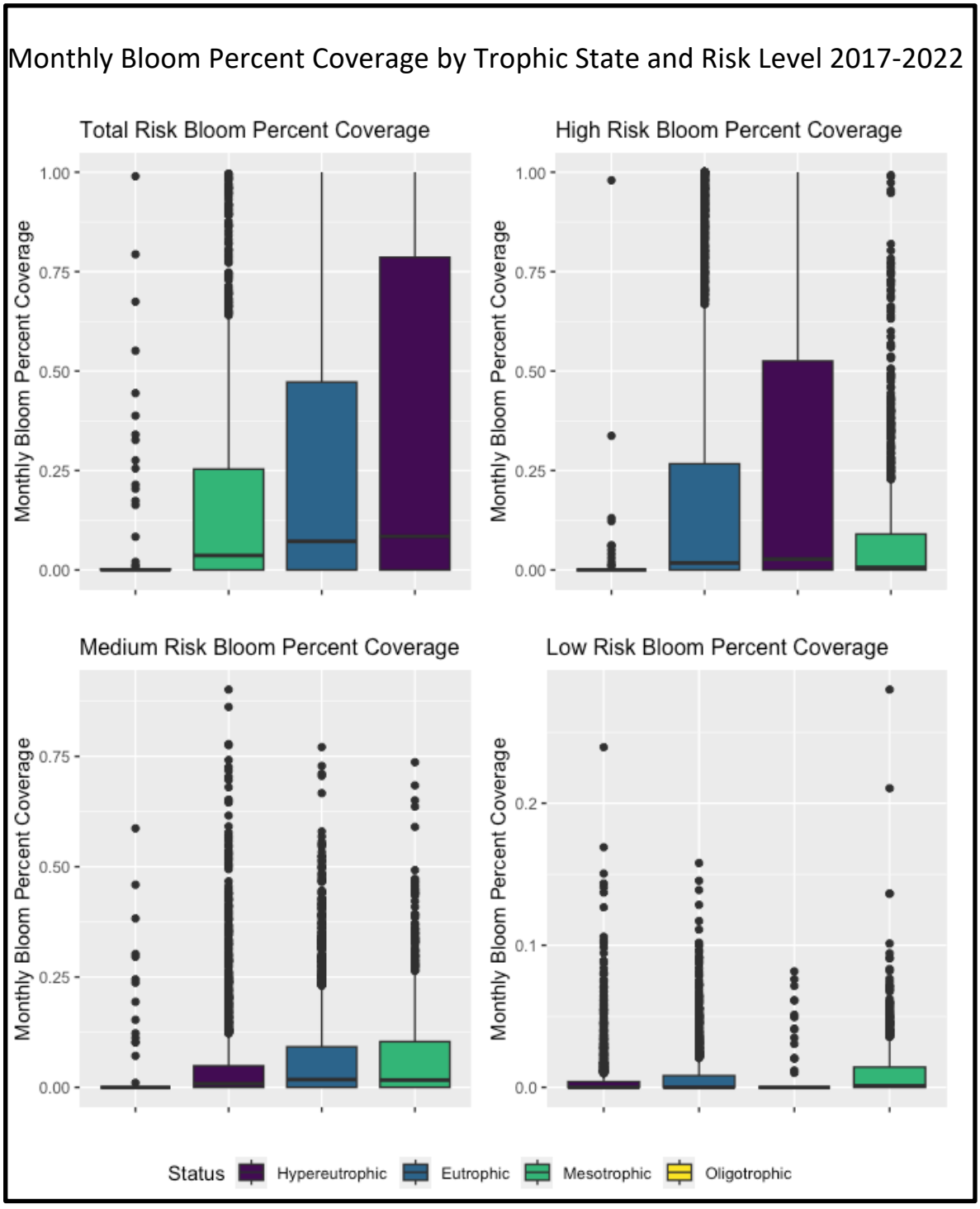

Figure E3: Monthly cyanoHAB bloom percent coverage of a waterbody by trophic state and risk level of bloom.

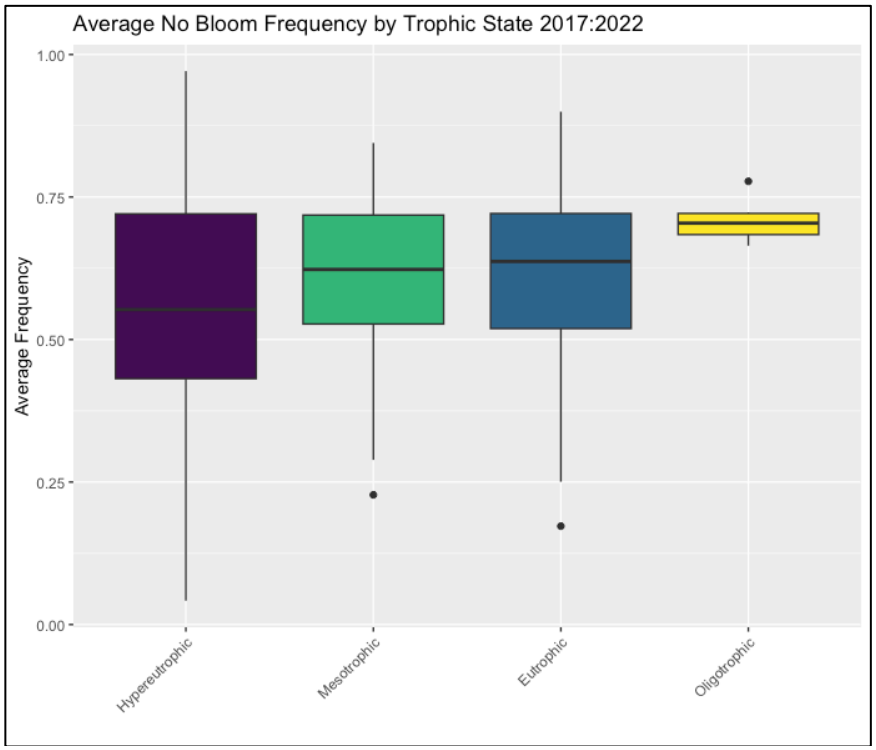

Figure E4: Average annual no bloom frequency by trophic states

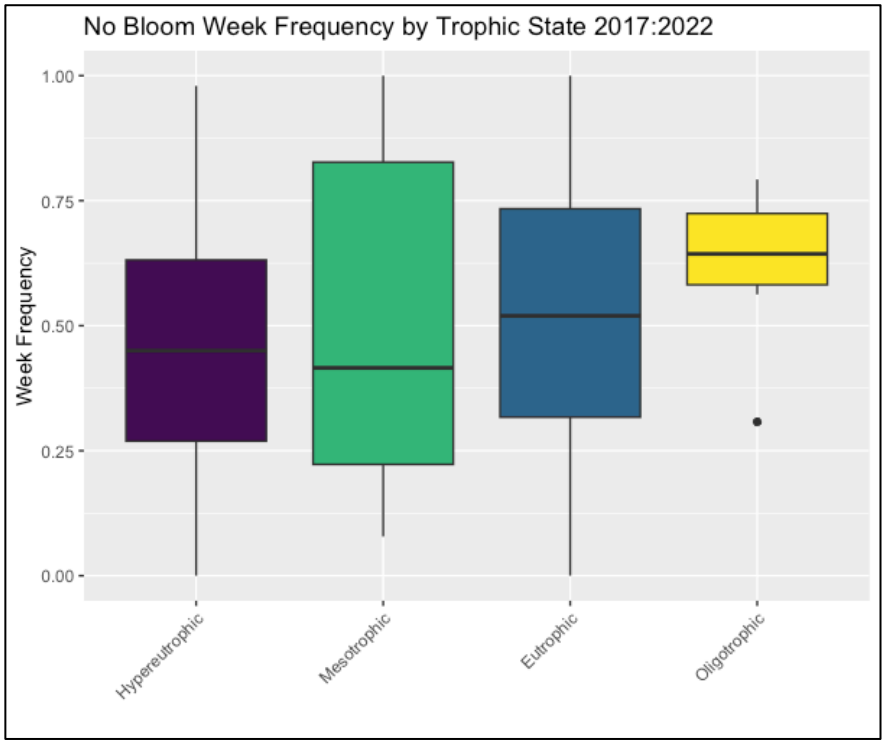

Figure E5: Weekly no bloom frequency by trophic state

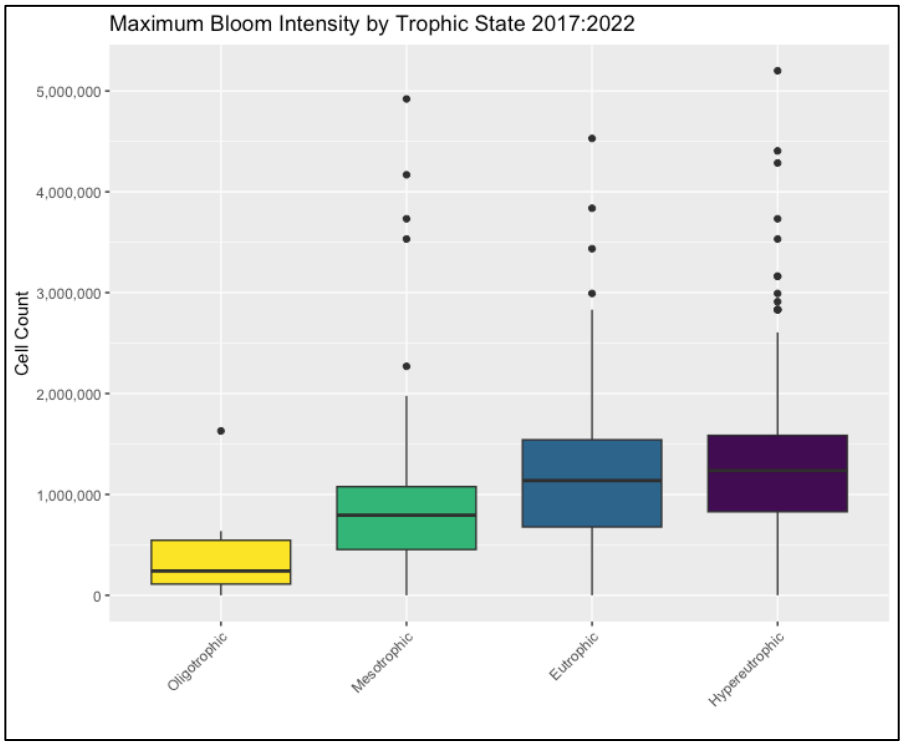

Figure E6: Max bloom severity by trophic status

APPENDIX F: Trophic trend analysis

Table F1: Mann-Kendall and Sen's Slope trend detection for high-risk bloom frequency by trophic states

Trophic State	Tau	MK p value	Sen's Slope	Sen's p value
Hypereutrophic	0.59999996	0.13285494	0.01026638	0.13285496
Eutrophic	**0.86666662**	**0.02417052**	**0.01194064**	**0.02417055**
Mesotrophic	0.33333331	0.45237041	0.00293533	0.45237036
Oligotrophic	0.41403931	0.33888781	0.00106838	0.33888783

Table F2: Mann-Kendall and Sen's slope for trends in average annual medium-risk bloom frequency by trophic states

Trophic State	Tau	MK p value	Sen's Slope	Sen's p value
Hypereutrophic	0.33333331	0.45237041	0.00280123	0.45237036
Eutrophic	**0.86666662**	**0.02417052**	**0.00258741**	**0.02417055**
Mesotrophic	**0.86666662**	**0.02417052**	**0.00343649**	**0.02417055**
Oligotrophic	0.59999996	0.13285494	0.00551994	0.13285496

Table F3: Mann-Kendall and Sen's slope for trends in average annual low-risk bloom frequency by trophic states

Trophic State	Tau	MK p value	Sen's Slope	Sen's p value
Hypereutrophic	0.73333329	0.06028914	0.00038804	0.06028917
Eutrophic	0.73333329	0.06028914	0.00026002	0.06028917
Mesotrophic	0.59999996	0.13285494	0.00072271	0.13285496
Oligotrophic	0.0860663	1	0	1

Table F4: Mann-Kendall and Sen's slope for trends in average annual no bloom frequency by trophic states

Trophic State	Tau	MK p value	Sen's Slope	Sen's p value
Hypereutrophic	-0.0666667	1	-0.0015347	1
Eutrophic	-0.0666667	1	-0.0053727	1
Mesotrophic	0.19999999	0.70711422	0.00713666	0.70711423
Oligotrophic	0.46666664	0.25965631	0.01021273	0.25965636

Table F5: Mann-Kendall and Sens slope for trends in average annual total bloom frequency by trophic state

Trophic State	Tau	MK p value	Sen's Slope	Sen's p value
Hypereutrophic	0.59999996	0.13285494	0.01327522	0.13285496
Eutrophic	**0.99999994**	**0.00853491**	**0.01506509**	**0.00853492**
Mesotrophic	0.73333329	0.06028914	0.00605263	0.06028917
Oligotrophic	0.33333331	0.45237041	0.0086254	0.45237036

Table F6: MK and Sen's slope for trends in annual high-risk bloom weekly frequency by trophic state

Trophic State	Tau	MK p value	Sen's Slope	Sen's p value
Hypereutrophic	0.59999996	0.13285494	0.03470944	0.13285496
Eutrophic	0.73333329	0.06028914	0.0271588	0.06028917
Mesotrophic	0.73333329	0.06028914	0.01780048	0.06028917
Oligotrophic	0.46666664	0.25965631	0.04846467	0.25965636

Table F7: MK and Sen's slope for trends in annual medium-risk bloom weekly frequency by trophic state

Trophic State	Tau	MK p value	Sen's Slope	Sen's p value
Hypereutrophic	-0.7333333	0.06028918	-0.0037707	0.06028917
Eutrophic	0.33333331	0.45237041	0.00263011	0.45237036
Mesotrophic	0.33333331	0.45237041	0.00375566	0.45237036
Oligotrophic	0.34641016	0.55818462	0	0.55818465

Table F8: MK and Sen's slope for trends in annual low-risk bloom weekly frequency by trophic state

Trophic State	Tau	MK p value	Sen's Slope	Sen's p value
Hypereutrophic	0.19999999	0.70711422	0.00024637	0.70711423
Eutrophic	0.46666664	0.25965631	0.00041262	0.25965636
Mesotrophic	-0.2	0.70711422	-0.0001664	0.70711423
Oligotrophic	-0.3464102	0.55818468	0	0.55818465

Table F9: MK and Sen's slope for trends in annual no bloom weekly frequency by trophic state

Trophic State	Tau	MK p value	Sen's Slope	Sen's p value
Hypereutrophic	-0.6	0.13285497	-0.030115	0.13285496
Eutrophic	**-0.8666666**	**0.02417055**	**-0.0315161**	**0.02417055**
Mesotrophic	-0.7333333	0.06028918	-0.0240769	0.06028917
Oligotrophic	-0.6	0.13285497	-0.055	0.13285496

Table F10: MK and Sen's slope for trends in annual total bloom weekly frequency

Trophic State	Tau	MK p value	Sen's Slope	Sen's p value
Hypereutrophic	**0.86666662**	**0.02417052**	**0.03151609**	**0.02417055**
Eutrophic	0.59999996	0.13285494	0.03011496	0.13285496
Mesotrophic	0.73333329	0.06028914	0.02407688	0.06028917
Oligotrophic	0.59999996	0.13285494	0.055	0.13285496

Table F11: MK and Sen's slope trend analysis for max bloom severity by trophic state

Trophic State	Tau	MK p value	Sen's Slope (cells/mL/year)	Sen's p value
Hypereutrophic	0.59999996	0.13285494	59964.3344	0.13285496
Eutrophic	0.73333329	0.06028914	80812.4484	0.06028917
Mesotrophic	0.73333329	0.06028914	45184.3958	0.06028917
Oligotrophic	0.46666664	0.25965631	90131.9333	0.25965636

VITA

Kelly Rose Hendrix

Candidate for the Degree of

Master of Science

Thesis: CHARACTERIZATION OF HARMFUL ALGAL BLOOM FREQUENCY, SEVERITY, AND SPATIAL EXTENT IN OKLAHOMA RESERVOIRS UTILIZING THE CYANOBACTERIA ASSESSMENT NETWORK

Major Field: Environmental Science

Biographical:

Education:

Completed the requirements for the Master of Science in Environmental Science at Oklahoma State University, Stillwater, Oklahoma in May, 2023.

Completed the requirements for the Bachelor of Science in your Environmental Science at Montana State University, Bozeman, Montana in 2021.